Laser ultrasonics for material characterization and defect detection

Christ Glorieux

Laboratory of Acoustics

Soft Matter and Biophysics

Department of Physics and Astronomy

KU Leuven, Belgium

Christ.Glorieux@fys.kuleuven.be

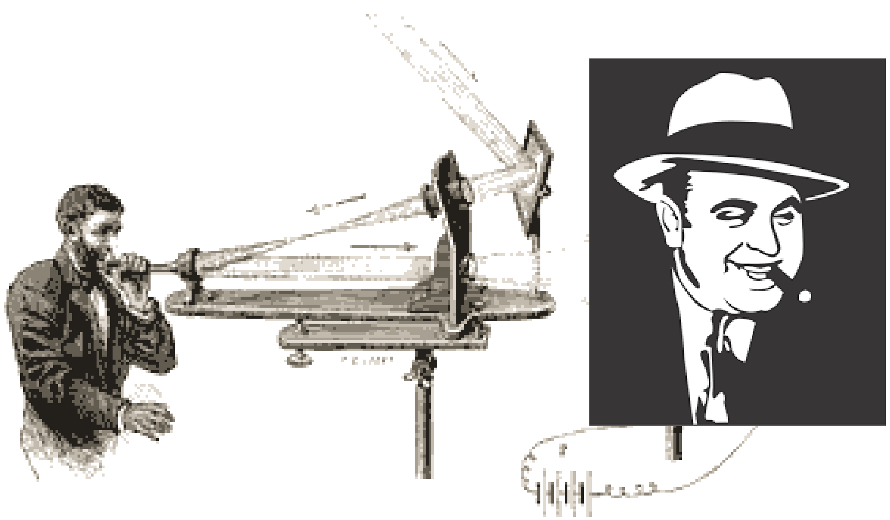

Alexander Graham Bell & Charles Sumner, 1880

Godfather of photoacoustics

KU LEUVEN

Photothermal and photoacoustic phenomena
⇒ optical, thermal and elastic properties

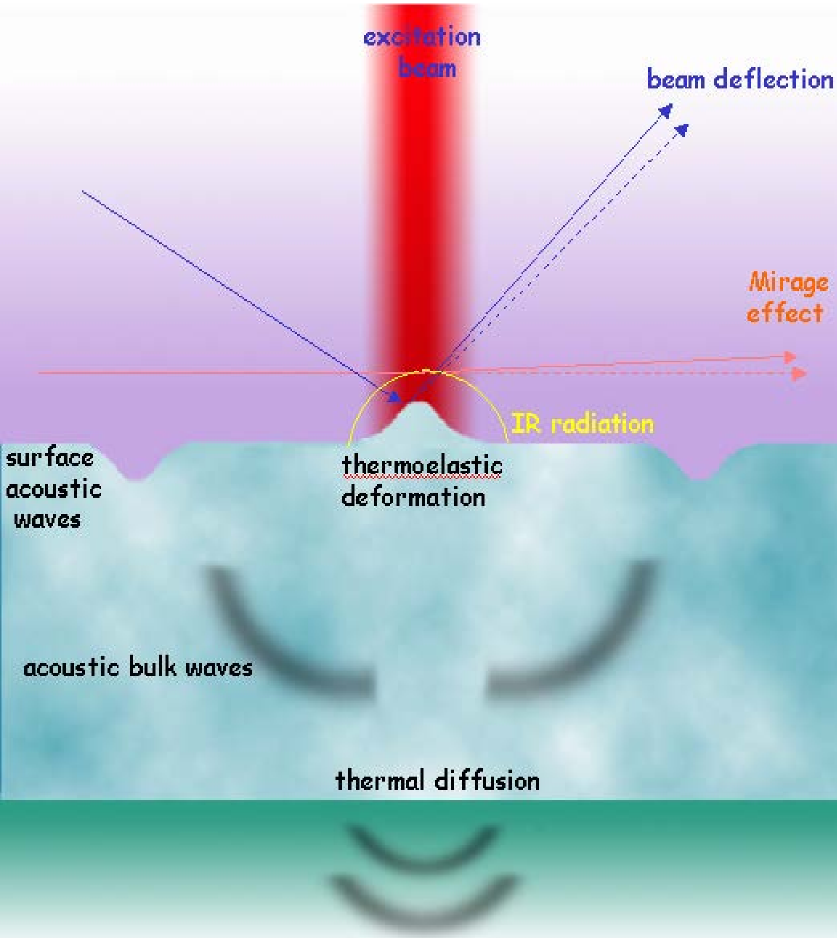

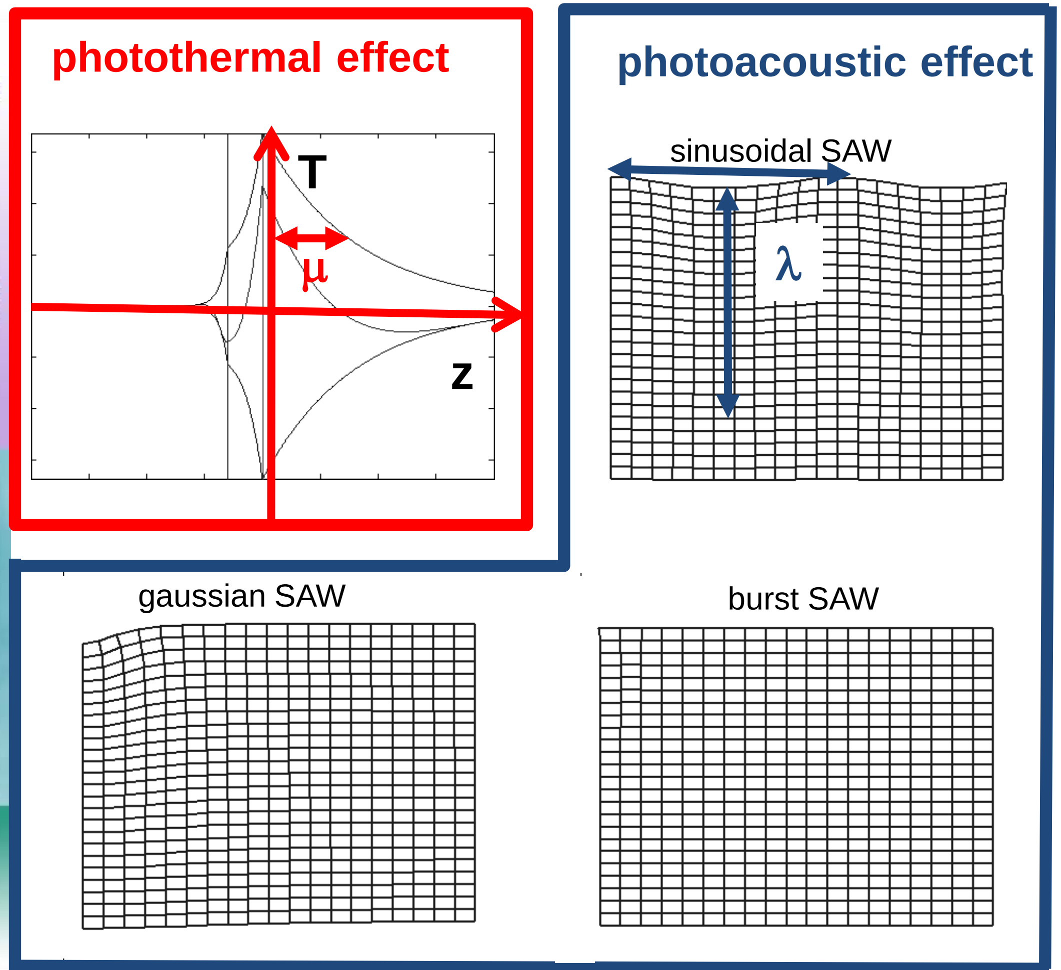

Photoacoustic tomography: optical information

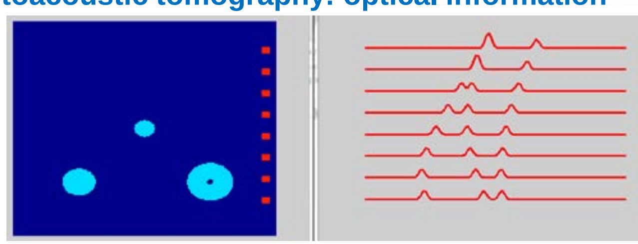

⇒ information on **transport properties**:
⇒ thermal diffusivity/diffusion length
& acoustic velocity and damping/wavelength

Overview

- Laser ultrasonics in layered samples: elastic/thermal depth information from dispersion
- Optical detection schemes
    - Michelson interferometer
    - Phase mask interferometer
    - Sagnac interferometer
    - Laser beam deflection
    - Speckle knife edge detection (SKED)
    - Laser Doppler vibrometry
    - Photorefractive interferometer
    - Modulated optical reflection
    - Brillouin oscillations
- Laser ultrasonics for material characterization: case studies
- Calculation of guided wave dispersion and photothermal and photoacoustic displacements
- Laser ultrasonics for defect detection and application for non-destructive testing

Laser ultrasonics on layered samples:

Elastic/thermal depth information
from dispersion

Laser ultrasonics on layered samples: elastic information from guided wave velocity dispersion

Rayleigh waves: wavelength dependent penetration depth

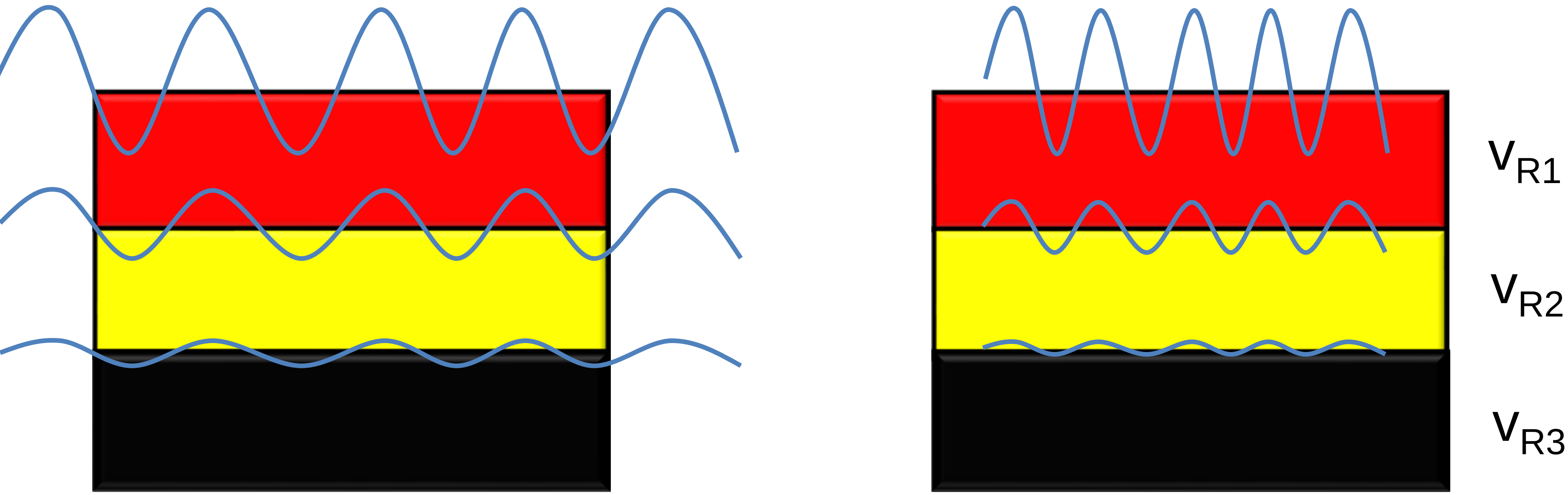

Laser ultrasonics on layered samples: elastic information from guided wave velocity dispersion

- Surface acoustic waves
  - Penetration depth ~λ
  - Multilayers: dispersion

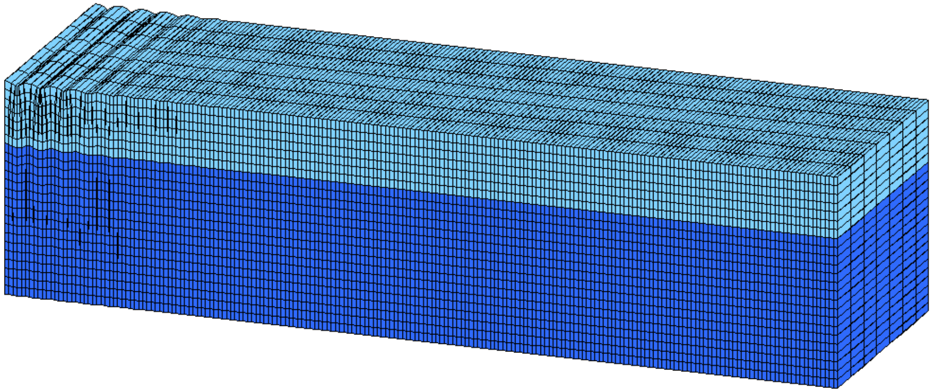

Dispersion curve:

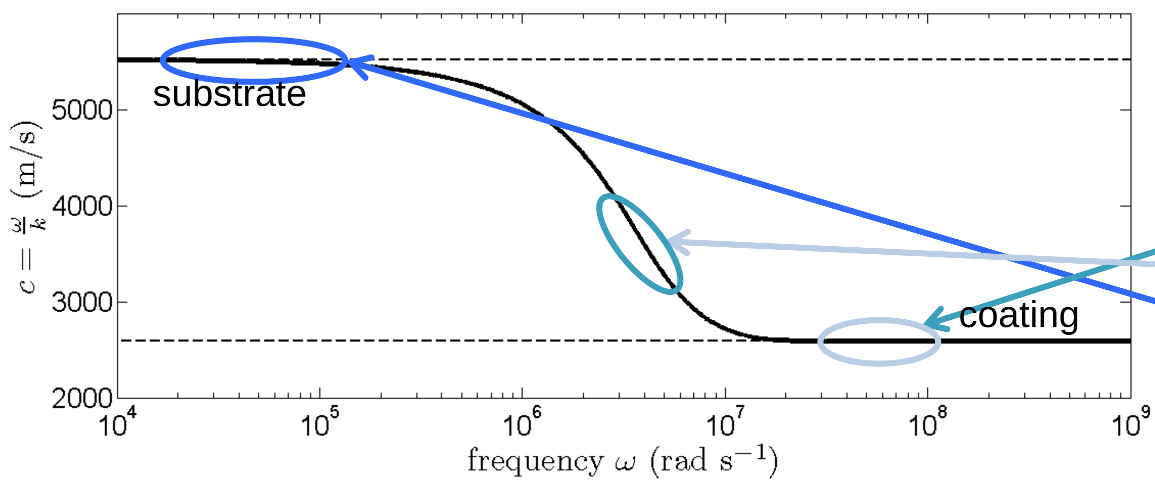

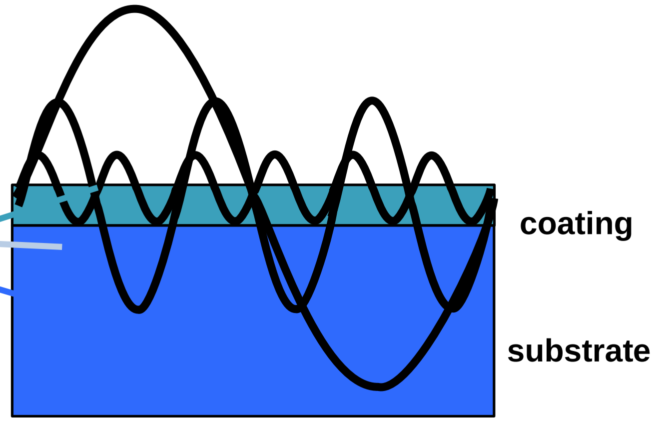

Photoacoustic characterization of elastic properties of (sub-)micron sub-surface layers

Rayleigh waves: wavelength dependent penetration depth

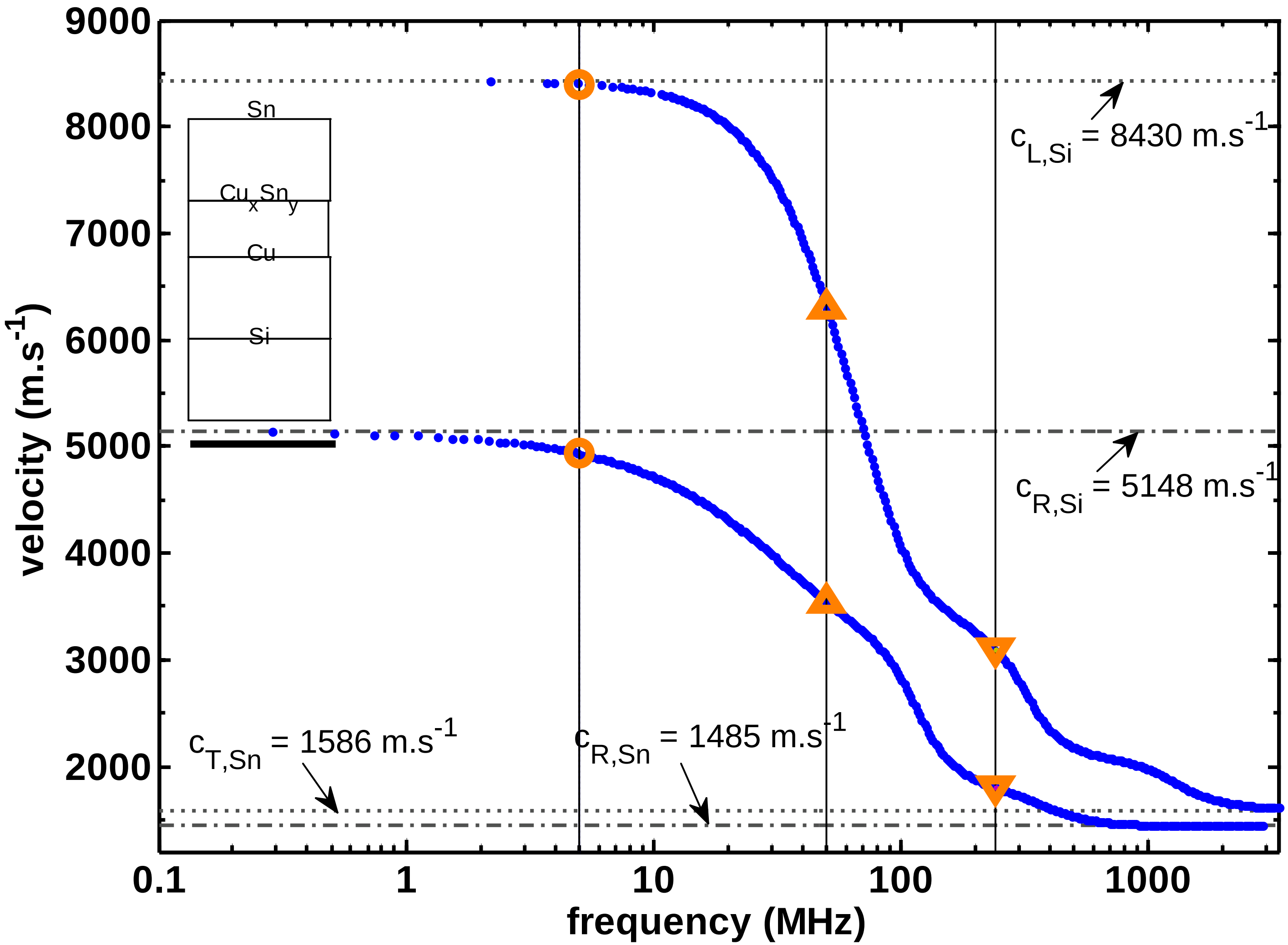

Multilayer sample

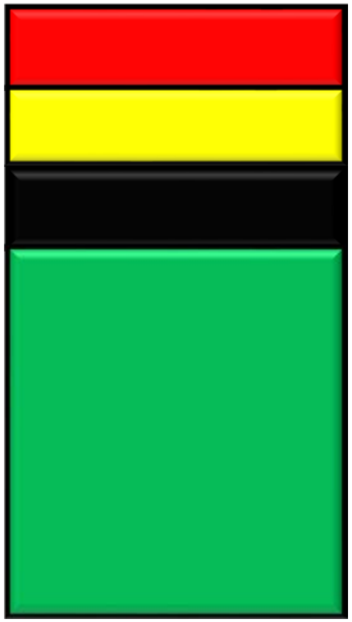

Photoacoustic characterization of elastic properties of (sub-)micron sub-surface layers

Rayleigh waves: wavelength dependent penetration depth

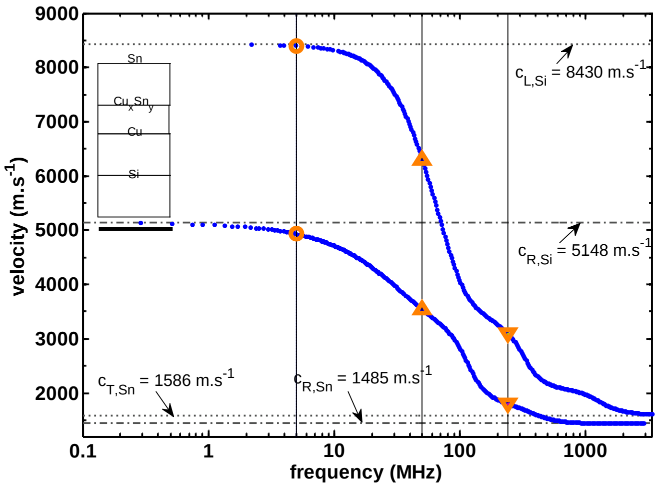

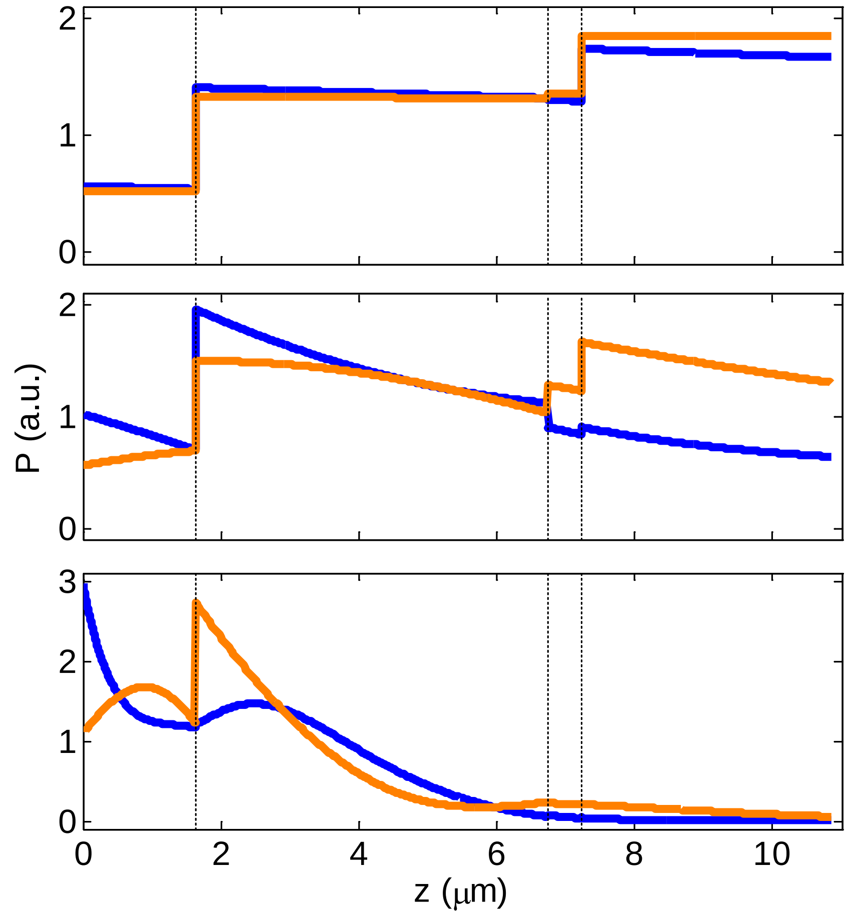

5 MHz

50 MHz

240 MHz

Rayleigh

Sezawa

KU LEUVEN

Photoacoustic characterization of elastic properties of free-standing films and plates: extraction of velocity dispersion

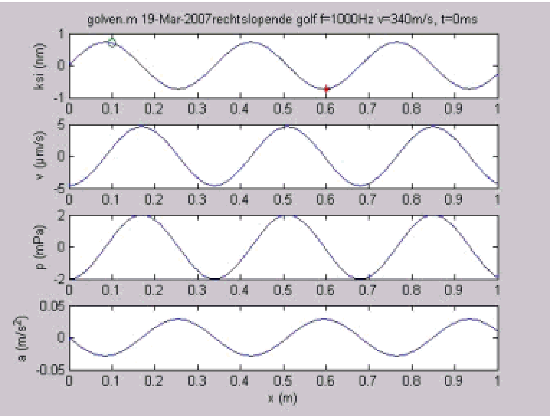

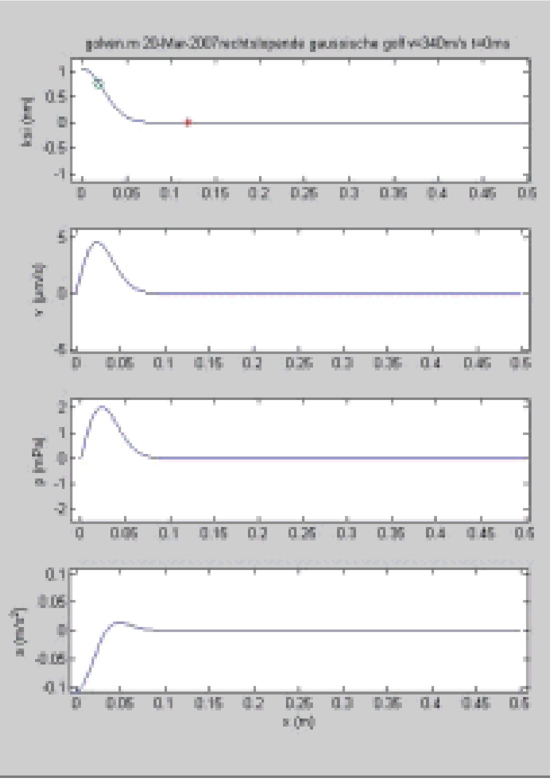

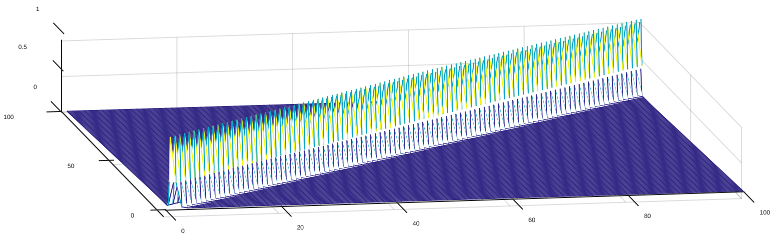

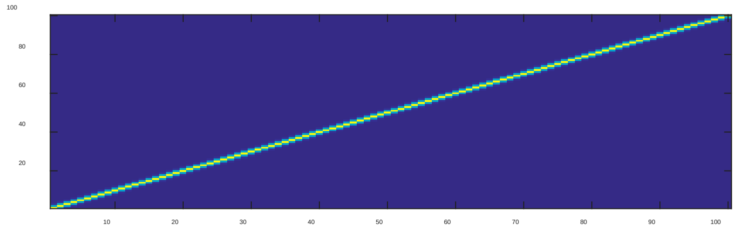

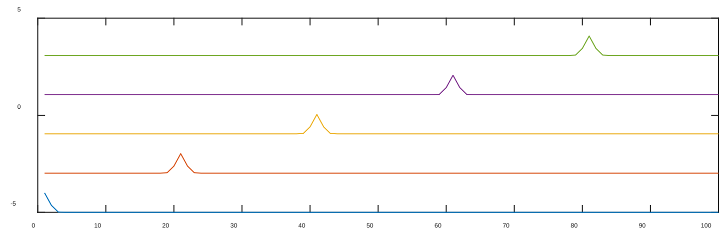

$$S(x,t) = S(x-ct)$$

$$= \int_{-\infty}^{+\infty} S(k)\exp(i\omega t - ikx)dk$$

with ω=kc

$$= \int_{-\infty}^{+\infty} dk \int_{-\infty}^{+\infty} \frac{d\omega}{2\pi} S(k,\omega)\delta(\omega - kc)\exp(i\omega t - ikx)$$

Photoacoustic characterization of elastic properties of free-standing films and plates: extraction of velocity dispersion

KU LEUVEN

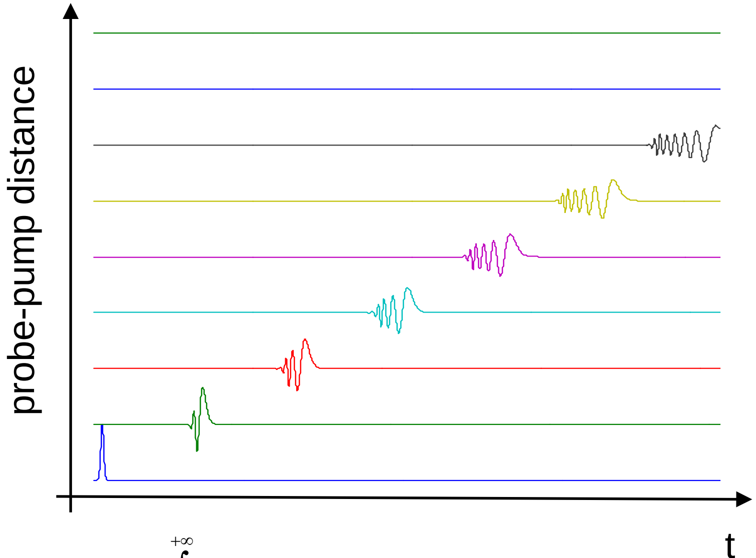

$$S(x,t) = \int_{-\infty}^{+\infty} S(k)\exp(i\omega t - ikx)dk \text{ with } \omega = \text{k c}(k)$$

$$= \int_{-\infty}^{+\infty} dk \int_{-\infty}^{+\infty} \frac{d\omega}{2\pi} S(k,\omega)\delta(\omega - kc(\omega))\exp(i\omega t - ikx)$$

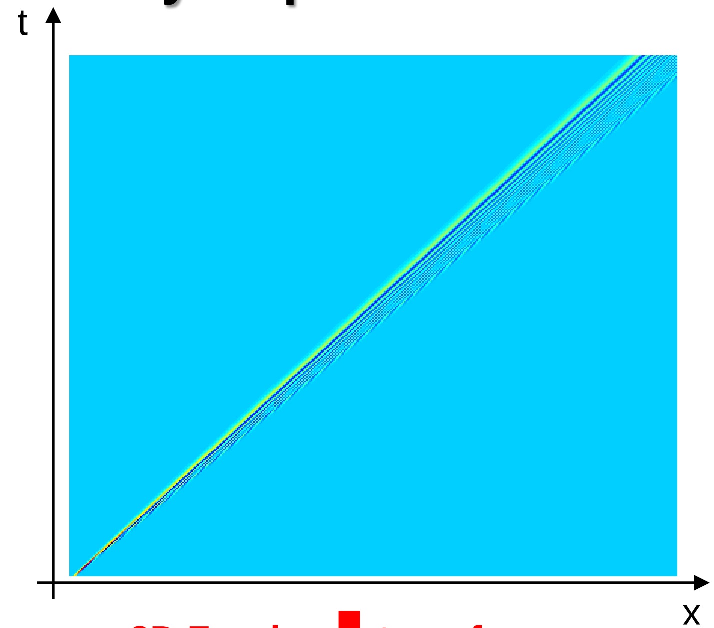

2D Fourier transform

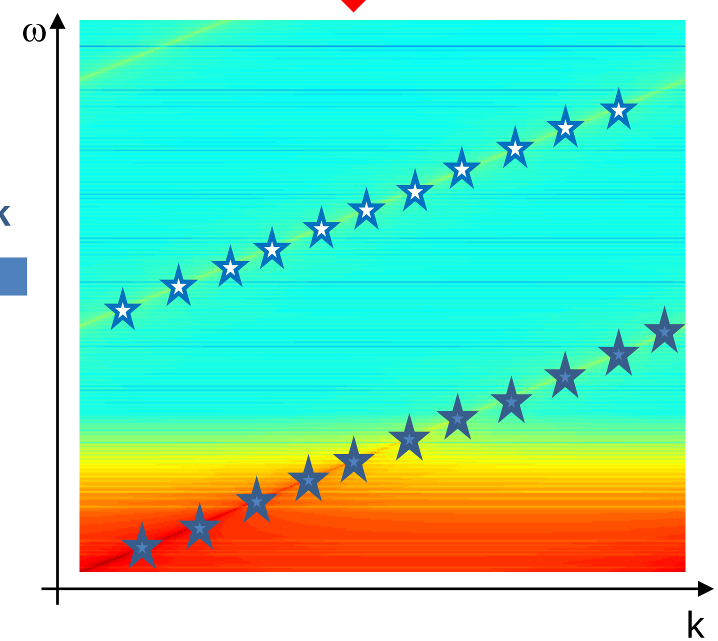

c=ω/k

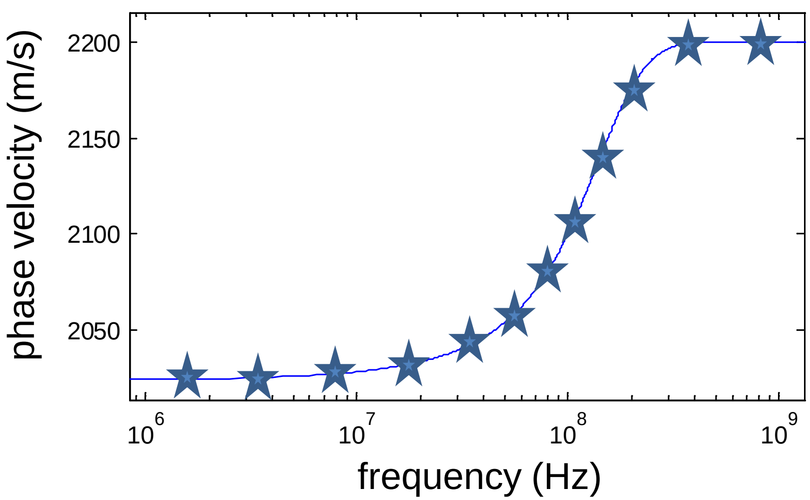

Photothermal characterization of thermal properties of free-standing films and plates: extraction of effective thermal diffusivity dispersion

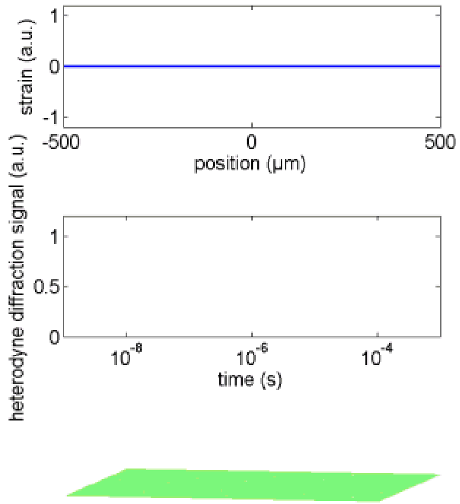

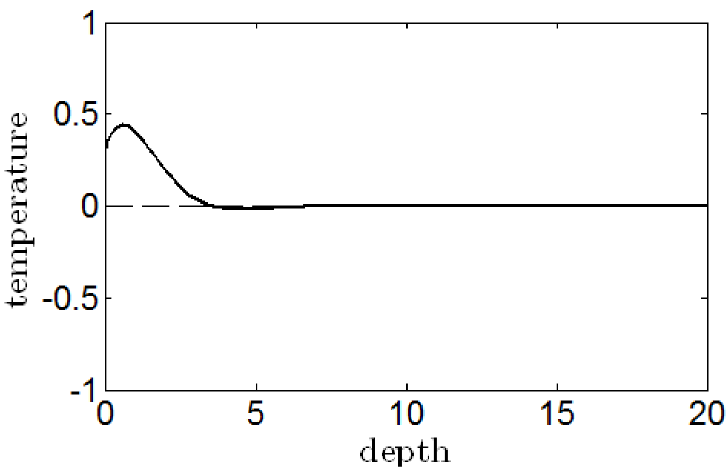

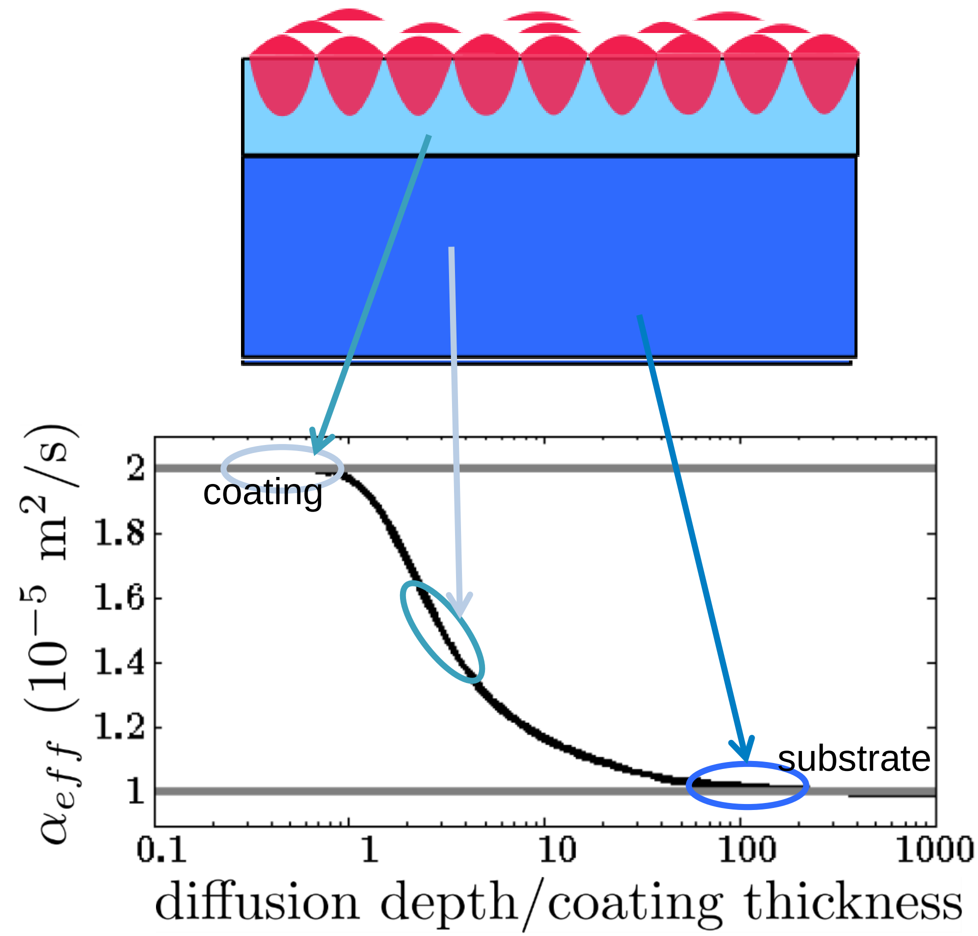

Optical detection schemes

Laser ultrasonics ⇒ detection schemes

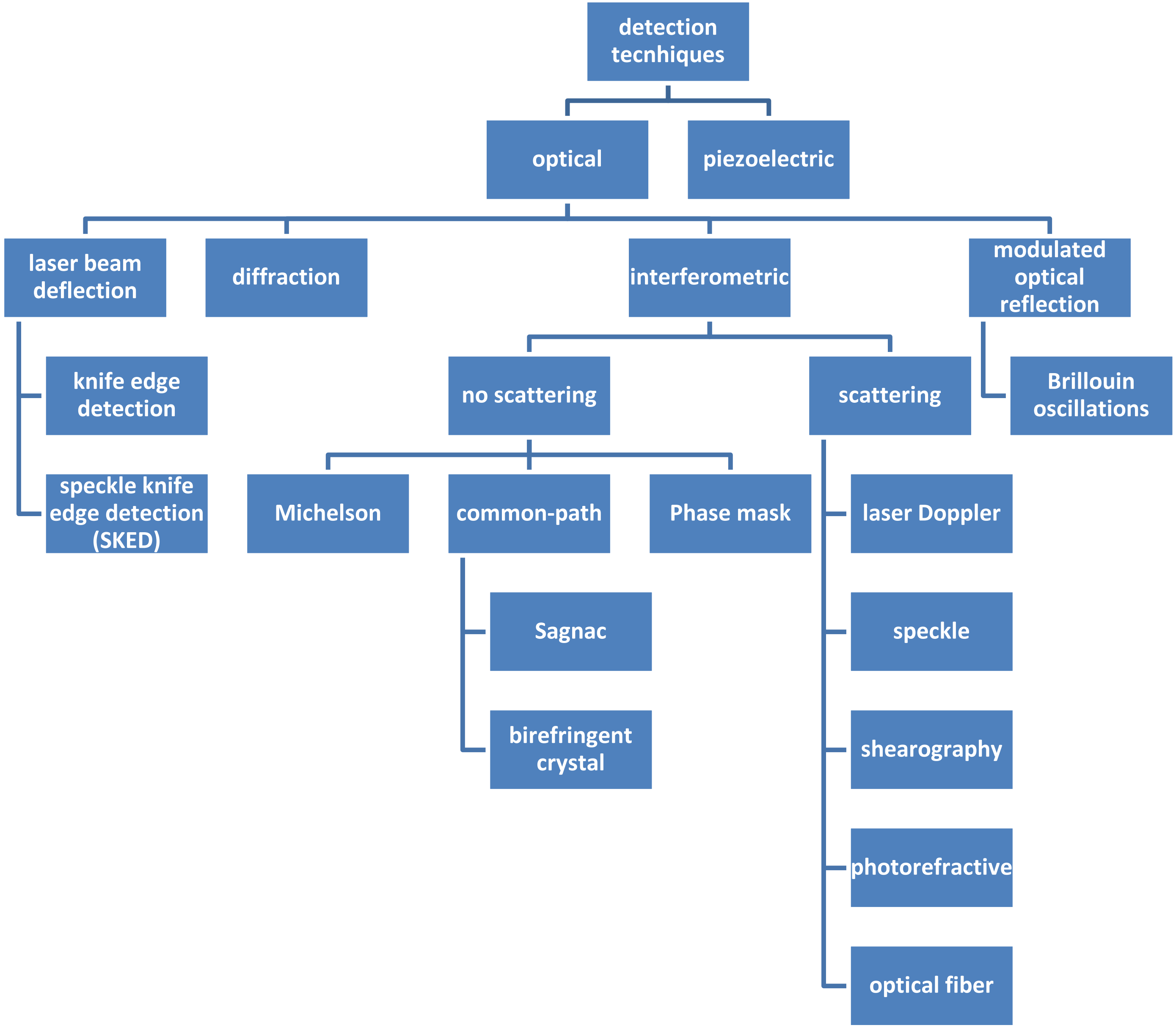

Laser ultrasonic detection schemes: laser beam deflection

Deflection displacement:
$\delta = \Delta\theta$
Relative differential intensity:
$\Delta I/I = \delta/\phi_2$
ϕ_2 is the diameter of the reflected beam at lens L_2
$\phi_2 = F_2/F_1\phi_1$
ϕ_1 is the diameter of the incoming beam at lens L_1

$$\frac{dI}{I} = \frac{2\int_0^{\xi} \exp\left(-\left(\frac{x}{\phi_2}\right)^2\right)dx}{\int_{-\infty}^{+\infty} \exp\left(-\left(\frac{x}{\phi_2}\right)^2\right)dx} \cong \frac{2\delta}{\phi_2\sqrt{\pi}} = O\left(\frac{\xi}{\phi_2}\right)$$

So that $\Delta I/I = \delta/\phi_2 = \Delta\theta\ F_1/\phi_1 = (\xi/w)(F_1/\phi_1)$

E.g.
$w = 10\ \mu m$, $F_1 = 50mm$, $\phi_1 = 5mm$
Displacement detection limit:
$\xi_{min} = (\Delta I/I)_{min}\ (F_1/\phi_1)^{-1}\ w = 10^{-10} w = 10^{-15}\ m(W/Hz)^{1/2}$

E.g.
300Hz bandwidth, 75μW probe laser power:
Typical light intensity change detection limit:
$10^{-9}(W/Hz)^{1/2}$
$\xi_{min,typ} = 2pm$

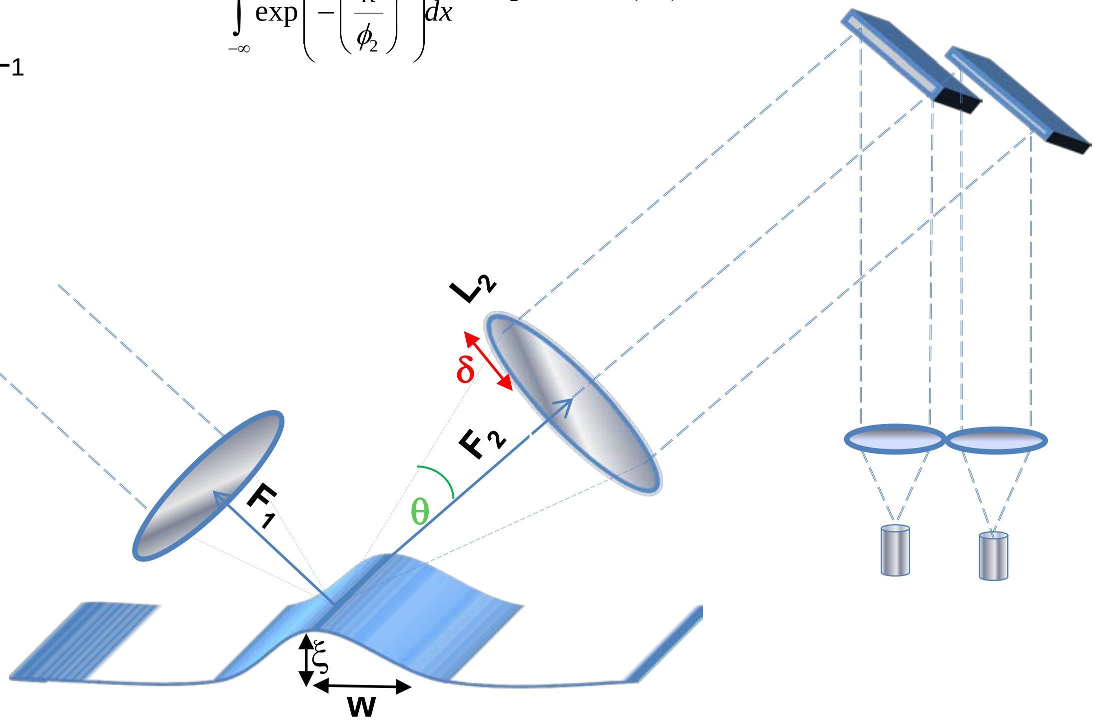

Deflection angle $\Delta\theta \cong \xi/w$ ~ spatial derivative of wave packet ~ high pass response

w = characteristic lateral dimension of wave packet
= displacement ξ or acoustic wavelength $\lambda_{acoustic}$

KU LEUVEN

Laser ultrasonic detection schemes: laser beam deflection

KU LEUVEN

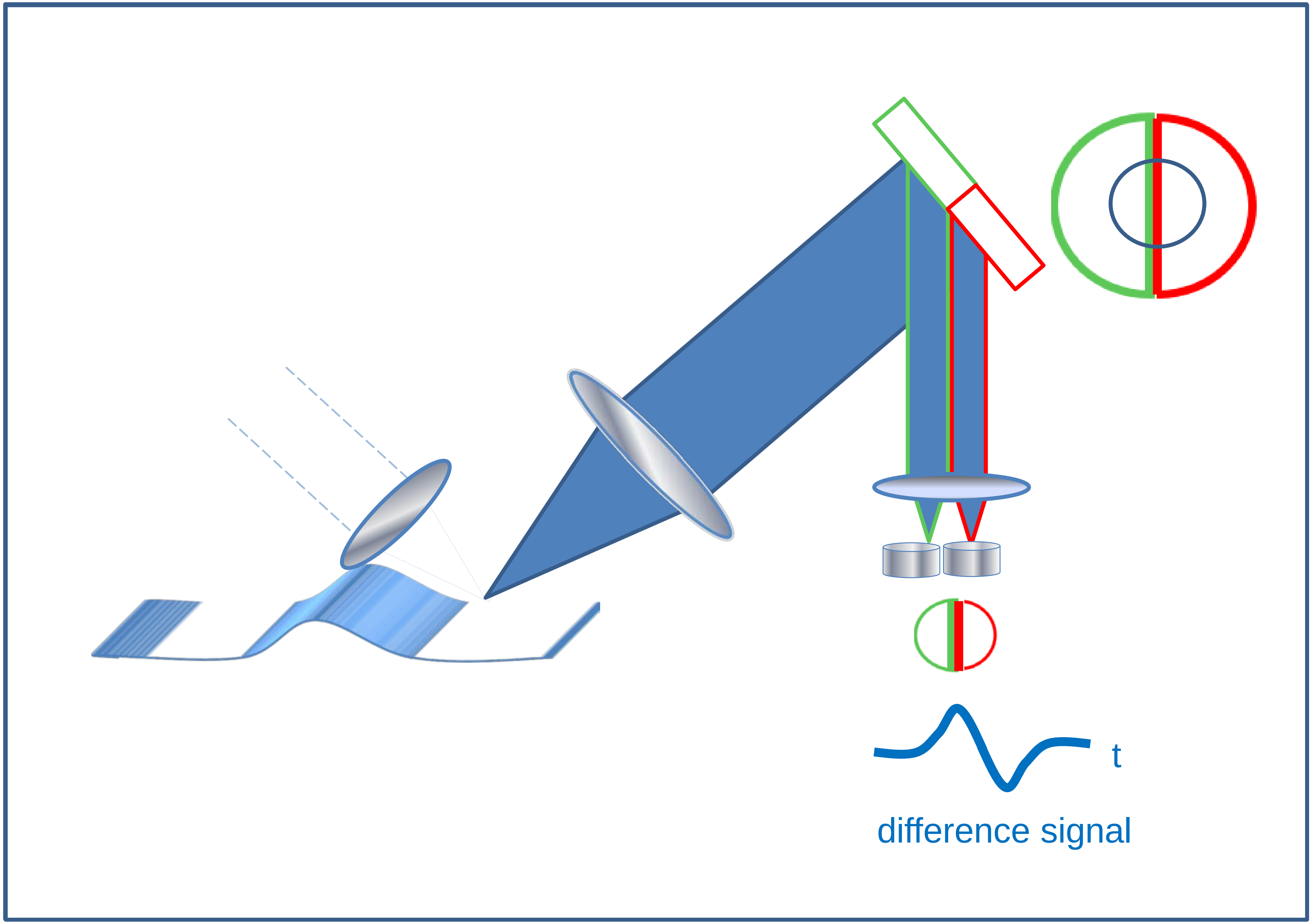

Laser ultrasonic detection schemes: speckle knife edge detector (SKED)

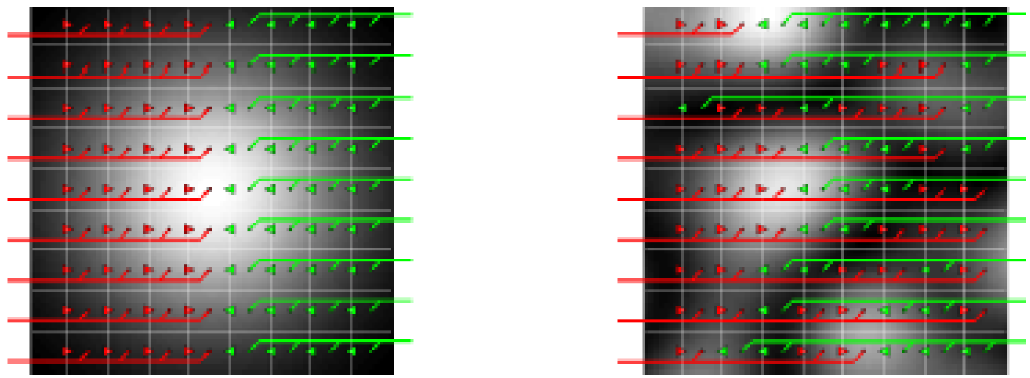

Figure 2. Schematic showing the operation of (left) the conventional knife edge detector, and (right) the speckle knife edge detector. The intensity gradient between adjacent pixels defines the output of one of those pixels.

3rd International Symposium on Laser Ultrasonics and Advanced Sensing IOP Publishing
Journal of Physics: Conference Series **520** (2014) 012004 doi:10.1088/1742-6596/520/1/012004

The SKED: speckle knife edge detector

SD Sharples, RA Light, SO Achamfuo-Yeboah, M Clark and MG Somekh
Electical Systems & Optics Research Division, Faculty of Engineering, University of Nottingham, University Park, Nottingham NG7 2RD, UK
E-mail: steve.sharples@nottingham.ac.uk

Abstract.
The knife edge detector—also known as optical beam deflection—is a simple and robust method of detecting ultrasonic waves using a laser. It is particularly suitable for detection of high frequency surface acoustic waves as the response is proportional to variation of the local tilt of the surface. In the case of a specular reflection of the incident laser beam from a smooth surface, any lateral movement of the reflected beam caused by the ultrasonic waves is easily detected by a pair of photodiodes. The major disadvantage of the knife edge detector is that it does not cope well with optically rough surfaces, those that give a speckled reflection. The optical speckles from a rough surface adversely affect the efficiency of the knife edge detector, because 'dark' speckles move synchronously with 'bright' speckles, and their contributions to the ultrasonic signal cancel each other out. We have developed a new self-adapting sensor which can cope with the optical speckles reflected from a rough surface. It is inelegantly called the SKED—speckle knife edge detector—and like its smooth surface namesake it is simple, cheap, compact, and robust. We describe the theory of its operation, and present preliminary experimental results validating the overall concept and the operation of the prototype device.

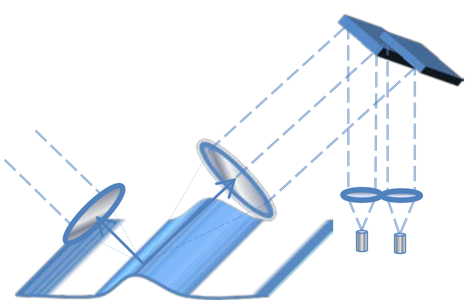

Pixel signal sign assignment based on steady state light pattern
32 x 32 photodiode pixel array

KU LEUVEN

Laser ultrasonic detection schemes: Michelson interferometer

- ☺ **NON-CONTACT**
- ☺ **FAST**
- ☺ **SENSITIVE**

$$I(t) = I_1 + I_2 + 2\sqrt{I_1 I_2}\cos(\Delta\phi)$$

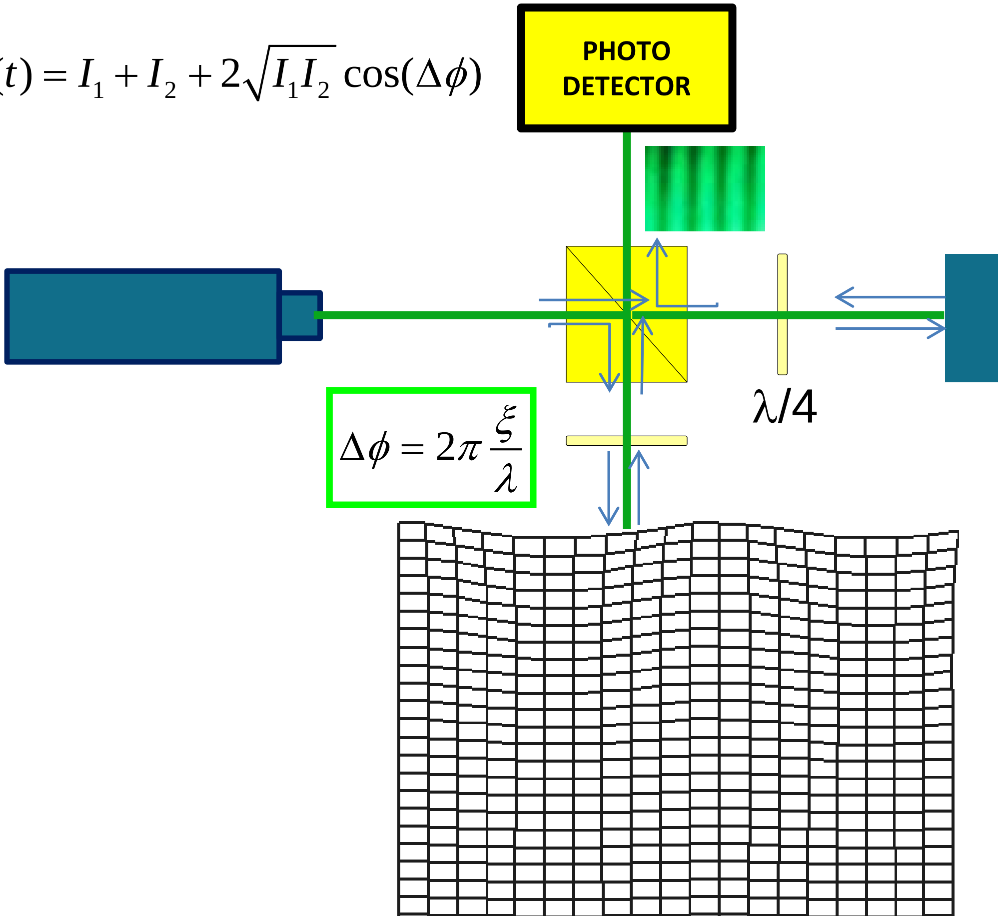

$$\boxed{\Delta\phi = 2\pi\frac{\xi}{\lambda}}$$

$$\frac{\partial V_{sig}}{\partial \xi} = -(V_{max} - V_{min})\frac{\pi}{\lambda}\sin(2\pi\xi/\lambda)$$

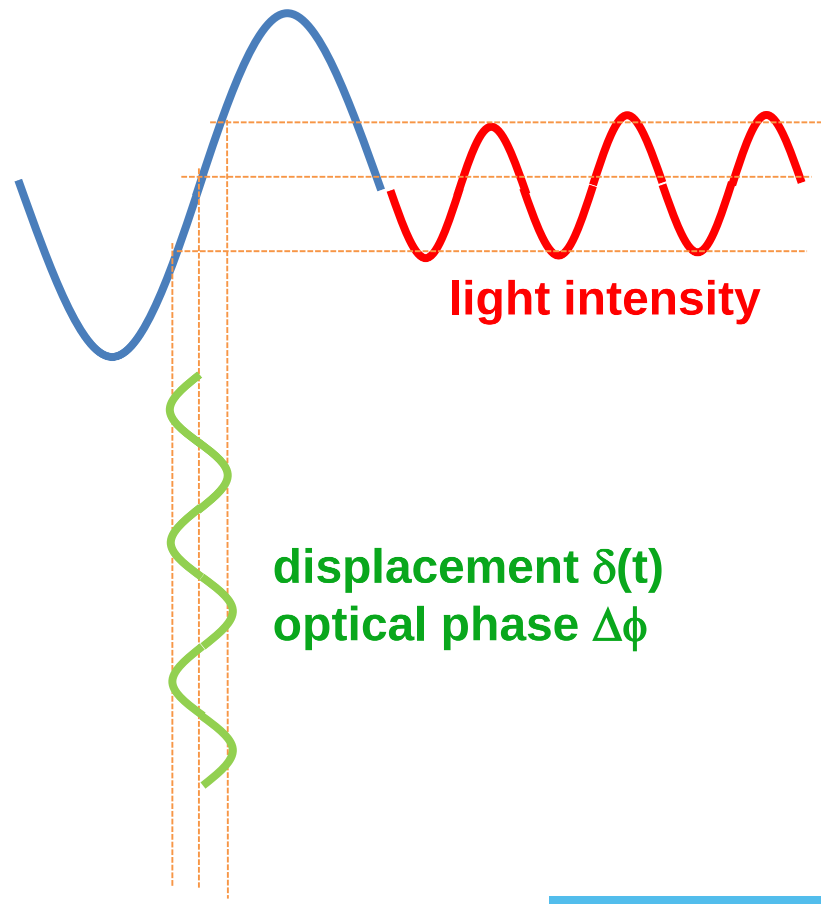

Laser ultrasonic detection schemes:
phase mask interferometer

Transmission mode

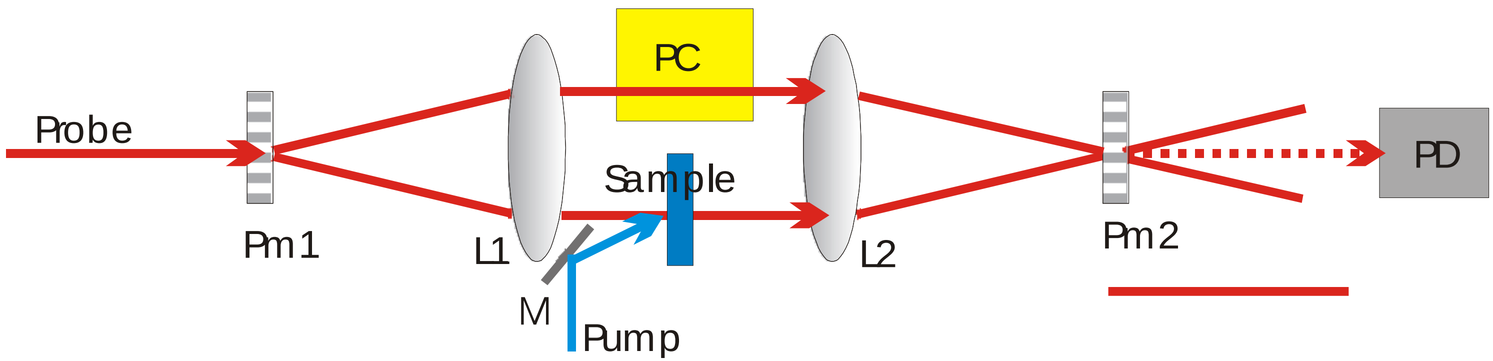

Reflection mode

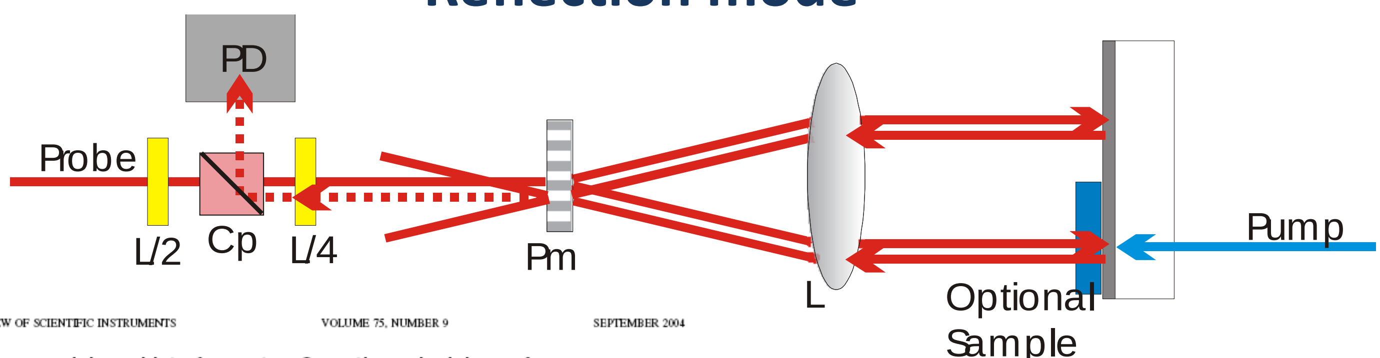

REVIEW OF SCIENTIFIC INSTRUMENTS VOLUME 75, NUMBER 9 SEPTEMBER 2004

Phase mask based interferometer: Operation principle, performance, and application to thermoelastic phenomena

C. Glorieux[a)]
Laboratorium voor Akoestiek en Thermische Fysica, Katholieke Universiteit Leuven, Celestijnenlaan 200D, B-3001 Leuven, Belgium

J. D. Beers
Department of Chemistry, Massachusetts Institute of Technology, 77 Massachusetts Avenue, Cambridge, Massachusetts 02139

E. H. Bentefour and K. Van de Rostyne
Laboratorium voor Akoestiek en Thermische Fysica, Katholieke Universiteit Leuven, Celestijnenlaan 200D, B-3001 Leuven, Belgium

Keith A. Nelson
Department of Chemistry, Massachusetts Institute of Technology, 77 Massachusetts Avenue, Cambridge, Massachusetts 02139

(Received 31 December 2003; accepted 14 June 2004)

A simple, versatile, sensitive optical interferometer based on diffractive optics is presented. The absence of a need for active stabilization, and a compact common-path design requiring two optical elements, make the interferometer ideal for time-resolved measurements in the picosecond through millisecond regimes. Its performance is characterized quantitatively, and its utility for local detection and scanning as well as spatially resolved imaging of thermoelastically induced strain is demonstrated. © *2004 American Institute of Physics.* [DOI: 10.1063/1.1781386]

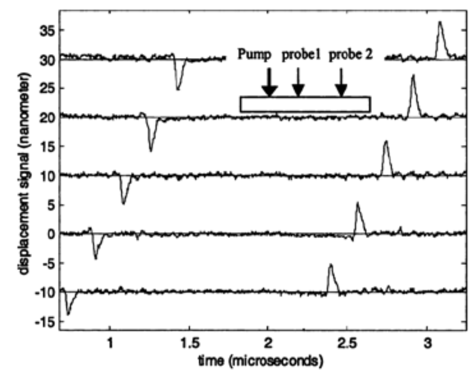

FIG. 10. Signal traces of SAWs on a thick aluminium sample, thermoelastically generated by a picosecond laser pulse cylindrically focused to a line source. The excitation beam was moved over a distance of 2 mm in steps of 0.5 mm (see inset), thus changing the pump-probe distance and the times of arrival at probe1 and probe2. The signals were recorded with a reflection-mode grating interferometer as in Fig. 2(b). For every signal trace, first, the left-going wave arrives at the nearest probe arm (negative signal excursion), then the right-going wave arrives at the second probe arm (positive signal excursion).

Laser ultrasonic detection schemes:
common path interferometer:
Sagnac configuration

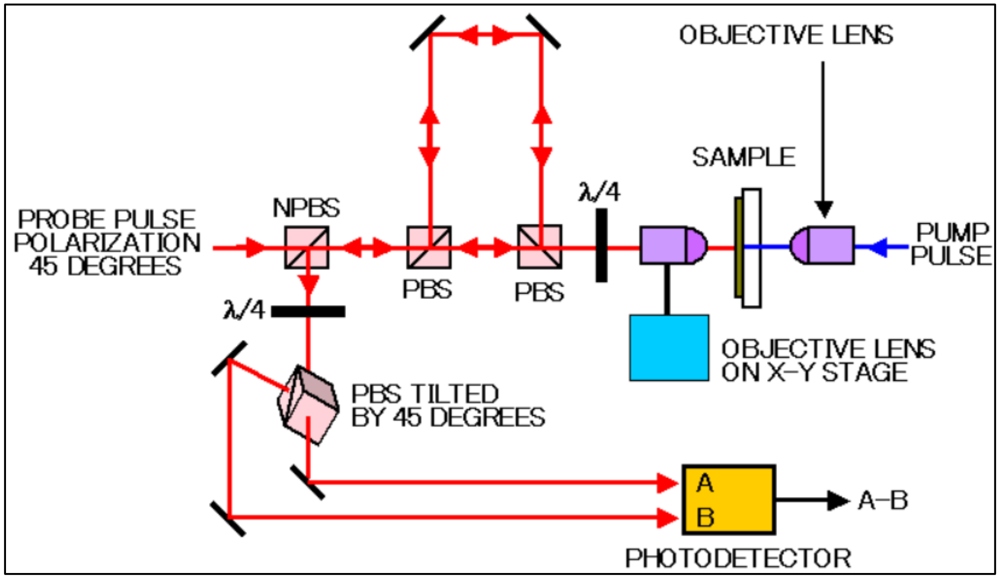

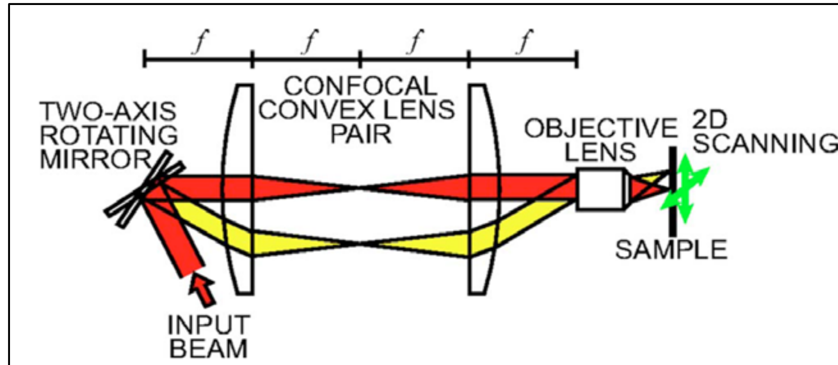

FIG. 4. (Color online) Schematic diagram of the 4f lens system. Examples of optical beam paths for two different angular positions of the rotating mirror are illustrated. The axis of rotation of the mirror is on the optical axis.

http://kino-ap.eng.hokudai.ac.jp/interferometer.html

REVIEW OF SCIENTIFIC INSTRUMENTS 77, 043713 (2006)

Scanning ultrafast Sagnac interferometry for imaging two-dimensional surface wave propagation

Takehiro Tachizaki, Toshihiro Muroya, and Osamu Matsuda[a)]
Department of Applied Physics, Graduate School of Engineering, Hokkaido University, Sapporo 060-8628, Japan

Yoshihiro Sugawara
School of Physics and Astronomy, University of Southampton, Southampton SO17 1BJ, United Kingdom

David H. Hurley
Idaho National Laboratory, Idaho Falls, Idaho 83415-2209

Oliver B. Wright
Department of Applied Physics, Graduate School of Engineering, Hokkaido University, Sapporo 060-8628, Japan

(Received 10 February 2006; accepted 16 March 2006; published online 24 April 2006)

We describe an improved two-dimensional optical scanning technique combined with an ultrafast Sagnac interferometer for delayed-probe imaging of surface wave propagation. We demonstrate the operation of this system, which involves the use of a single focusing objective, by monitoring surface acoustic wave propagation on opaque substrates with picosecond temporal and micron lateral resolutions. An improvement in the lateral resolution by a factor of 3 is achieved in comparison with previous setups for similar samples. © *2006 American Institute of Physics.* [DOI: 10.1063/1.2194518]

September 15, 1999 / Vol. 24, No. 18 / OPTICS LETTERS 1305

Detection of ultrafast phenomena by use of a modified Sagnac interferometer

David H. Hurley and Oliver B. Wright
Department of Applied Physics, Faculty of Engineering, Hokkaido University, Sapporo 060-8628, Japan

Received April 12, 1999

We describe a time-division interferometer based on the Sagnac geometry for monitoring ultrafast changes in the real and the imaginary components of the refractive index as well as phase changes that are due to surface displacement. Particular advantages of this interferometer are its simple common-path design and operation at normal incidence with a microscope objective for both pumping and probing. Operation is demonstrated by detection of temperature changes and coherent phonon generation in a gold film. © 1999 Optical Society of America

OCIS codes: 320.7130, 120.3180, 320.7120.

Laser ultrasonic detection schemes: common path interferometer: time delay by birefringent crystal

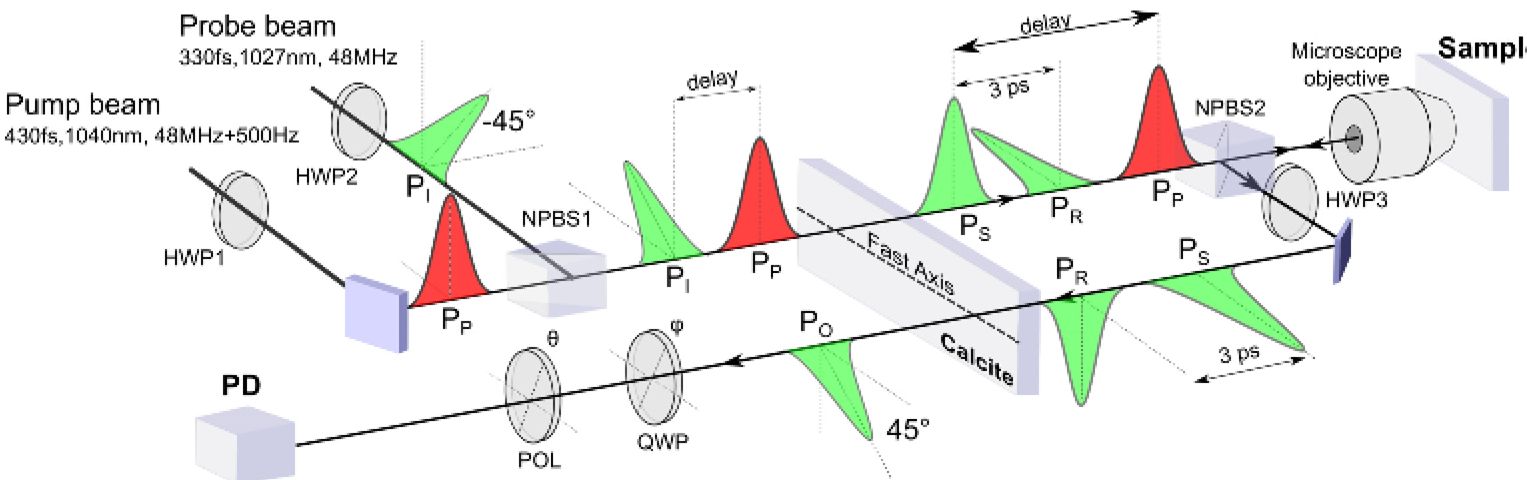

Fig. 1. Scheme of the in-line femtosecond common-path interferometer coupled to an ASOPS pump-probe experiment. HWP1 to HWP3: half-wave plates, NPBS1 and NPBS2: non-polarizing beam-splitters, QWP: quarter-wave plate, Pol: polarizer, P_P: pump pulse, P_I: pulse at the input of the interferometer, P_O: pulse at the output of the interferometer, P_S: probe pulse, P_R: reference pulse. The time zero is defined as the overlap between the pump and the probe pulses. Angles are given relatively to the fast optical axis of the birefringent calcite crystal. See text for a detailed description.

In-line femtosecond common-path interferometer in reflection mode

J. Chandezon,[1,2] J.-M. Rampnoux,[2] S. Dilhaire,[2] B. Audoin,[1] and Y. Guillet[1,*]

[1]Univ. Bordeaux, I2M, UMR 5295, F-33405 Talence, France
[2]Univ. Bordeaux, LOMA, UMR 5798, F-33405 Talence, France

Received 1 Sep 2015; revised 1 Oct 2015; accepted 1 Oct 2015; published 5 Oct 2015
19 Oct 2015 | Vol. 23, No. 21 | DOI:10.1364/OE.23.027011 | OPTICS EXPRESS 27011

Laser ultrasonic detection schemes: laser Doppler vibrometry

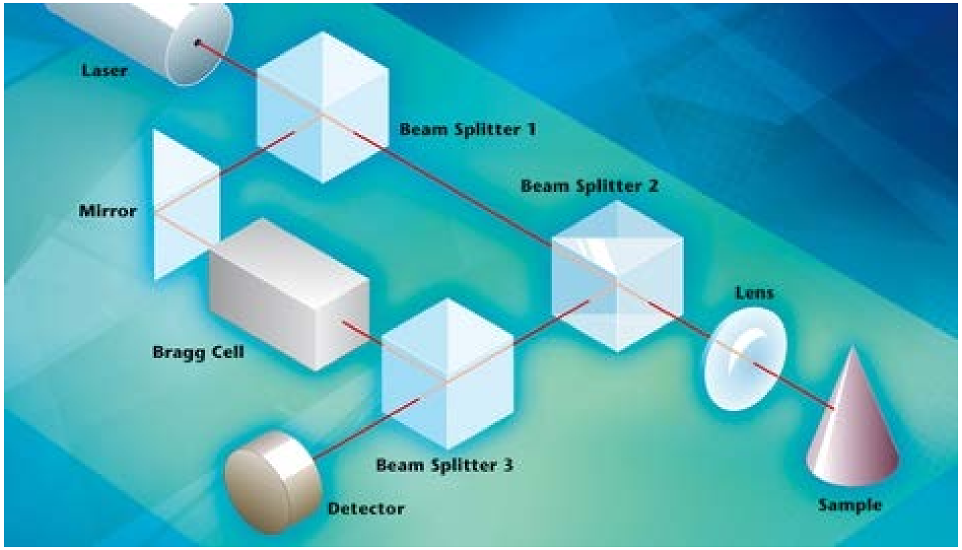

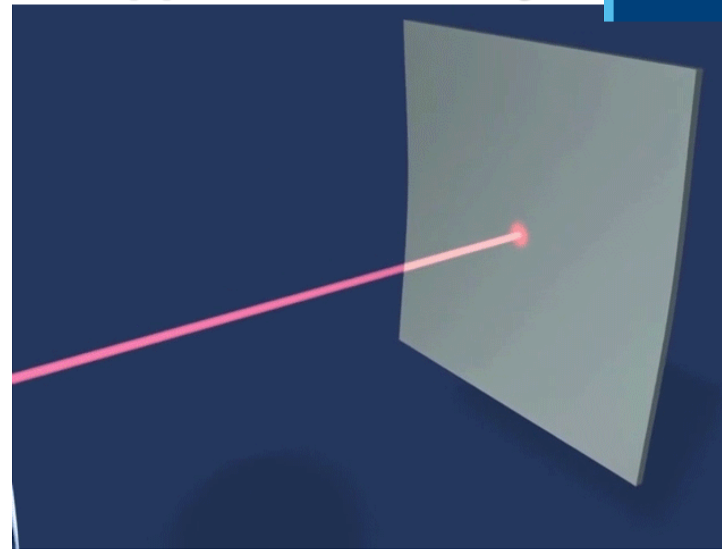

- $I_{tot} = E_r(t)^2 + E_s(t)^2 + 2 * |E_r(t)| * |E_s(t)| * \cos(\varphi)$
- with $\varphi = k * \Delta x = 2\pi\Delta x/\lambda$
- $I_{tot} = E_r(t)^2 + E_s(t)^2 + 2 * |E_r(t)| * |E_s(t)| * \cos\left[\frac{2\pi(r_r - r_s)}{\lambda}\right]$
- $I_{tot} = I_r + I_s + 2 * \sqrt{I_1 I_2}\cos\left[\frac{2\pi(r_r - r_s)}{\lambda}\right]$

$$\cos\left[\frac{2\pi(r_r - r_s)}{\lambda}\right] = \cos[(\omega_r - \omega_s) * t] = \cos[(\omega_0 + \omega_{AOM} - \omega_o - \Delta\omega_{sample}) * t]$$

$$\cos\left[\frac{2\pi(r_r - r_s)}{\lambda}\right] = \cos[(\omega_{AOM} - \Delta\omega_{sample}) * t]$$

$$\boxed{I_{tot} = I_r + I_s + 2 * \sqrt{I_1 I_2}\cos[(\omega_{AOM} - \Delta\omega_{sample}) * t]}$$

detected by photodetector

Doppler effect

$$\Delta\omega_{sample}(t) = (\omega_0 + \omega_{AOM})\frac{v_{sample}(t)}{c}$$

Phase locked loop PLL-detector

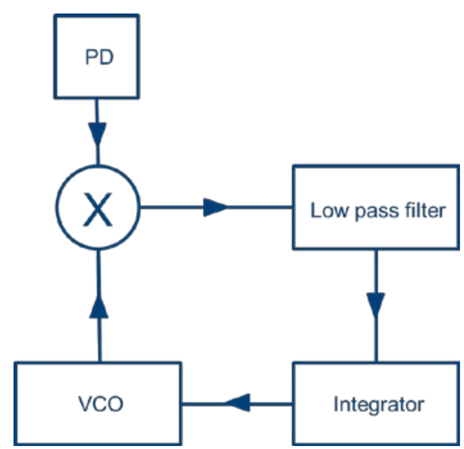

Laser ultrasonic detection schemes: Fabry-Perot interferometer

KU LEUVEN

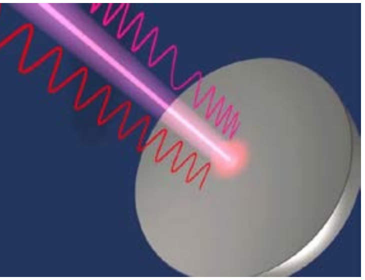

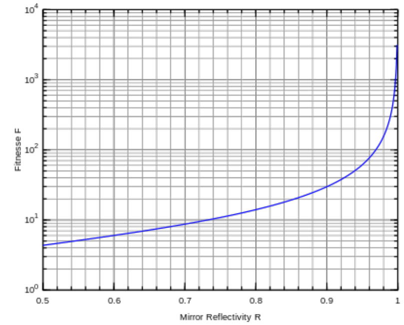

$$I_{transmitted} = I_0 \frac{1}{1 + F\sin^2(\Delta\phi_{etalon}/2)}$$

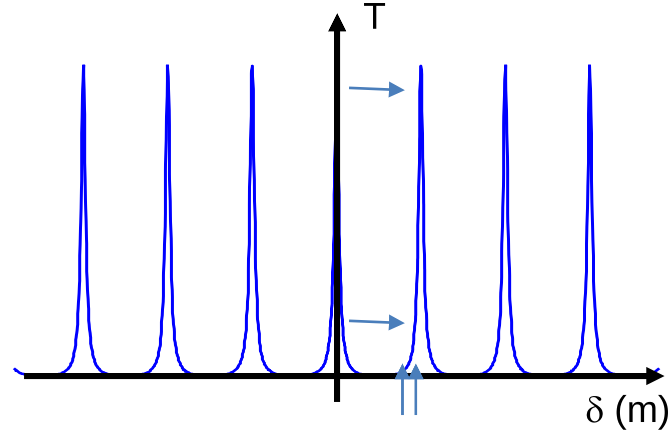

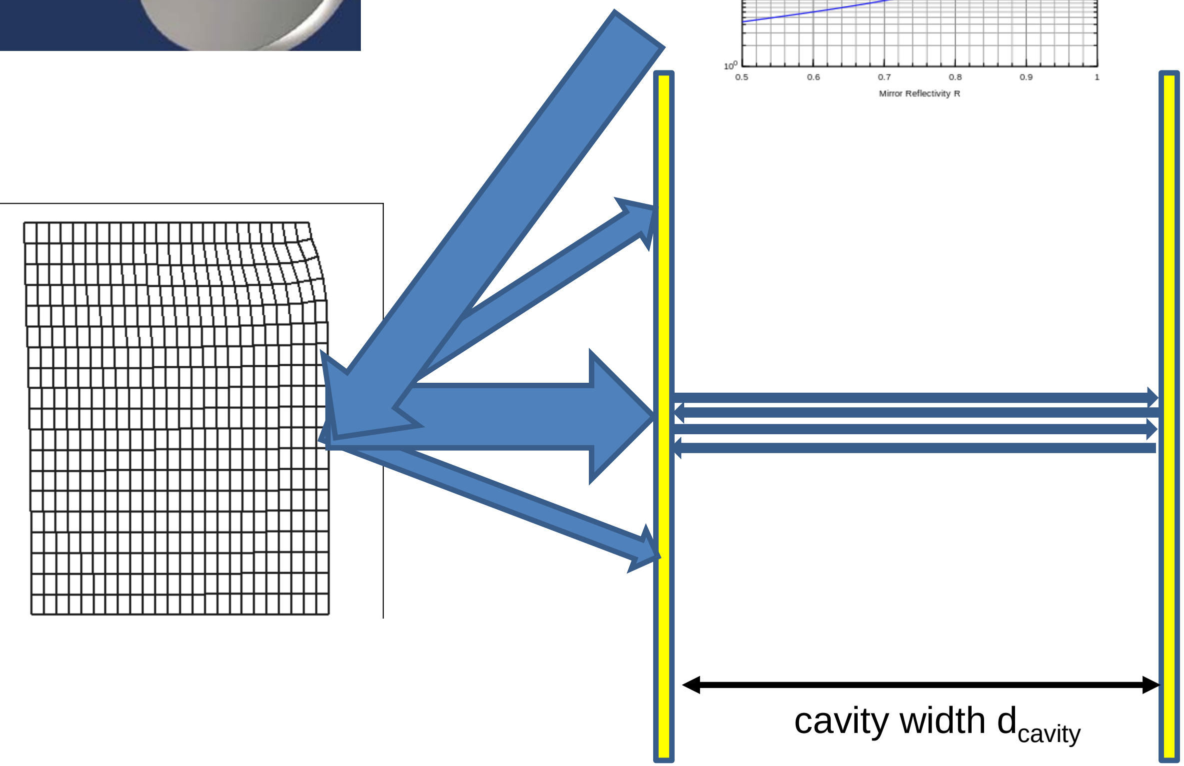

$$I_{reflected} = I_0 - I_0 \frac{1}{1 + F\sin^2(\Delta\phi_{etalon}/2)}$$

$$= I_0 \frac{F\sin^2(\Delta\phi_{etalon}/2)}{1 + F\sin^2(\Delta\phi_{etalon}/2)}$$

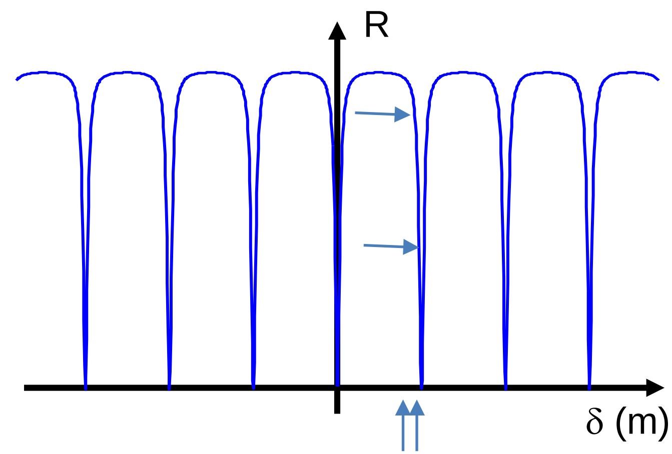

R: mirror reflectivity
$F=4R/(1-R)^2$: Finesse
$\Delta\phi_{etalon}=2\pi\Delta(\xi/\lambda_{optical})$
$\Delta\lambda_{optical}/\lambda_{0,optical}=d\xi/dt/c$

Cavity resonance time:
$\tau_{cavity} \sim Fd_{cavity}/c$
e.g. $d_{cavity=}10$mm, F=100:
bandwidth $\Delta f=\tau_{cavity}^{-1}=300$MHz

Laser ultrasonic detection schemes:
broadband ←→ narrowband excitation

Broadband

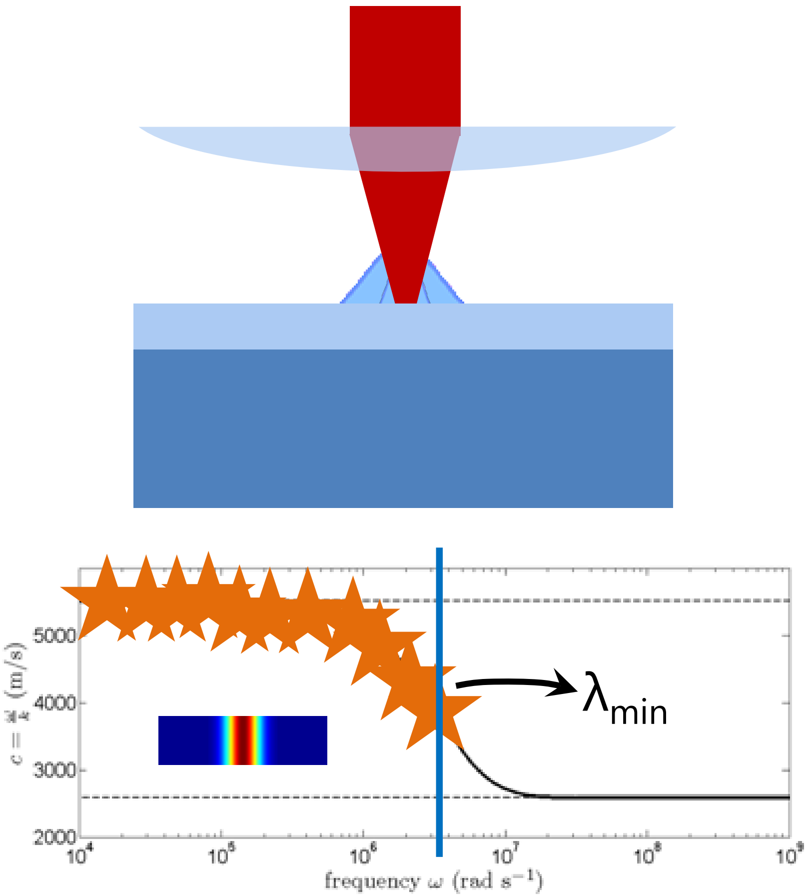

Narrowband

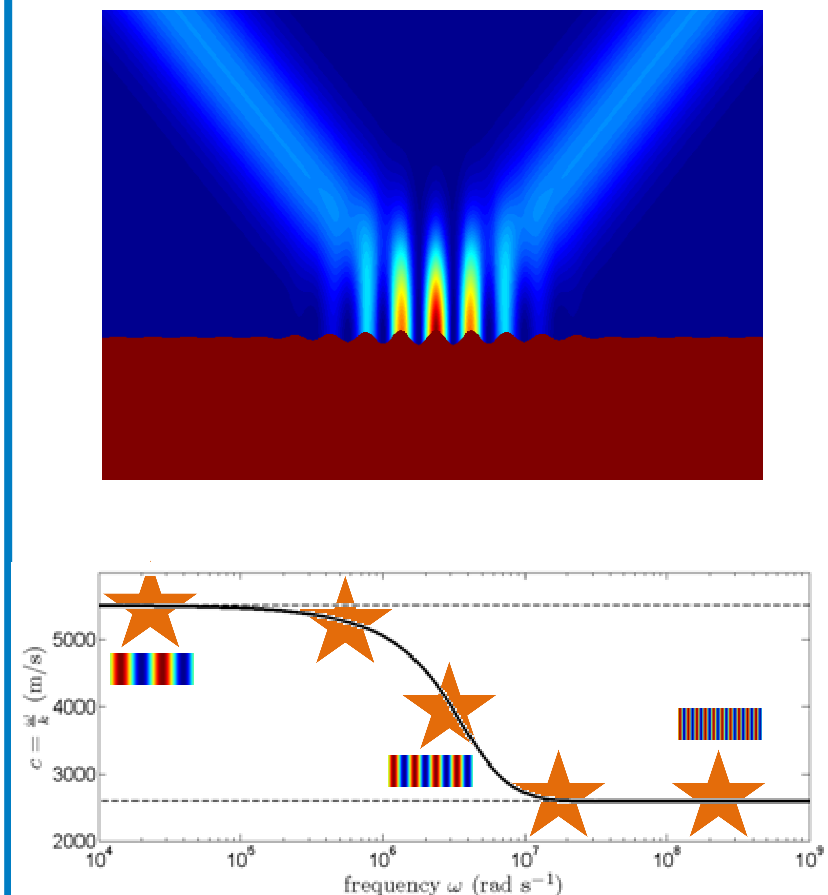

KU LEUVEN

Laser ultrasonic detection schemes: transient grating excitation

Heterodyne diffraction configuration

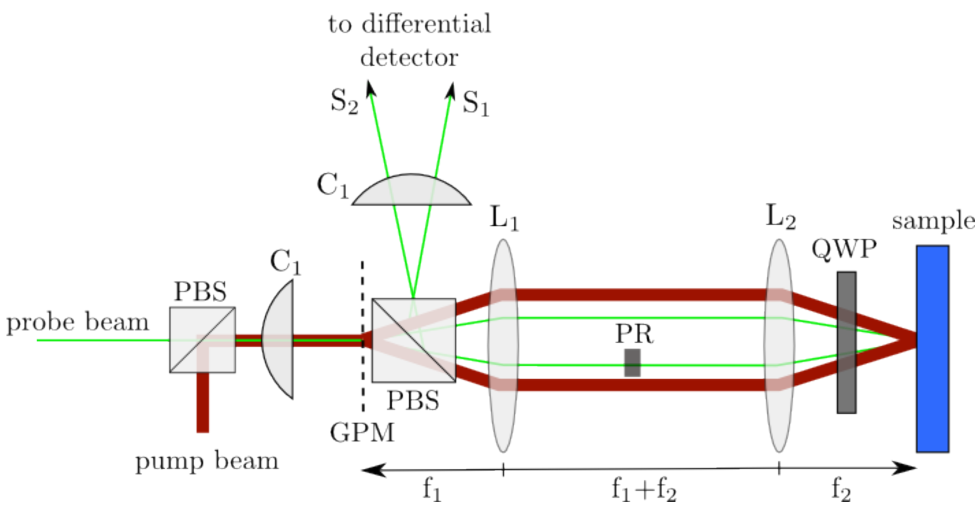

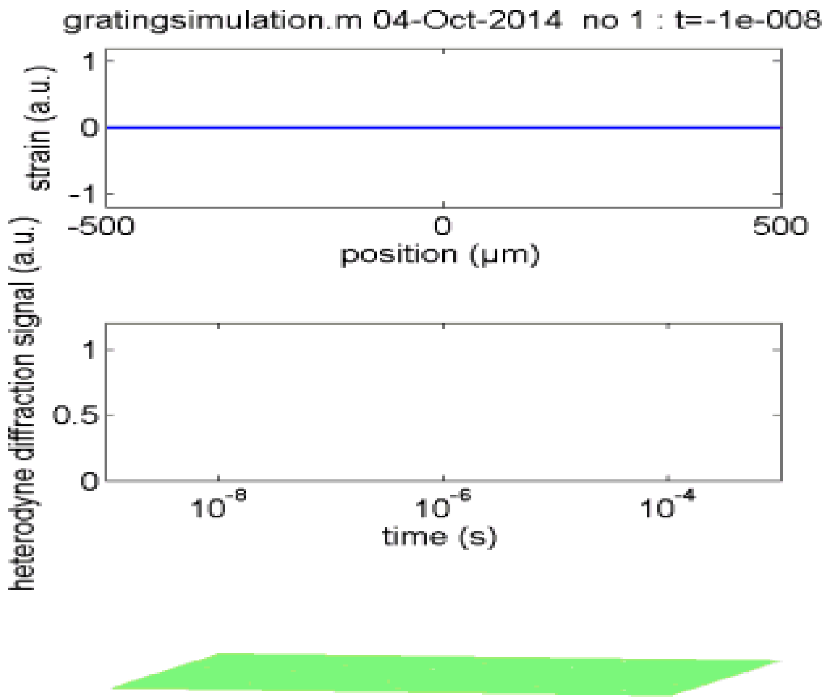

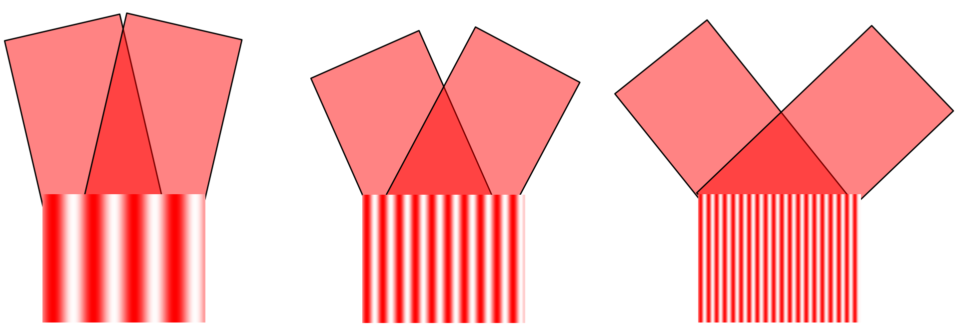

KU LEUVEN

Laser ultrasonics:

material characterization

case studies

Laser ultrasonic applications: elastic characterization of hardened steel

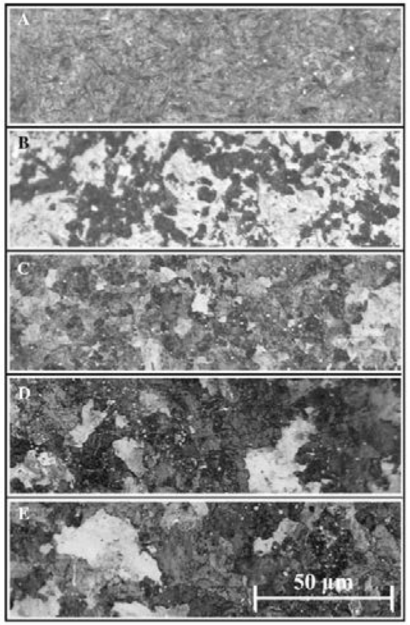

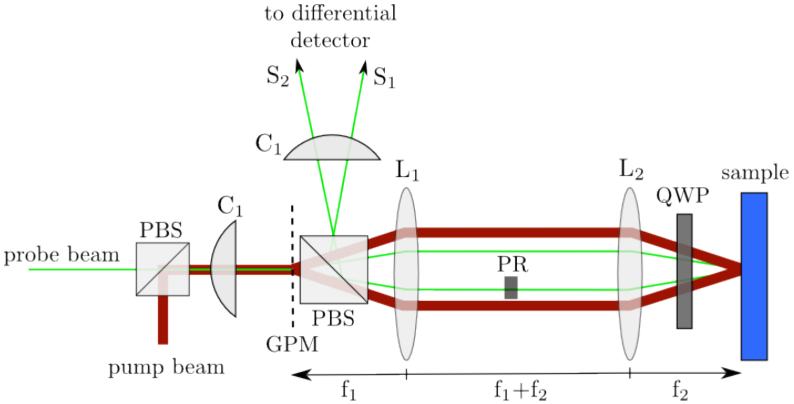

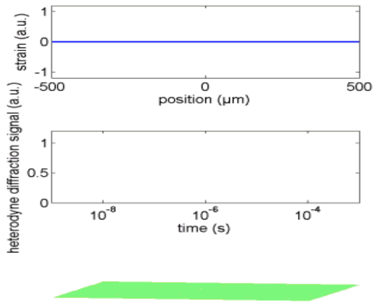

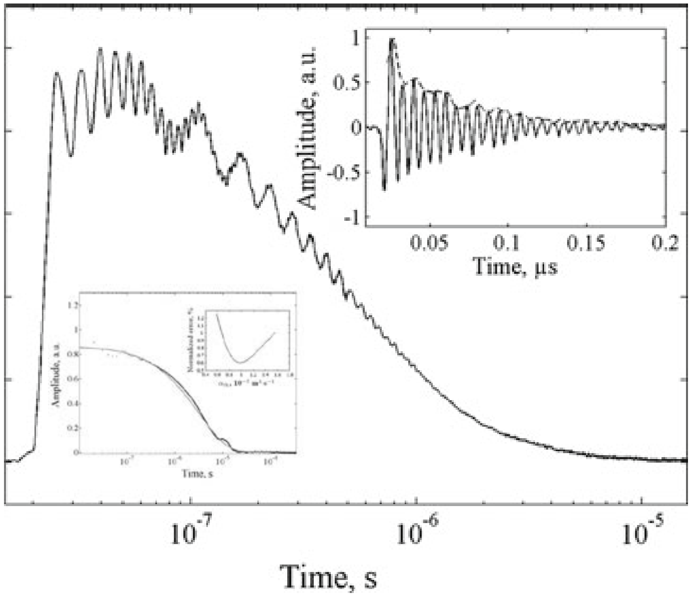

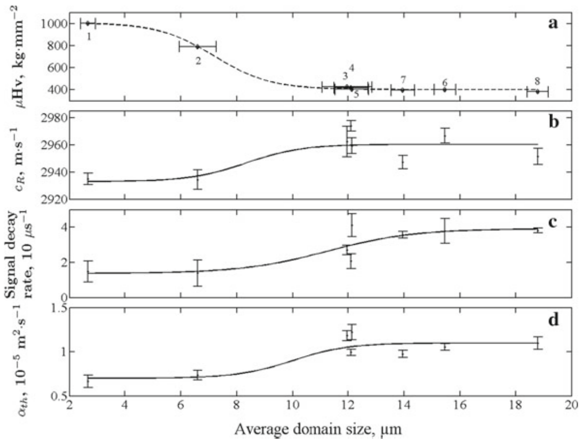

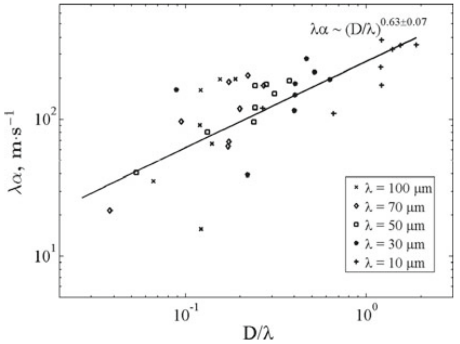

Laser ultrasonic applications:
elastic characterization of protective layer on fuel cladding

Oxide layers

Natural protective barrier

Increased dissolution resistance

0.1 ~ 10 µm

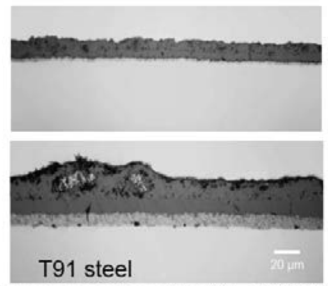

[A. Weisenburger et. al., Journ. Nucl. Mat., **376** (2008) 274-281]

Engineered layers

- Synthetic protective barrier
- Strong oxide-formers
- Self-healing
- Higher temperatures (>500°C)

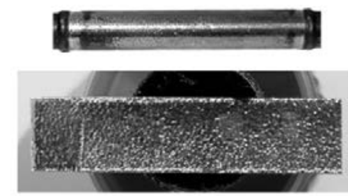

[A. Weisenburger et. al., Journ. Nucl. Mat., **376** (2008) 274-281]

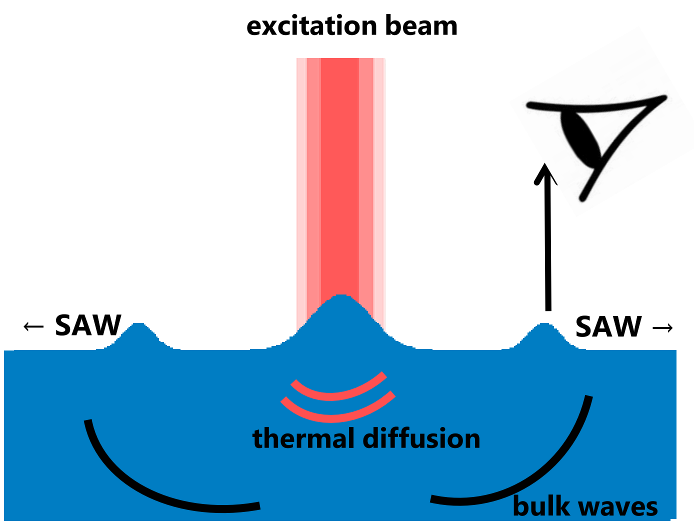

- Laser excitation of
  - surface acoustic waves (SAW)
  - bulk waves
  - thermal diffusion field
- Optical detection

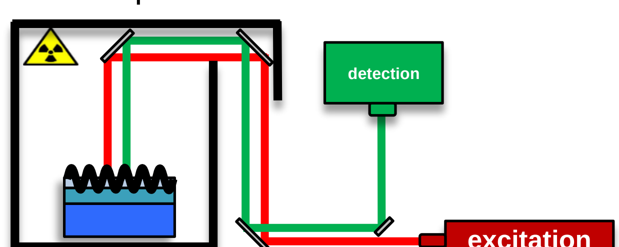

Laser ultrasonic applications:
elastic characterization of protective layer on fuel cladding

Thermoelasticity GESA remelted 20 μm FeCrAlY on T91 steel

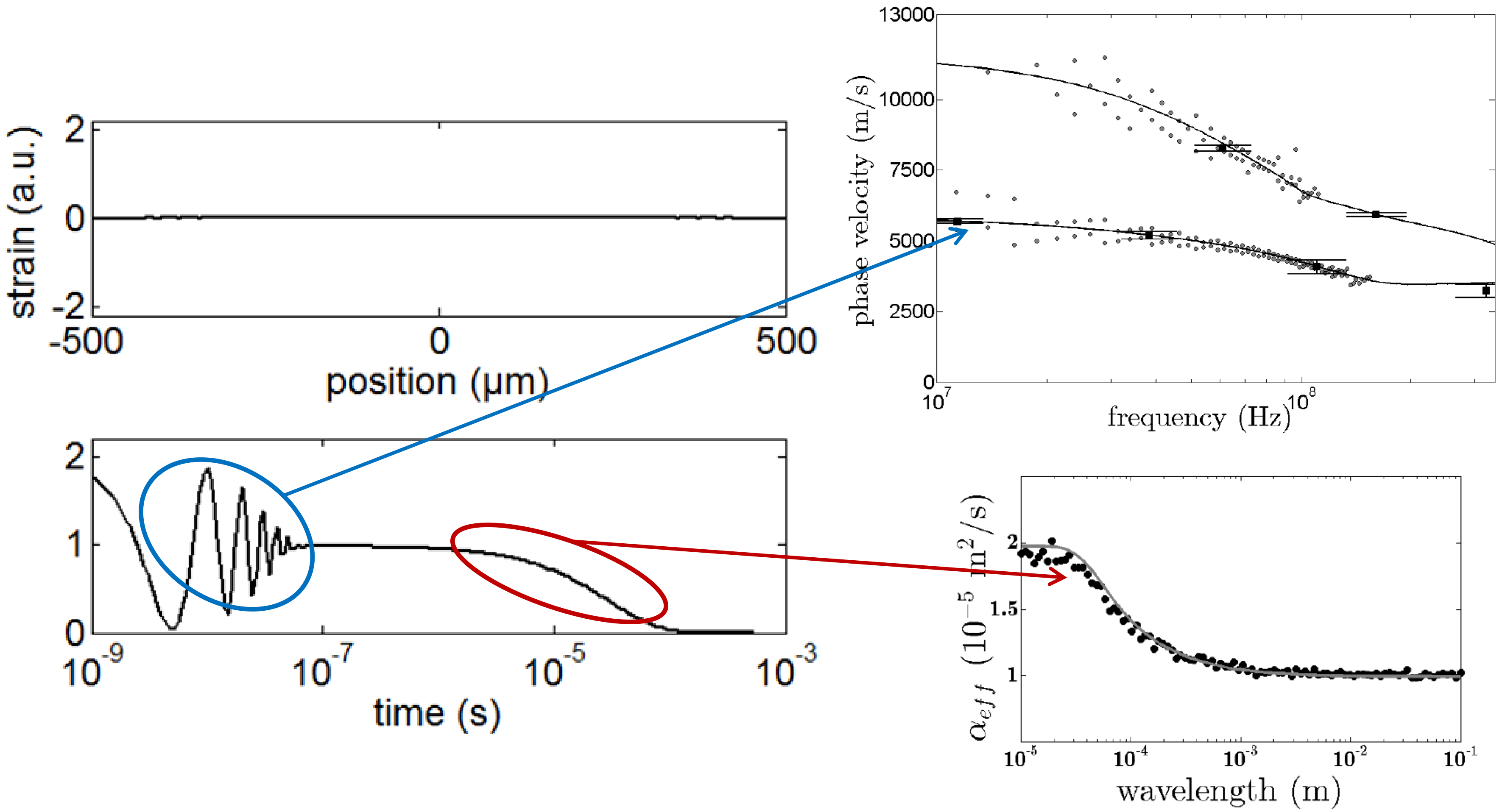

Laser ultrasonic applications:
elastic characterization of protective layer on fuel cladding

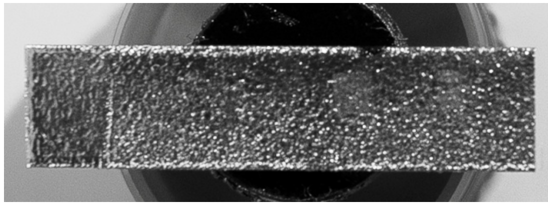

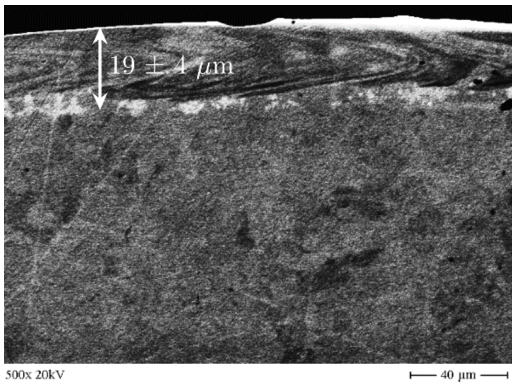

GESA sample

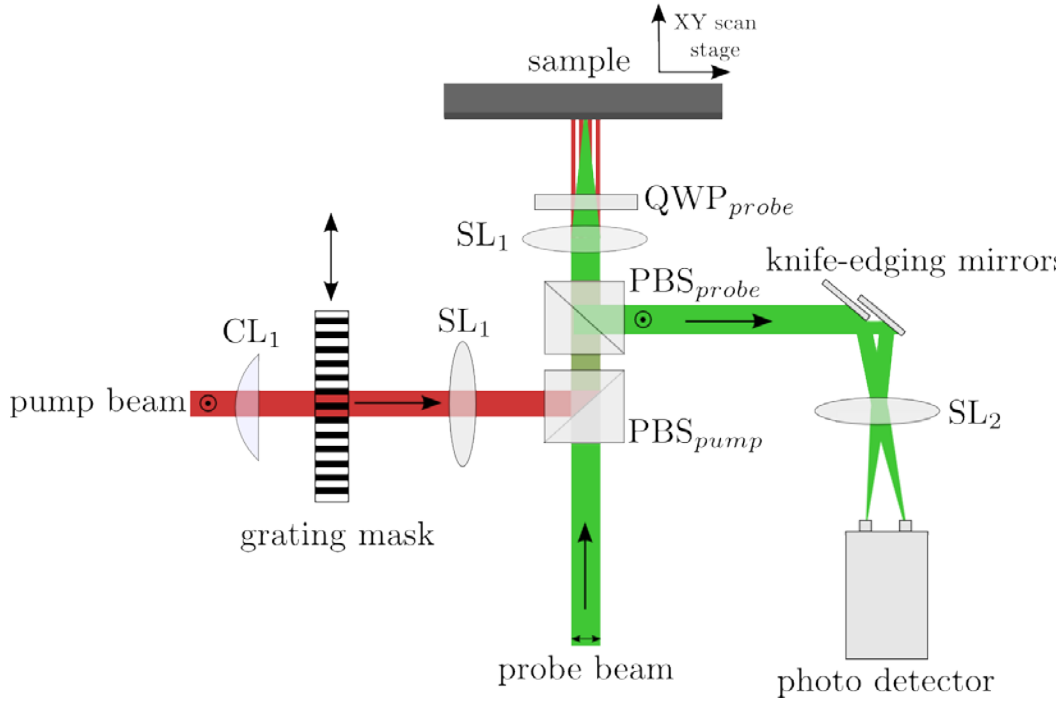

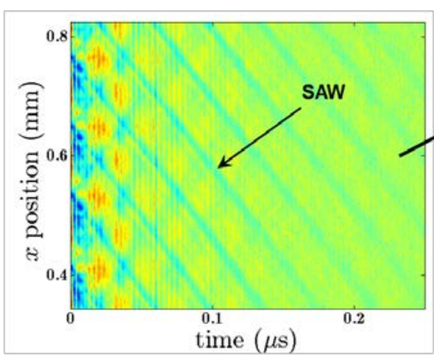

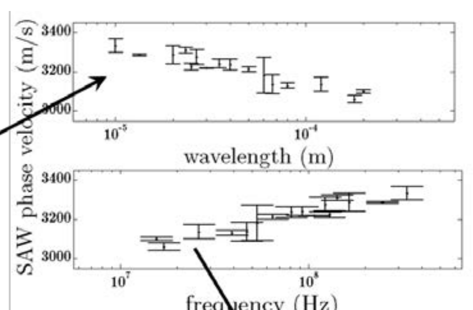

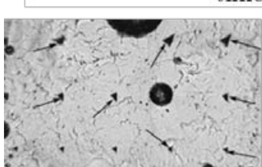

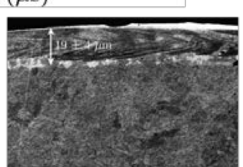

	E (GPa)	ν	d (μm)
coating	191±50	0.3	22±4
substrate	202	0.3	

Validation by nano-indentation: E_1=207 GPa

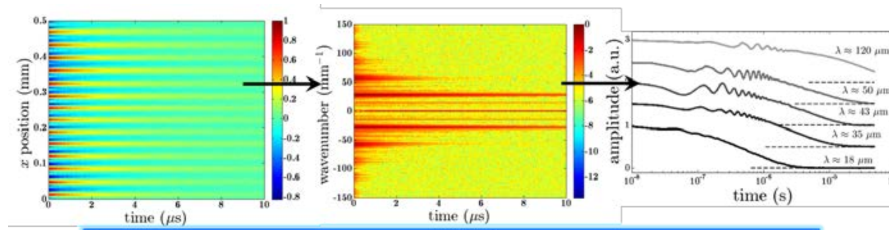

Extracted thermal diffusivities

	α (10^{-5} m²/s)
coating	5.0 ± 1.6
substrate	7.5

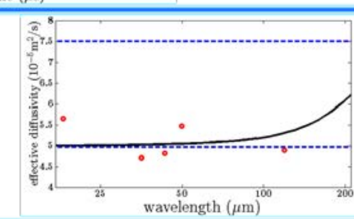

Laser ultrasonic applications:
elastic characterization of protective layer on fuel cladding

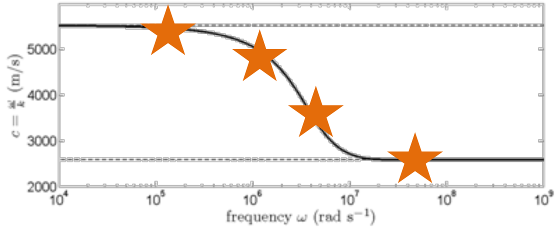

SAW velocity at different grating spacings

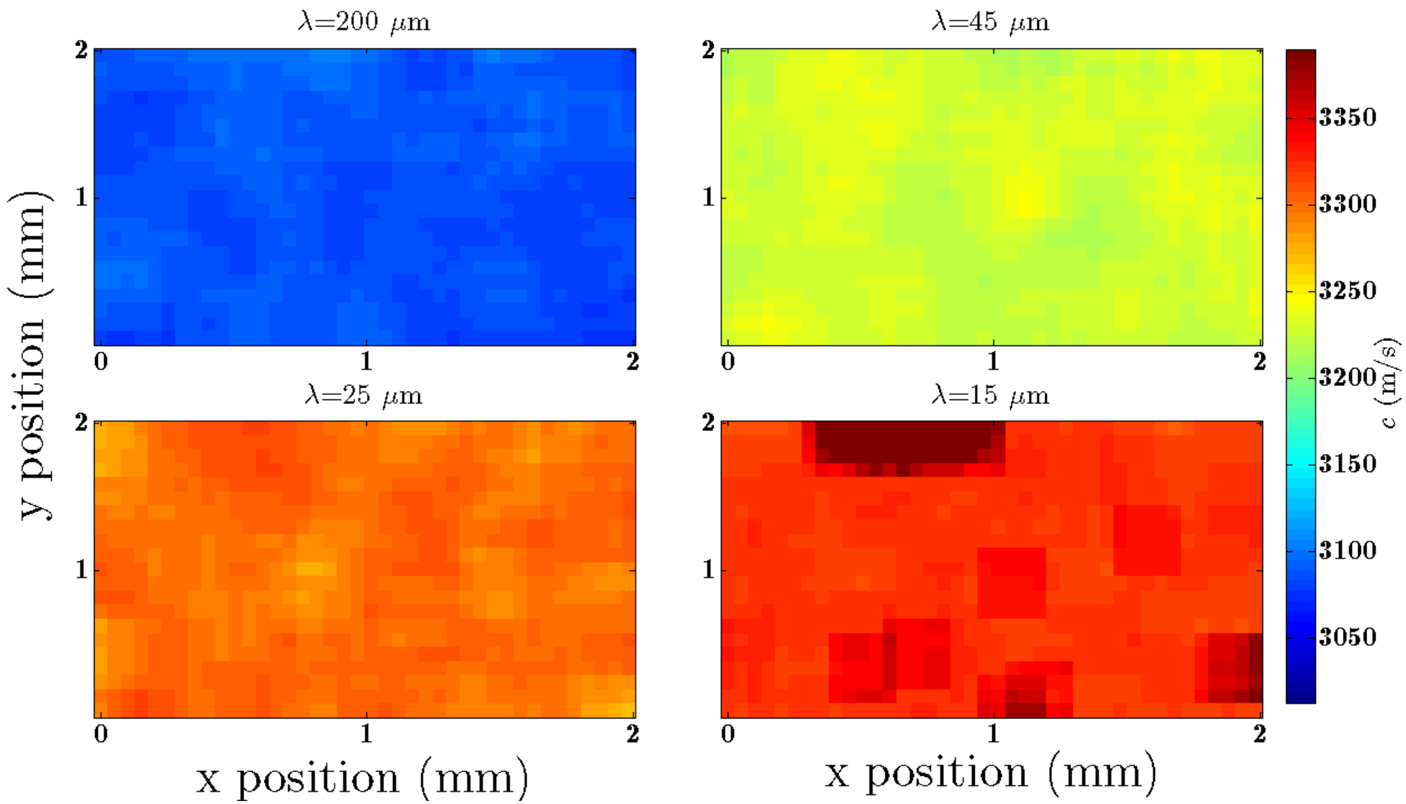

Laser ultrasonic applications:
elastic characterization of protective layer on fuel cladding

KU LEUVEN

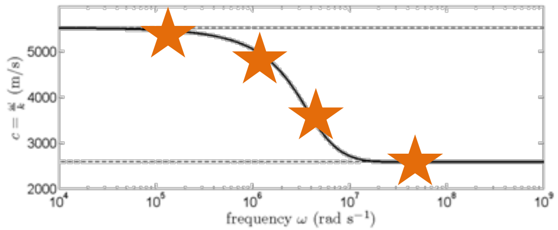

Extracted coating thickness

from xy-scan

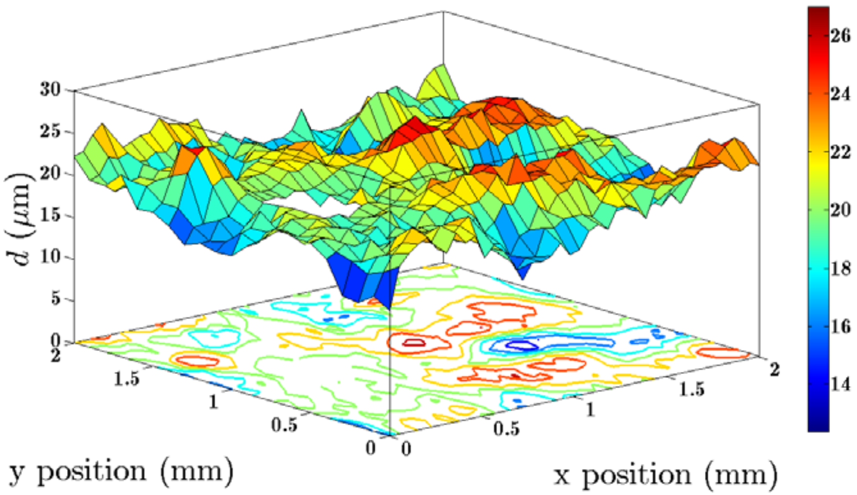

from yx-scan

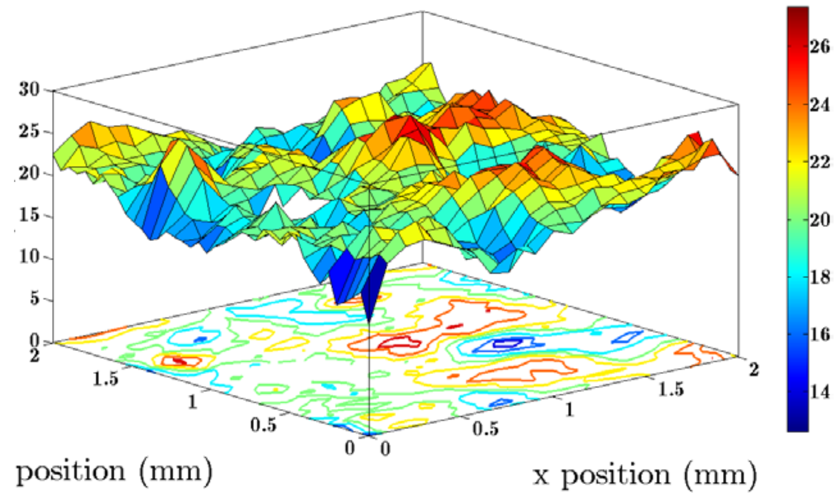

Laser ultrasonic applications: elastic characterization of protective layer on fuel cladding

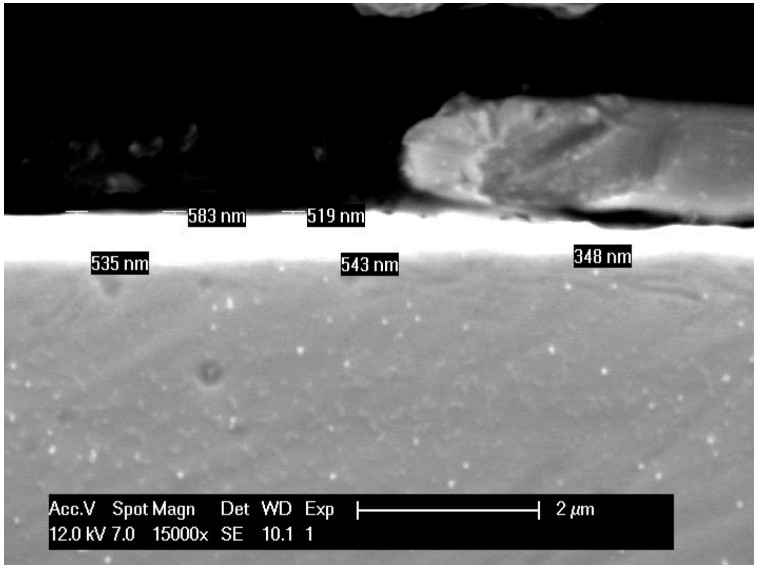

Submicron oxide layer

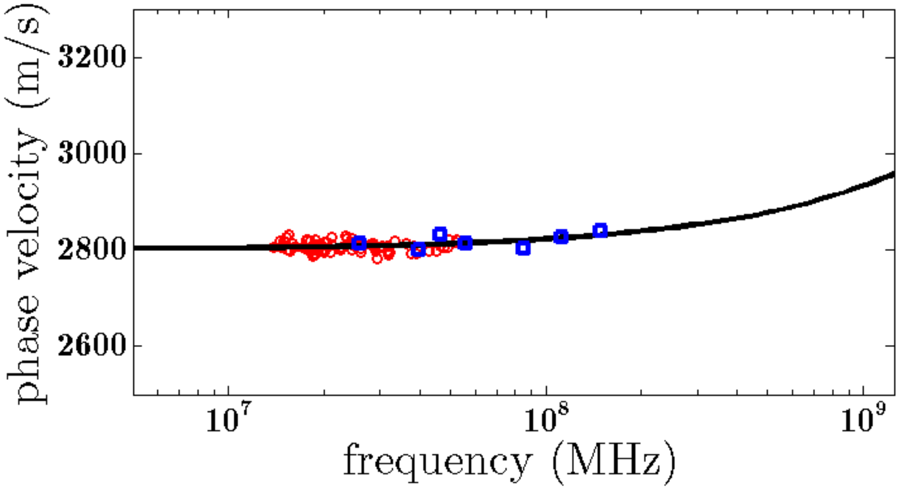

	d (µm)	c_R (m/s)	ρ (kg/m³)
coating	0.6±1.0	(3.2±0.7) 10^3	(7±11) 10^3
substrate		2826	7990

Laser ultrasonic applications:
elastic characterization of rough polymer coated steel sample

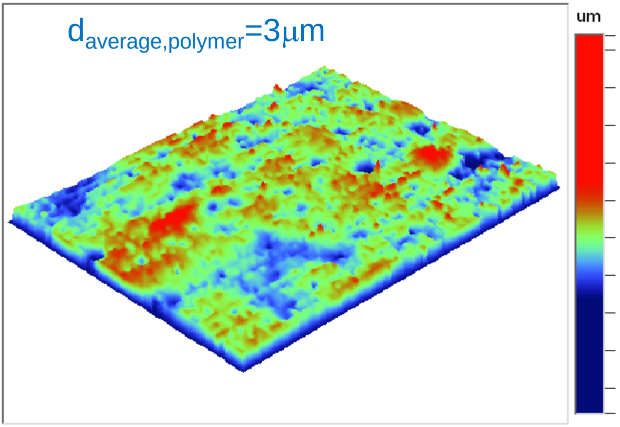

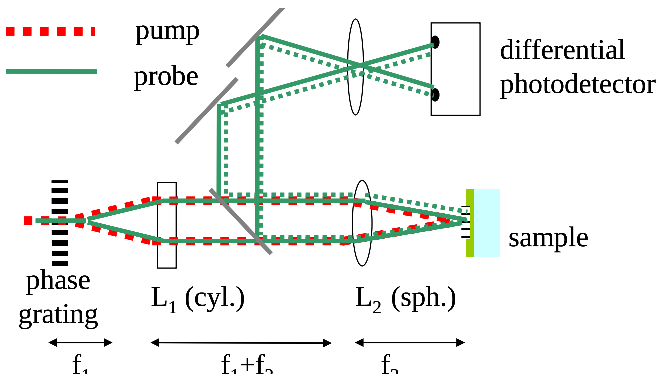

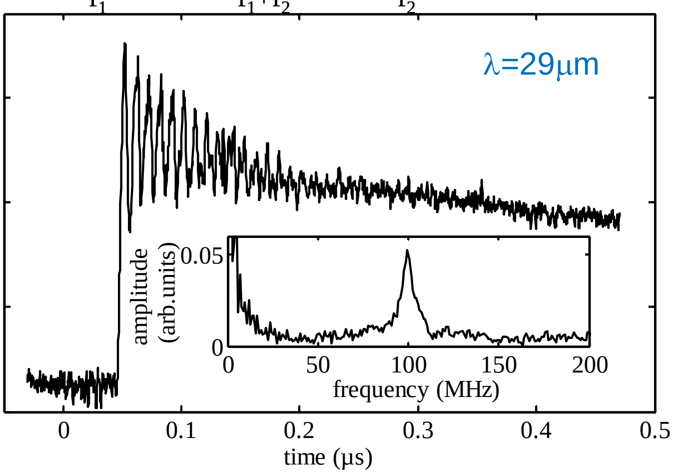

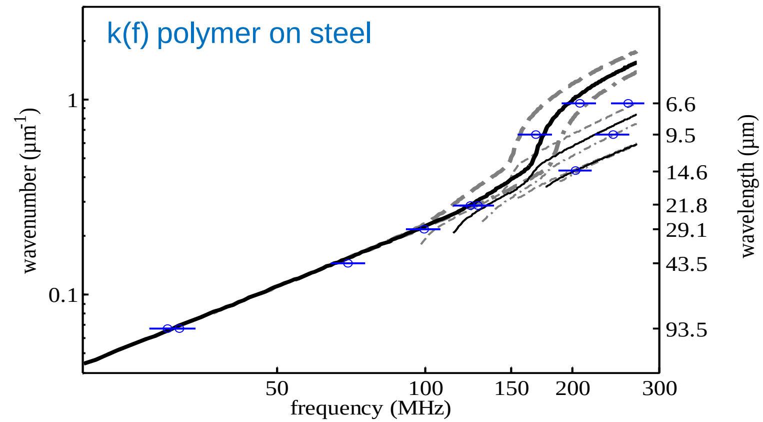

polymer on steel

340 nm Al on polymer on steel

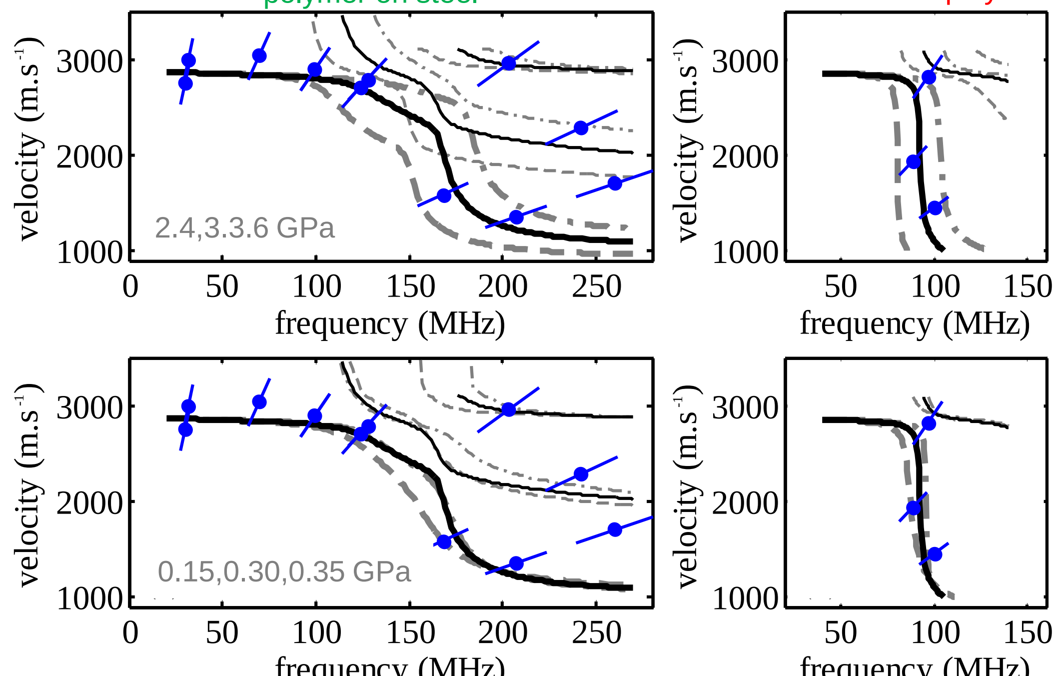

E_p=3.0±0.6 GPa

E_p=1.6±0.4 GPa

nanoindentation: E=2.2±0.5 GPa

Laser ultrasonic applications:
elastic characterization of rubber layer

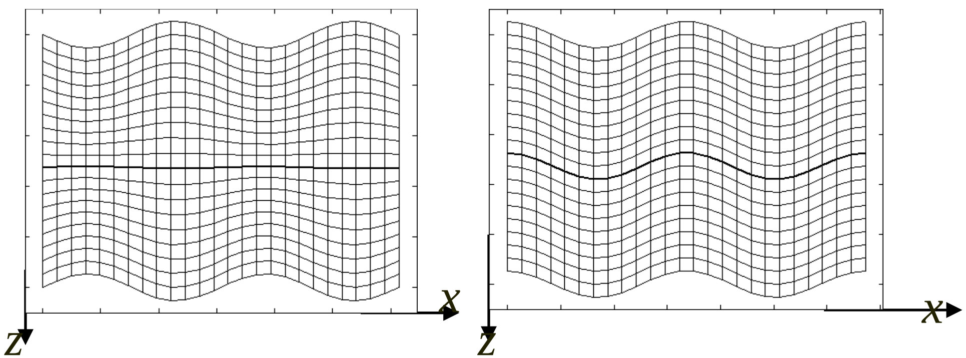

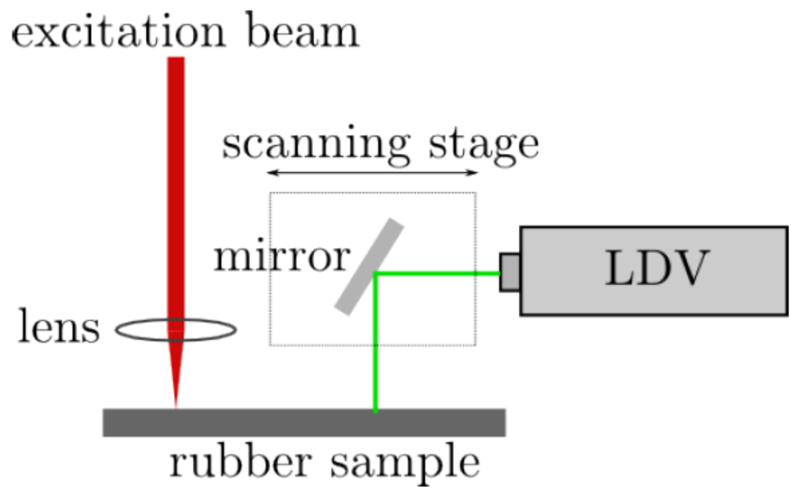

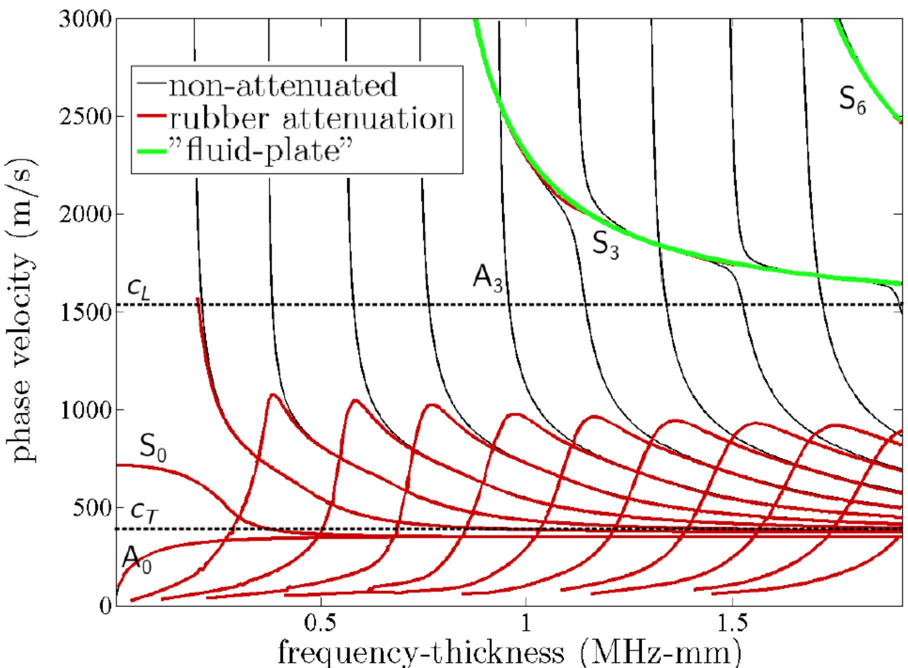

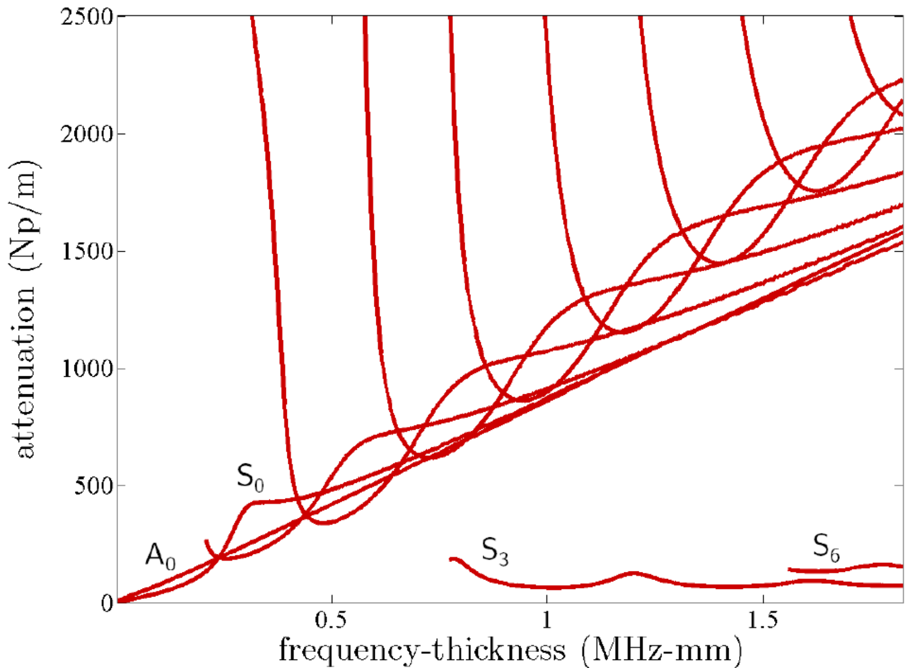

Laser ultrasonic applications: elastic characterization of rubber layer

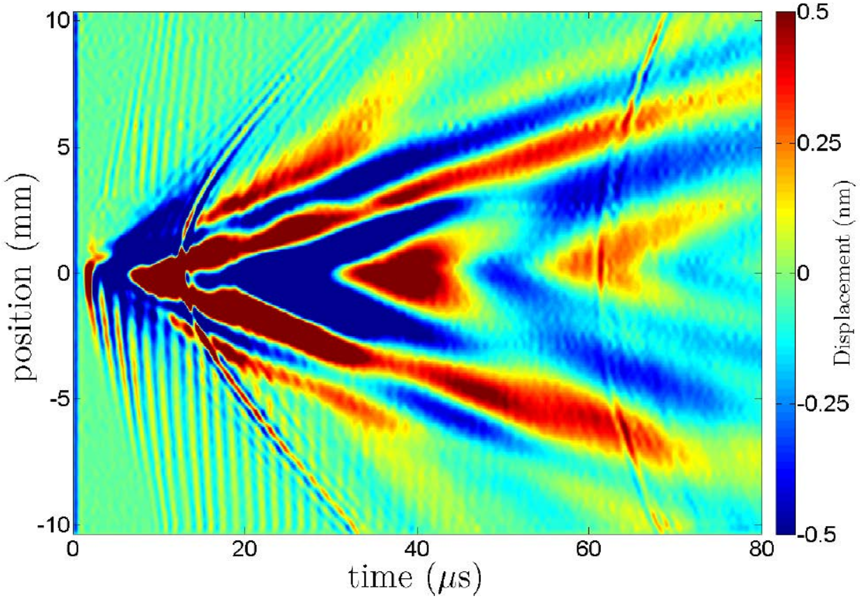

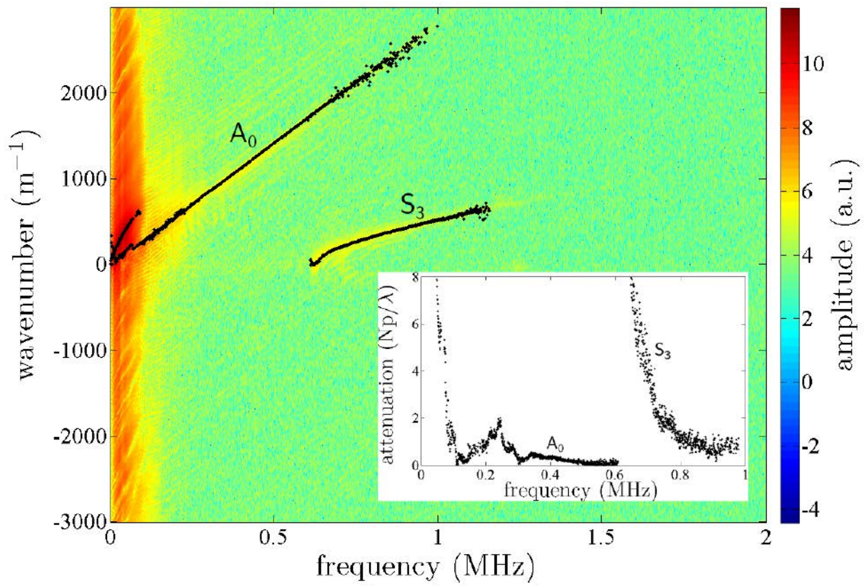

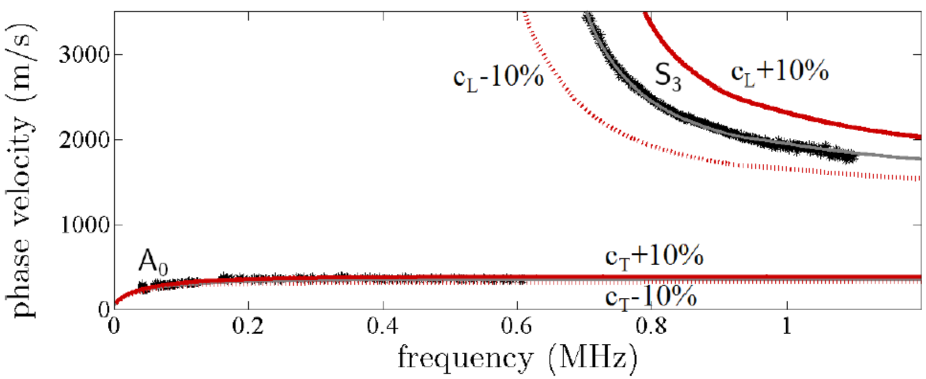

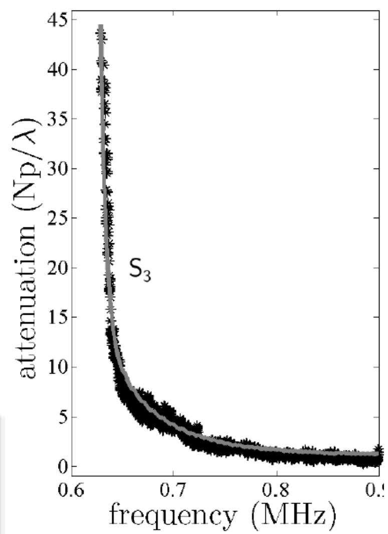

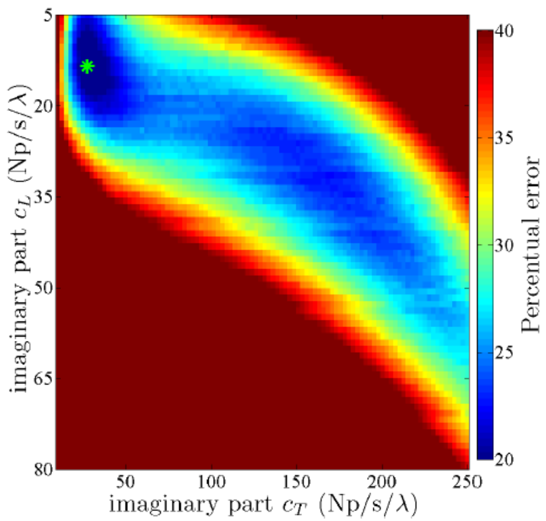

Elastic parameter	Real part	Imaginary part
Longitudinal velocity	1510 ± 3 m/s	11 ± 5 Np/s/λ
Shear velocity	370 ± 19 m/s	25 ± 11 Np/s/λ
Sample thickness	1.194 ± 0.003 mm	

Laser ultrasonic applications: elastic characterization of sub-micron intermetallic layer

KU LEUVEN

Sn-Cu interdiffusion layer

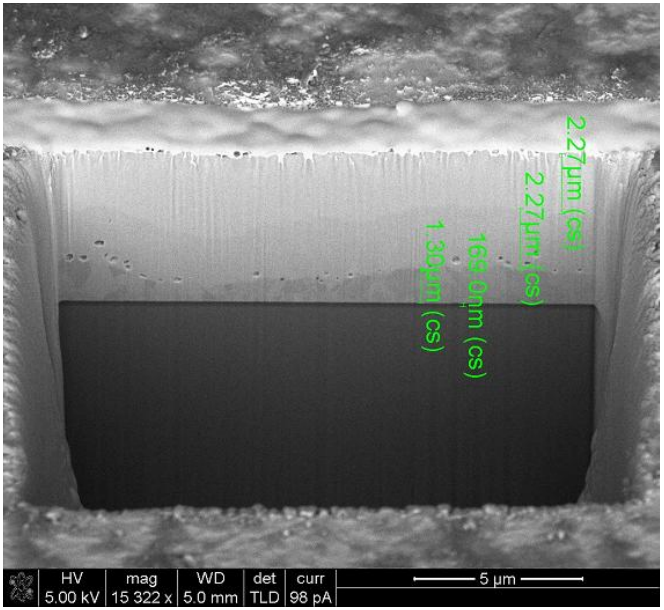

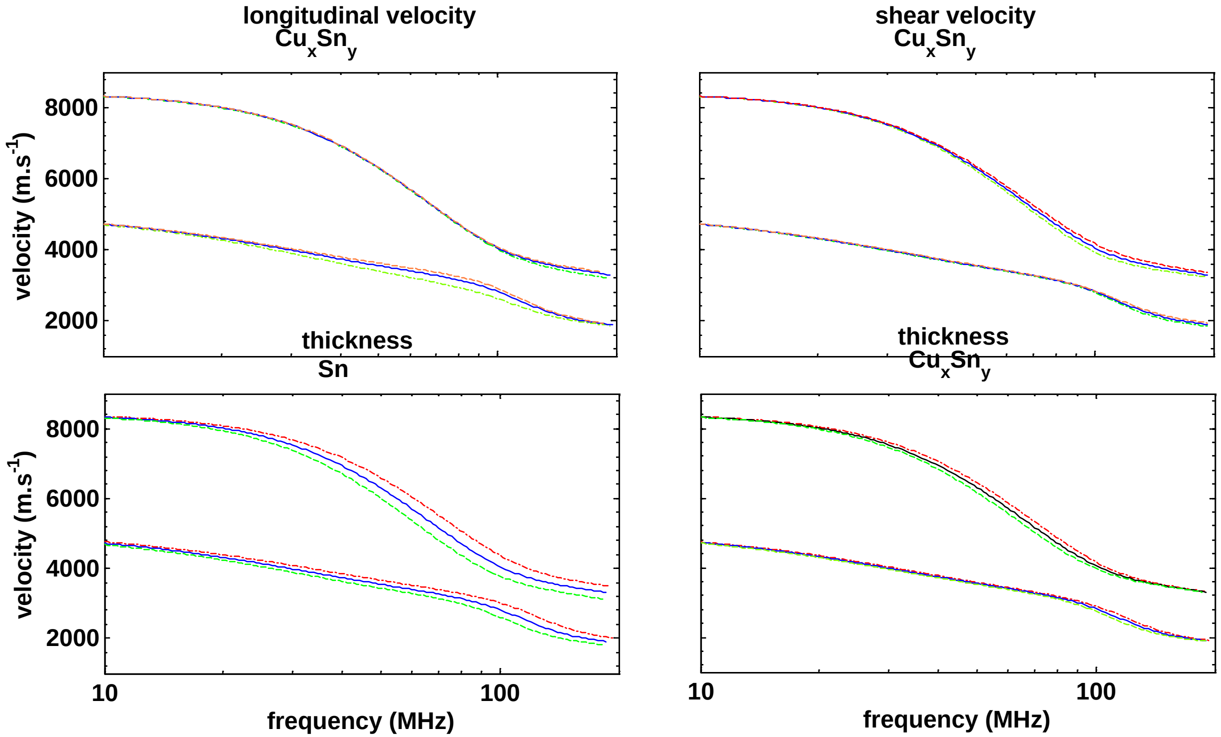

Fitting parameters:

v_L = 5400 m/s
v_T = 2100 m/s
d_1 = 1.63 µm
d_2 = 5.10 µm
d_3 = 0.50 µm
ρ = 7900 kg/m³

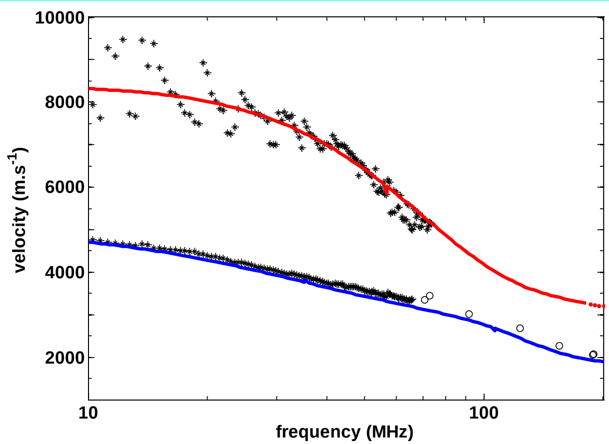

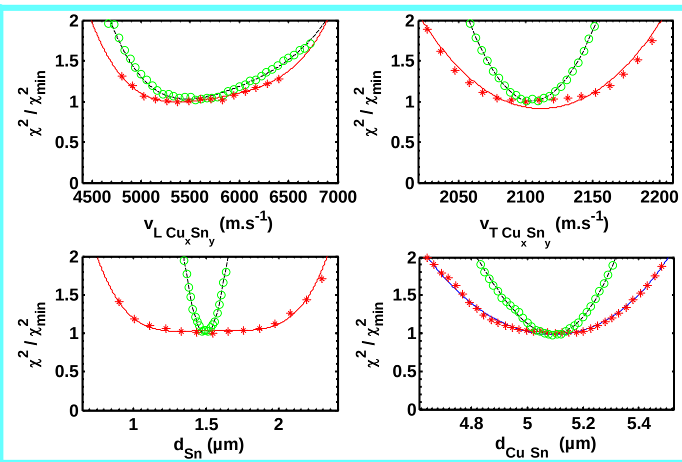

Laser ultrasonic applications: elastic depth profiling of functionally graded materials

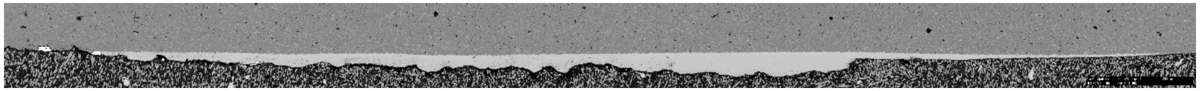

Glass layer diffused in porous ceramic
parameter study

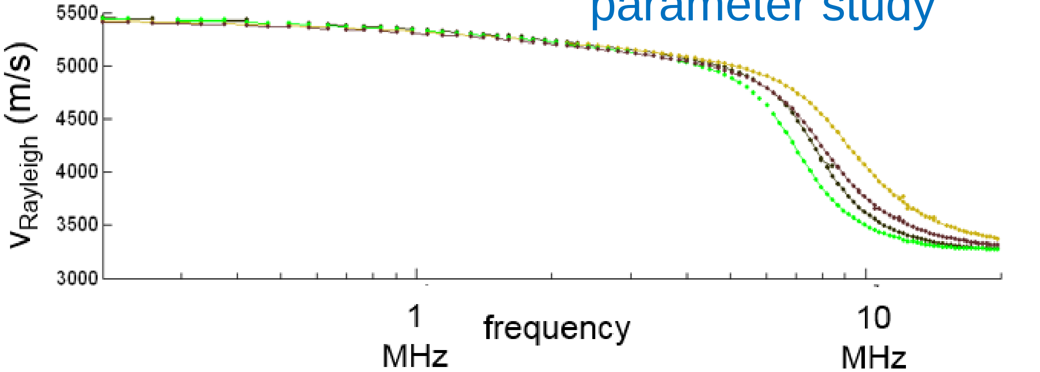

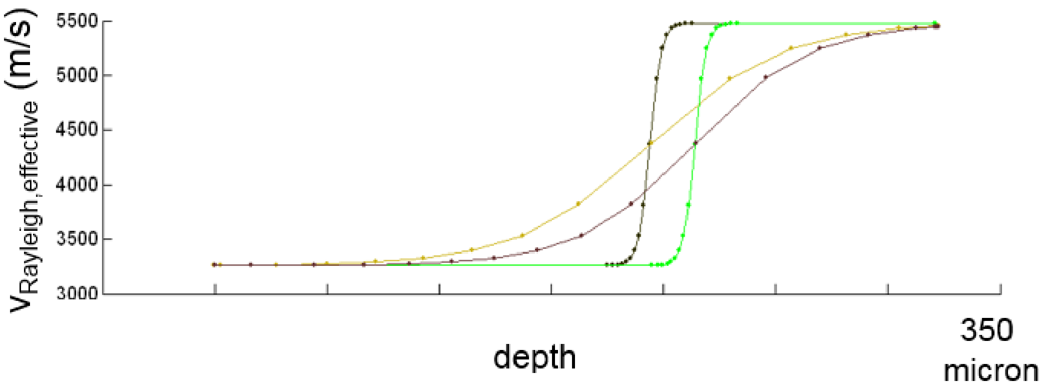

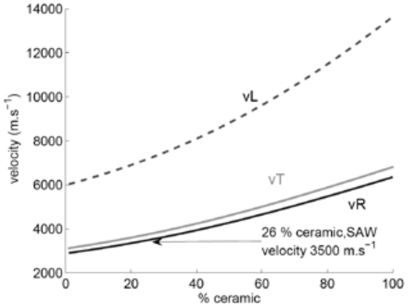

Experimental result

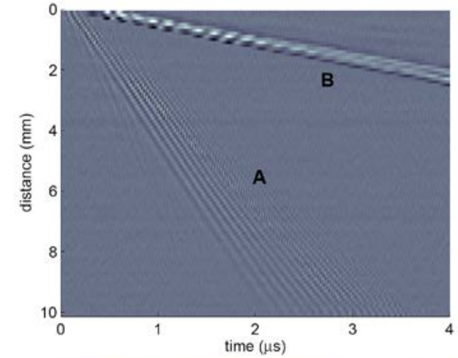

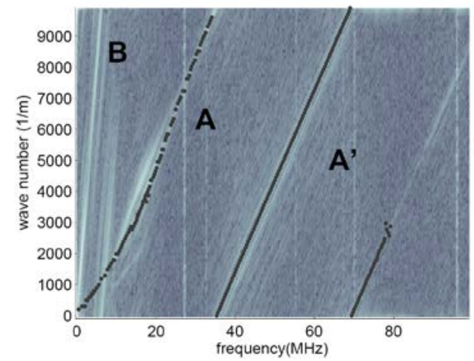

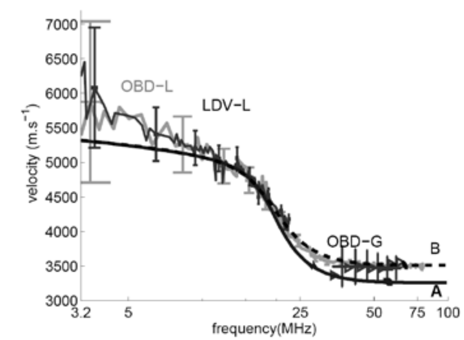

Laser ultrasonic applications: elastic characterization of sub-micron nanocrystalline diamond layer

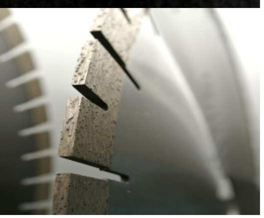

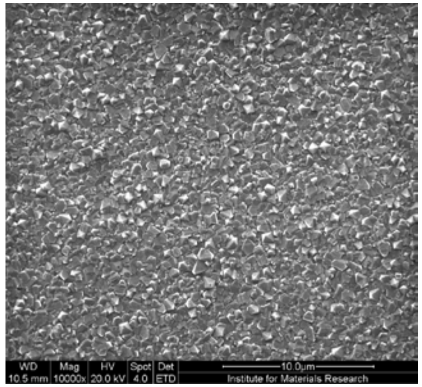

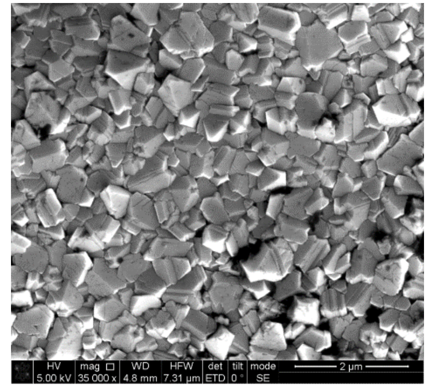

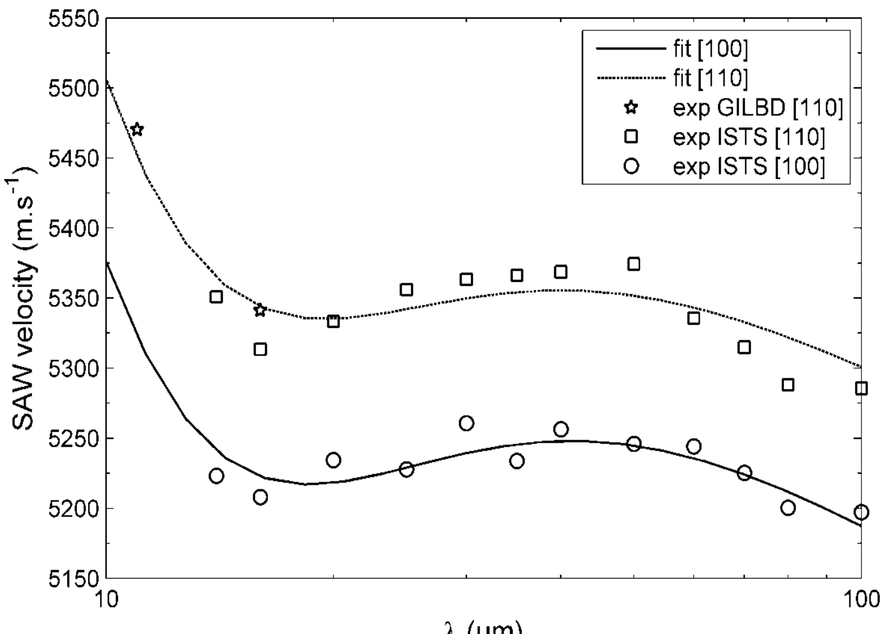

$E = 770 \pm 26$ GPa

$\rho = 3250 \pm 50$ kg.m^{-3}

$L = 1.4 \pm 0.04$ μm

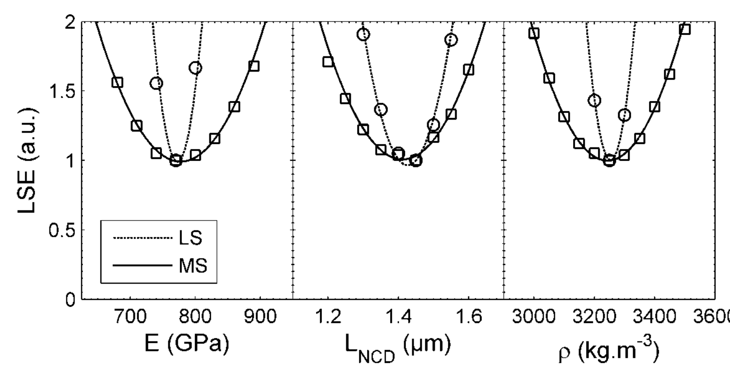

Laser ultrasonic applications: thermal characterization of sub-micron nanocrystalline diamond layer

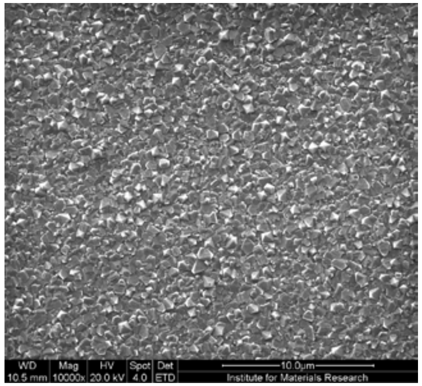

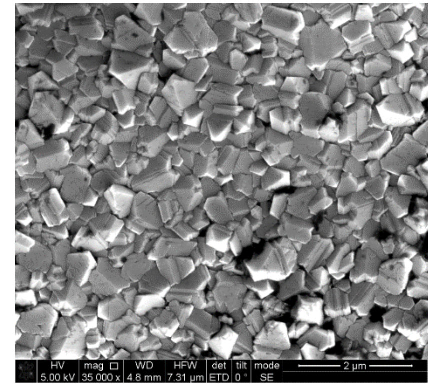

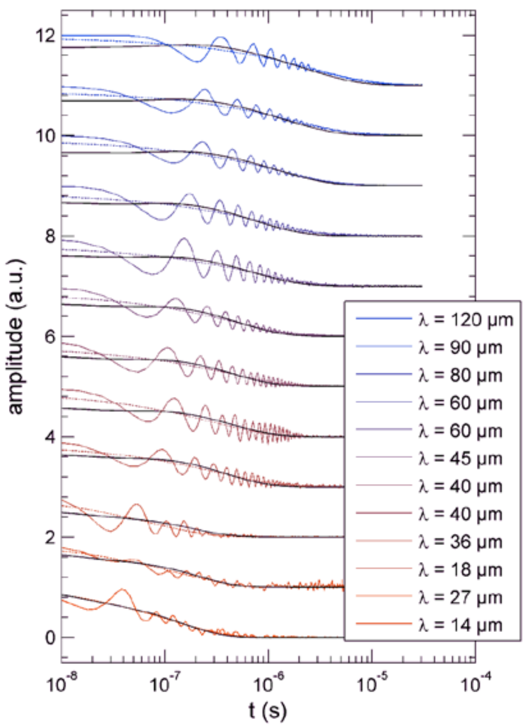

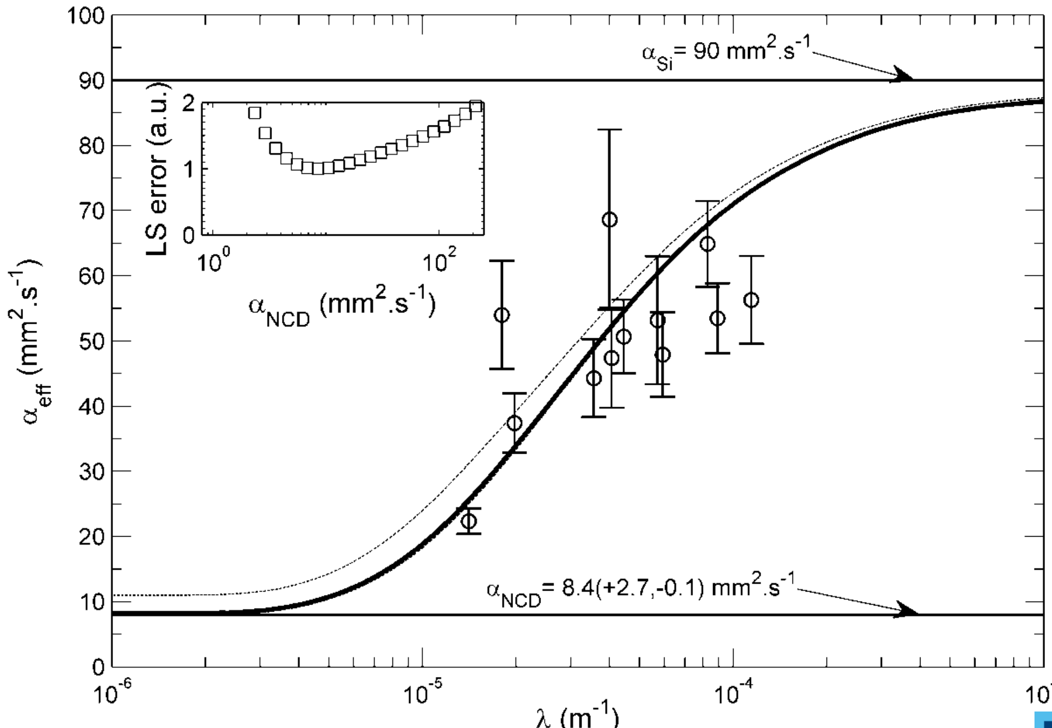

Laser ultrasonic applications: elastic characterization of Ni_2MnGa layer

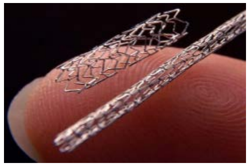

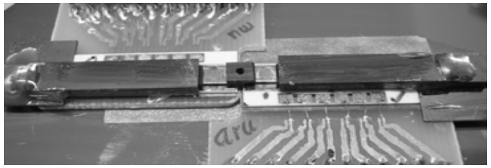

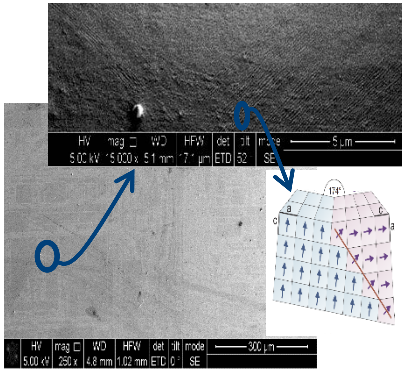

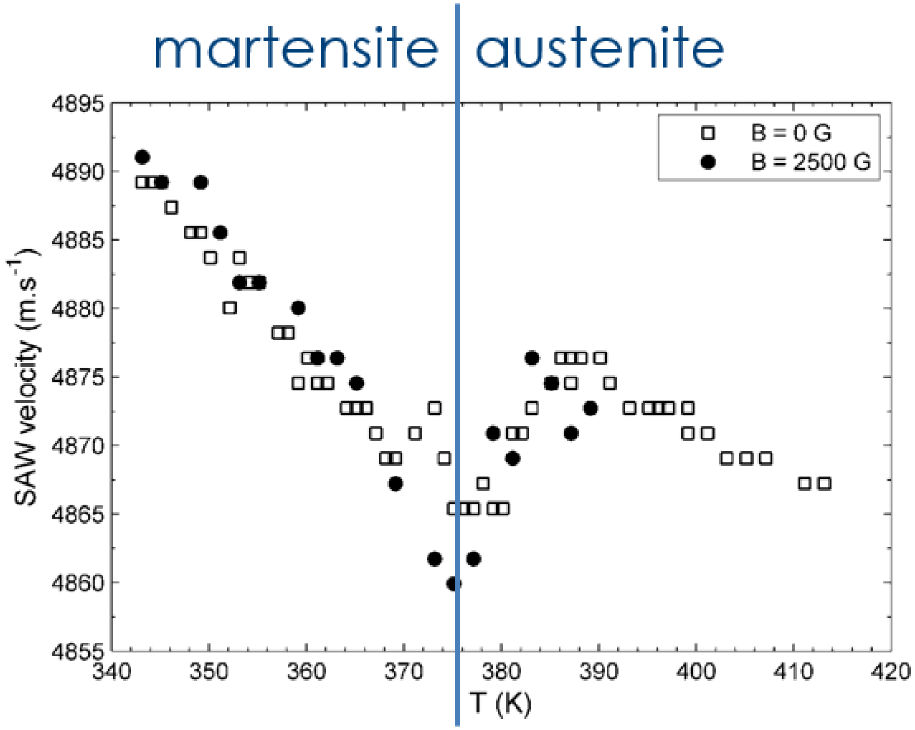

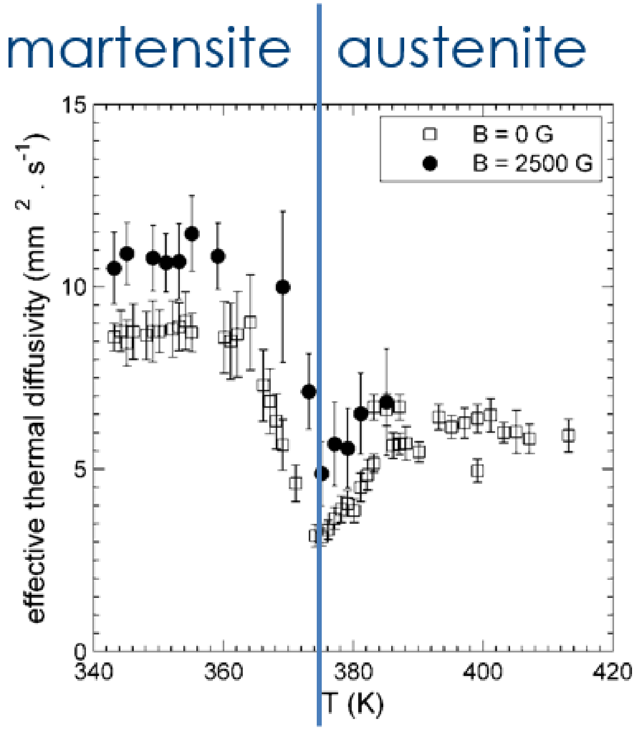

Calculation of guided wave dispersion and photothermal and photoacoustic displacements

Bulk wave propagation in solids

Propagating quantities:

- density ρ
- displacement vector u_i
- strain tensor $\varepsilon_{ij} = ½(\partial u_i/\partial x_j + \partial u_j/\partial x_i) \equiv ½(u_{i,j}+u_{j,i})$
- stress components σ_{ij}
- velocity vector v_i

Governing equations:

- **Newton**

$$\boxed{\rho_0 \ddot{u}_i \equiv \rho_0 \frac{\partial^2 u_i}{\partial t^2} = \frac{\partial \sigma_{ij,j}}{\partial x_j} \equiv \sigma_{ij,j}}$$

- **Hooke**

$$\boxed{\begin{aligned} \sigma_{ij} &= c_{ijkl}\varepsilon_{kl} \\ \sigma_{ij} &= \rho_0\left(\left(c_L{}^2 - 2c_T{}^2\right)\varepsilon_{kk}\delta_{ij} + 2c_T{}^2\varepsilon_{ij}\right) \\ &= \rho_0\left(\left(c_L{}^2 - 2c_T{}^2\right)u_{k,k}\delta_{ij} + c_T{}^2\left(u_{i,j} + u_{j,i}\right)\right) \end{aligned}}$$

	(c_L, c_T)	(λ, μ)	(E, ν)
c_L		$\sqrt{\frac{\lambda+2\mu}{\rho}}$	$\sqrt{\frac{E(1-\nu)}{\rho(1+\nu)(1-2\nu)}}$
c_T		$\sqrt{\frac{\mu}{\rho}}$	$\sqrt{\frac{E}{2\rho(1+\nu)}}$
λ	$\rho(c_L^2 - 2c_T^2)$		$\frac{\nu E}{(1+\nu)(1-2\nu)}$
μ	ρc_T^2		$\frac{E}{2(1+\nu)}$
E	$\rho c_T^2 \frac{3c_L^2-4c_T^2}{c_L^2-c_T^2}$	$\frac{3\lambda\mu}{2\lambda+\mu}$	
ν	$\frac{c_L^2-2c_T^2}{2c_L^2-2c_T^2}$	$\frac{\lambda}{2\lambda+\mu}$	

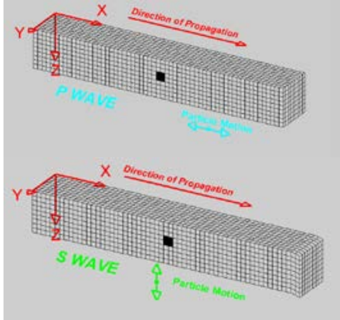

Strain

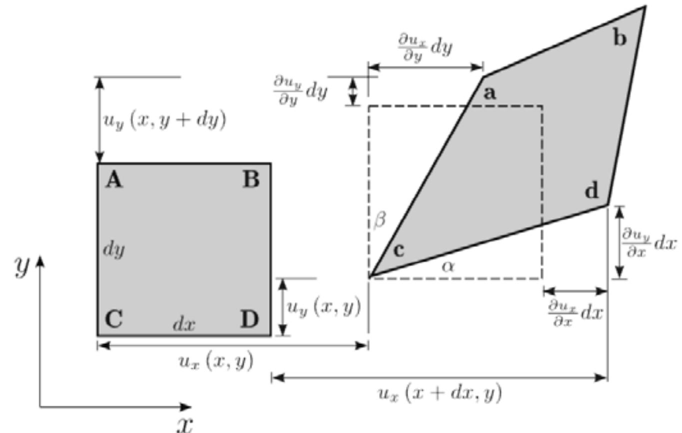

Stress

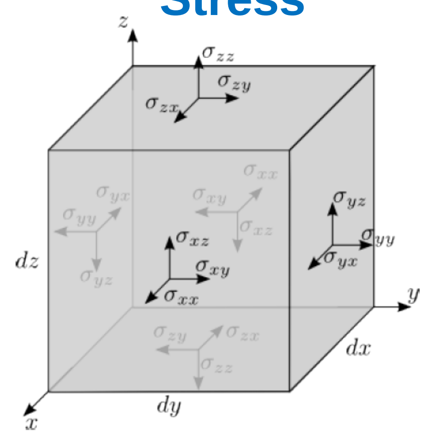

Bulk wave propagation in solids

Combining Newton and Hooke:

$$\rho_0 \ddot{u}_i \equiv \rho_0 \frac{\partial^2 u_i}{\partial t^2} = \frac{\partial \sigma_{ij,j}}{\partial x_j} \equiv \sigma_{ij,j}$$

$$\sigma_{ij} = c_{ijkl}\varepsilon_{kl}$$

$$\sigma_{ij} = \rho_0\left(\left(c_L{}^2 - 2c_T{}^2\right)\varepsilon_{kk}\delta_{ij} + 2c_T{}^2\varepsilon_{ij}\right)$$

$$= \rho_0\left(\left(c_L{}^2 - 2c_T{}^2\right)u_{k,k}\delta_{ij} + c_T{}^2\left(u_{i,j} + u_{j,i}\right)\right)$$

$$\rho_0 \ddot{u}_i = \rho_0\left(\left(c_L{}^2 - 2c_T{}^2\right)u_{k,kj}\delta_{ij} + c_T{}^2\left(u_{i,jj} + u_{j,ii}\right)\right)$$

$$\ddot{u}_i = \left(c_L{}^2 - 2c_T{}^2\right)u_{j,ji} + c_T{}^2 u_{i,jj}$$

$$\ddot{\mathbf{u}} = c_T^2 \Delta \mathbf{u} + \left(c_L^2 - c_T^2\right)\nabla\left(\nabla \cdot \mathbf{u}\right)$$

$$\mathbf{u} = \nabla\varphi + \nabla \times \boldsymbol{\psi}$$

$$\nabla \cdot \boldsymbol{\psi} = 0$$

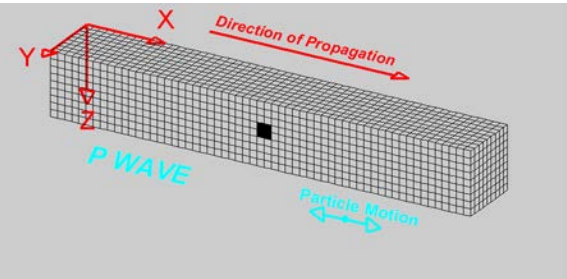

$$\Delta\varphi = \frac{1}{c_L^2}\ddot{\varphi}$$

$$\Delta\psi = \frac{1}{c_T^2}\ddot{\psi}$$

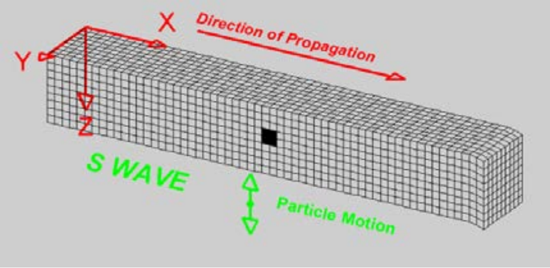

Bulk wave propagation in solids: harmonic solutions in 2D

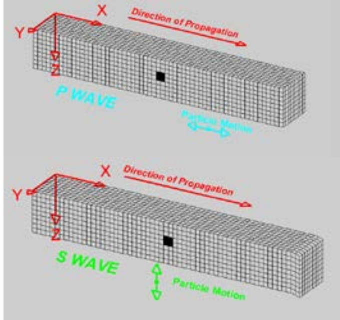

Combining Newton and Hooke:

$$\Delta\varphi = \frac{1}{c_L^2}\ddot{\varphi}$$
$$\Delta\psi = \frac{1}{c_T^2}\ddot{\psi}$$

Harmonic proposal solution for plane waves running in the positive x-direction

$$\varphi(x,z,t) = \varphi(x,z)\exp(i\omega t - ikx)$$
$$\psi(x,z,t) = \psi(x,z)\exp(i\omega t - ikx)$$

$$-k^2\varphi + \frac{\partial^2\varphi}{\partial z^2} = -\frac{\omega^2}{c_L^2}\frac{\partial^2\varphi}{\partial t^2}$$
$$-k^2\psi + \frac{\partial^2\psi}{\partial z^2} = -\frac{\omega^2}{c_T^2}\frac{\partial^2\psi}{\partial t^2}$$

$$\frac{\partial^2\varphi}{\partial z^2} = \left(k^2 - \frac{\omega^2}{c_L^2}\right)\frac{\partial^2\varphi}{\partial t^2} \equiv p_L^2\varphi$$
$$\frac{\partial^2\psi}{\partial z^2} = \left(k^2 - \frac{\omega^2}{c_T^2}\right)\frac{\partial^2\psi}{\partial t^2} \equiv p_T^2\psi$$

Harmonic plane waves running in the positive x-direction with a depth profile in the z-direction.

$$\varphi(x,z,t) = \left(A\exp(p_L z) + B\exp(-p_L z)\right)\exp(i\omega t - ikx)$$
$$\psi(x,z,t) = \left(C\exp(p_T z) + B\exp(-p_T z)\right)\exp(i\omega t - ikx)$$

Surface wave propagation in semi-infinite solids

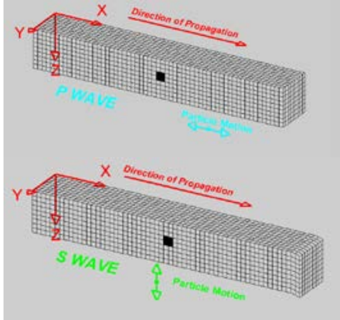

Harmonic plane wave components running in the positive x-direction with a depth profile in the z-direction.

$$\varphi(x,z,t)=\left(A\exp(p_L z)+B\exp(-p_L z)\right)\exp(i\omega t-ikx)$$
$$\psi(x,z,t)=\left(C\exp(p_T z)+D\exp(-p_T z)\right)\exp(i\omega t-ikx)$$

Surface waves: no energy far away from the surface

$$\varphi(x,z,t)=B\exp(-p_L z)\exp(i\omega t-ikx)$$
$$\psi(x,z,t)=D\exp(-p_T z)\exp(i\omega t-ikx)$$

Surface waves: no normal and no shear stress at the free surface: $\sigma_{zz}=0$ and $\sigma_{xz}=0$

$$\mathbf{u}=\nabla\varphi+\nabla\times\boldsymbol{\psi}$$

$$\sigma_{ij}=\rho_0\left(\left(c_L{}^2-2c_T{}^2\right)u_{k,k}\delta_{ij}+c_T{}^2\left(u_{i,j}+u_{j,i}\right)\right)$$

$$\begin{aligned}\sigma_{xz} &= \rho c_T^2\left[\frac{\partial^2\psi}{\partial x^2}-\frac{\partial^2\psi}{\partial z^2}+2\frac{\partial^2\varphi}{\partial xz}\right]\\ &\rightarrow \rho c_T^2\left[-k^2\psi-\frac{\partial^2\psi}{\partial z^2}+2ik\frac{\partial\varphi}{\partial z}\right]=0\\ \sigma_{zz} &= \rho\left[c_L^2\left(\frac{\partial^2\varphi}{\partial x^2}+\frac{\partial^2\varphi}{\partial z^2}\right)-2c_T^2\left(\frac{\partial^2\varphi}{\partial x^2}-\frac{\partial^2\psi}{\partial xz}\right)\right]\\ &\rightarrow \rho\left[c_L^2\left(-k^2\varphi+\frac{\partial^2\varphi}{\partial z^2}\right)-2c_T^2\left(-k^2\varphi-ik\frac{\partial\psi}{\partial z}\right)\right]=0\end{aligned}$$

$$\begin{pmatrix}k^2+p_T^2 & -2ikp_T\\ 2ikp_L & k^2+p_T^2\end{pmatrix}\begin{pmatrix}B\\ D\end{pmatrix}=0$$

Rayleigh determinant of homogeneous set of equations should be zero

$$k^4+2k^2p_T^2+p_T^4-4k^2p_Tp_L=0$$

Implicit condition relation between wave number k and angular frequency ω: dispersion relation

$$k^4\left(1+2\left(1+\frac{\omega^2}{k^2c_T^2}\right)+\left(1+\frac{\omega^2}{k^2c_T^2}\right)^2-4\left(1+\frac{\omega^2}{k^2c_T^2}\right)^{1/2}\left(1+\frac{\omega^2}{k^2c_L^2}\right)^{1/2}\right)=0$$

NO DISPERSION

$$c_R\equiv\omega/k=f(c_L,c_T,\cancel{\rho,\omega,k})$$

KU LEUVEN

Guided wave propagation in a free-standing plate

with thickness L

Harmonic plane wave components running in the positive x-direction with a depth profile in the z-direction.

$$\varphi(x,z,t) = \left(A\exp(p_L z) + B\exp(-p_L z)\right)\exp(i\omega t - ikx)$$
$$\psi(x,z,t) = \left(C\exp(p_T z) + D\exp(-p_T z)\right)\exp(i\omega t - ikx)$$

4 unknowns A,B,C,D to be found from 4 boundary condition equations:
No normal and shear stress at plate boundaries z=0 and z=L:
$\sigma_{zz}(z=0)=0$
$\sigma_{zx}(z=0)=0$
$\sigma_{zz}(z=L)=0$
$\sigma_{zx}(z=L)=0$

$$\mathbf{u} = \nabla\varphi + \nabla\times\boldsymbol{\psi}$$

$$\sigma_{ij} = \rho_0\left(\left(c_L{}^2 - 2c_T{}^2\right)u_{k,k}\delta_{ij} + c_T{}^2\left(u_{i,j} + u_{j,i}\right)\right)$$

$$\begin{aligned}
\sigma_{xz} &= \rho c_T^2\left[\frac{\partial^2\psi}{\partial x^2} - \frac{\partial^2\psi}{\partial z^2} + 2\frac{\partial^2\varphi}{\partial x z}\right] \\
&\rightarrow \rho c_T^2\left[-k^2\psi - \frac{\partial^2\psi}{\partial z^2} + 2ik\frac{\partial\varphi}{\partial z}\right] \\
\sigma_{zz} &= \rho\left[c_L^2\left(\frac{\partial^2\varphi}{\partial x^2} + \frac{\partial^2\varphi}{\partial z^2}\right) - 2c_T^2\left(\frac{\partial^2\varphi}{\partial x^2} - \frac{\partial^2\psi}{\partial x z}\right)\right] \\
&\rightarrow \rho\left[c_L^2\left(-k^2\varphi + \frac{\partial^2\varphi}{\partial z^2}\right) - 2c_T^2\left(-k^2\varphi - ik\frac{\partial\psi}{\partial z}\right)\right]
\end{aligned}$$

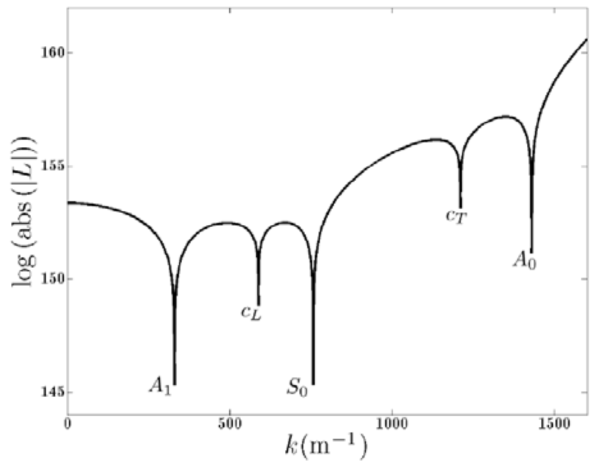

Lamb determinant of homogeneous set of equations should be zero

$$\begin{pmatrix}
-2i\rho v_T^2 p_L k & -\rho v_T^2(p_T^2+k^2) & 2i\rho v_T^2 p_L k & \rho v_T^2(p_T^2+k^2) \\
\rho((2v_T^2 - v_L^2)k^2 + v_L^2 p_L^2) & -2i\rho p_T k v_T^2 & \rho((2v_T^2 - v_L^2)k^2 + v_L^2 p_L^2) & 2i\rho p_T k v_T^2 \\
-2i\rho v_T^2 p_L e^{-p_L L} k & -\rho v_T^2 e^{-p_T L}(p_T^2+k^2) & 2i\rho v_T^2 p_L e^{p_L L} k & -\rho v_T^2 e^{p_T L}(p_T^2+k^2) \\
\rho e^{-p_L L}(-k^2 v_L^2 + 2k^2 v_T^2 + v_L^2 p_L^2) & -2i\rho p_T e^{-p_T L} k v_T^2 & \rho e^{p_L L}(-k^2 v_L^2 + 2k^2 v_T^2 + v_L^2 p_L^2) & 2i\rho p_T e^{p_T L} k v_T^2
\end{pmatrix}
\begin{pmatrix} A \\ C \\ B \\ D \end{pmatrix} = 0$$

$$f(c_L, c_T, \cancel{\rho}, \omega, k, L) = 0$$

Zero search of determinant of set of equations, looking for root k-values for every value of ω

$$c_{Lamb}(c_L, c_T, \cancel{\rho}, \omega, L)$$

DISPERSION

MULTIPLE SOLUTIONS PER FREQUENCY

KU LEUVEN

Guided wave propagation in a free-standing plate

$$f(c_L, c_T, \cancel{\rho,} \omega, k, L) = 0$$

with thickness L

- Dispersion
- Multiple modes
- Both
  running (Im(k)=0)
  and
  local modes (Im(k)≠0)

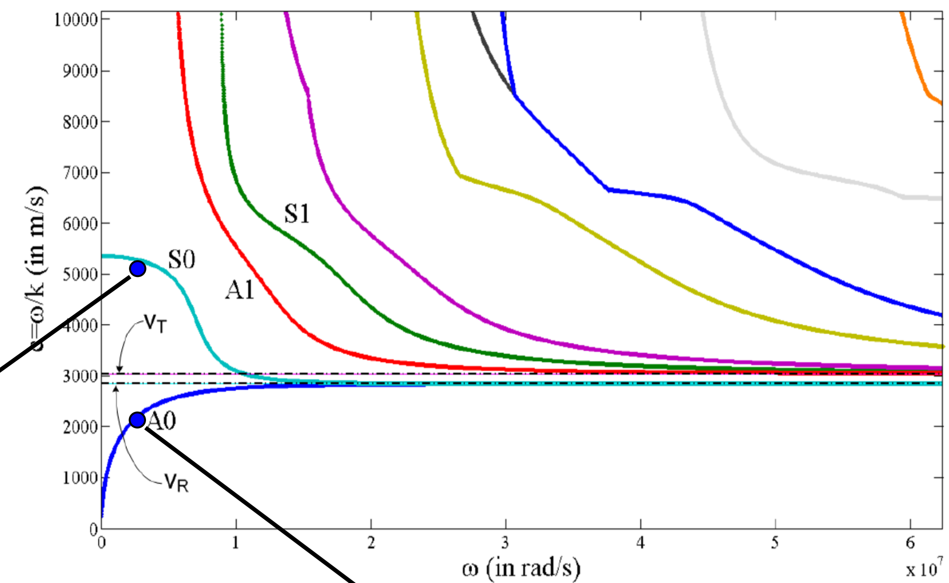

S_0-mode

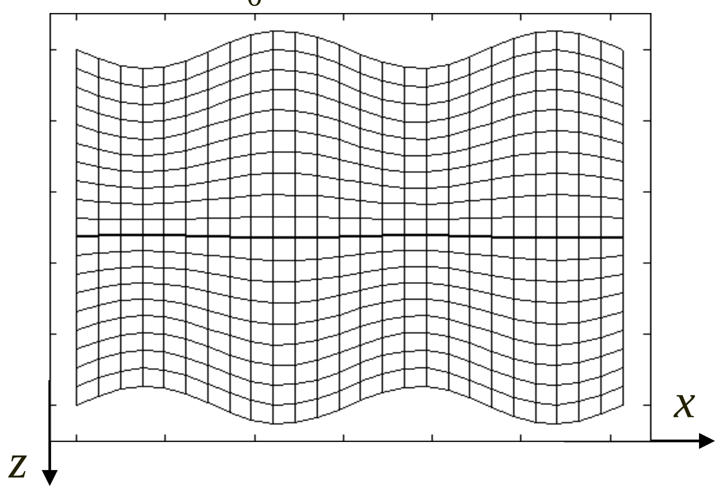

A_0-mode

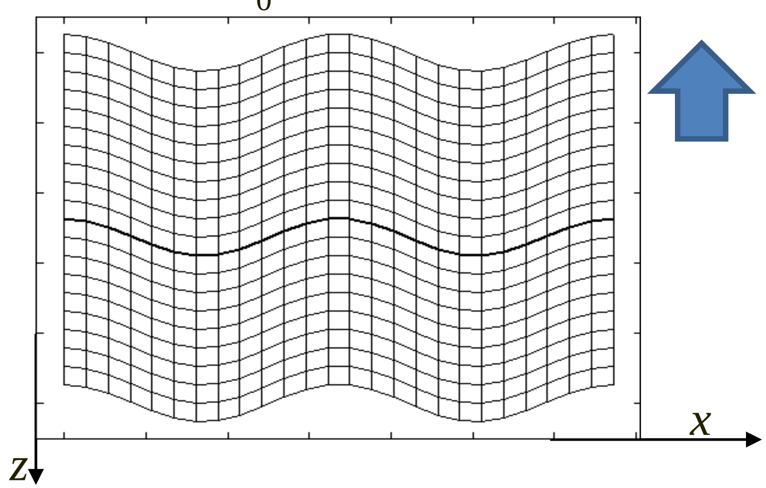

Aluminium plate L = 2 mm, ρ = 2700 kg/m³, v_T = 3040 m/s, v_L =6420 m/s, v_R = 2846 m/s

Guided wave propagation in multilayers

$$\varphi_1(x,z,t)=\left(A_1\exp(p_{L_1}z)+B_1\exp(-p_{L_1}z)\right)\exp(i\omega t-ikx)$$

$$\psi_1(x,z,t)=\left(C_1\exp(p_{T_1}z)+D_1\exp(-p_{T_1}z)\right)\exp(i\omega t-ikx)$$

$$\varphi_2(x,z,t)=\left(A_2\exp(p_{L_2}z)+B_2\exp(-p_{L_2}z)\right)\exp(i\omega t-ikx)$$

$$\psi_2(x,z,t)=\left(C_2\exp(p_{T_2}z)+D_2\exp(-p_{T_2}z)\right)\exp(i\omega t-ikx)$$

$$\varphi_3(x,z,t)=\left(A_3\exp(p_{L_3}z)+B_3\exp(-p_{L_3}z)\right)\exp(i\omega t-ikx)$$

$$\psi_3(x,z,t)=\left(C_3\exp(p_{T_3}z)+D_3\exp(-p_{T_3}z)\right)\exp(i\omega t-ikx)$$

What if there is a delamination?

What if there is a source?

layer

12 equations

0

$\sigma_{zz}(z=0)=0$
$\sigma_{zx}(z=0)=0$

1

$\sigma_{zz}^{+}(z=d_1)=\sigma_{zz}^{-}(z=d_1)$
$\sigma_{zx}^{+}(z=d_1)=\sigma_{zx}^{-}(z=d_1)$
$u_z^{+}(z=d_1)=u_z^{-}(z=d_1)$
$u_x^{+}(z=d_1)=u_x^{-}(z=d_1)$

2

$\sigma_{zz}^{+}(z=d_1+d_2)=\sigma_{zz}^{-}(z=d_1+c$
$\sigma_{zx}^{+}(z=d_1+d_2)=\sigma_{zx}^{-}(z=d_1+($
$u_z^{+}(z=d_1+d_2)=u_z^{-}(z=d_1+d_2$
$u_x^{+}(z=d_1+d_2)=u_x^{-}(z=d_1+d_2)$

3

$A_3=0$
$C_3=0$

12 unknowns

A_1,B_1,C_1,D_1
A_2,B_2,C_2,D_2
A_3,B_3,C_3,D_3

$c_{Lamb}(c_L,c_T,\cancel{\rho},\omega,L)$

Zero search of determinant of set of equations, looking for root k-values for every value of ω

$f(c_L,c_T,\cancel{\rho},\omega,k,L)=0$

$$\begin{pmatrix} M_{1,1} & M_{1,2} & M_{1,3} & M_{1,4} & M_{1,5} & M_{1,6} & M_{1,7} & M_{1,8} & M_{1,9} & M_{1,10} & M_{1,11} & M_{1,12} \\ M_{2,1} & & & & & & & & & & & \\ M_{3,1} & & & & & & & & & & & \\ M_{4,1} & & & & & & & & & & & \\ M_{5,1} & & & & & & & & & & & \\ M_{6,1} & & & & & & & \dots & & & & \\ M_{7,1} & & & & & & & & & & & \\ M_{8,1} & & & & & & & & & & & \\ M_{9,1} & & & & & & & & & & & \\ M_{10,1} & & & & & & & & & & & \\ M_{11,1} & & & & & & & & & & & \\ M_{12,1} & & & & & & & & & & & M_{12,12} \end{pmatrix} \begin{pmatrix} \\ \\ \\ D_1 \\ A_2 \\ B_2 \\ C_2 \\ D_2 \\ A_3 \\ B_3 \\ C_3 \\ D_3 \end{pmatrix} = 0$$

Determinant of homogeneous set of equations should be zero

f(material properties,ω,k,L)=0

DISPERSION CURVE SOLUTIONS k(ω), c(ω)

KU LEUVEN

Guided wave propagation in multilayers

Rayleigh waves: wavelength dependent penetration depth

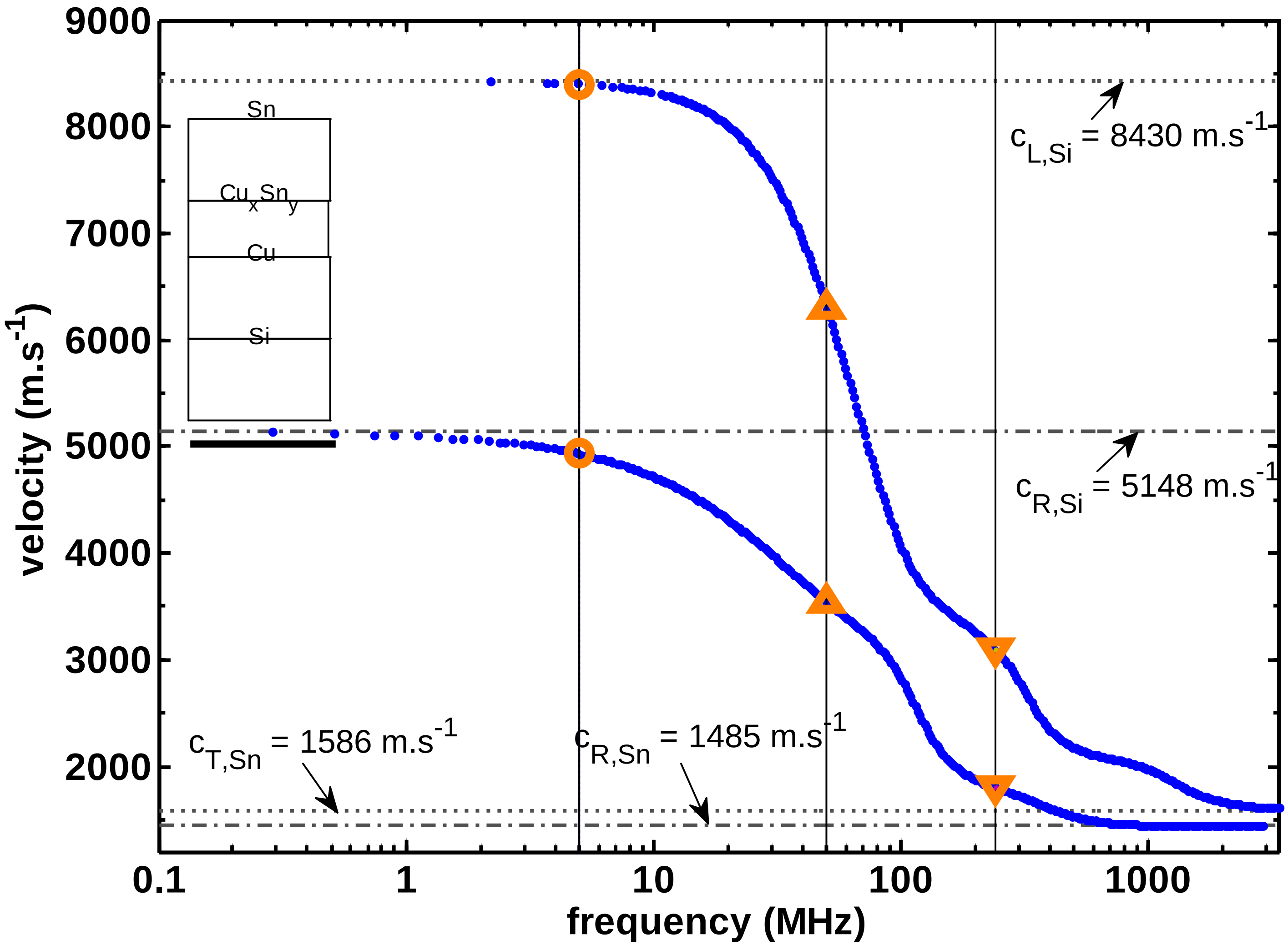

Multilayer sample

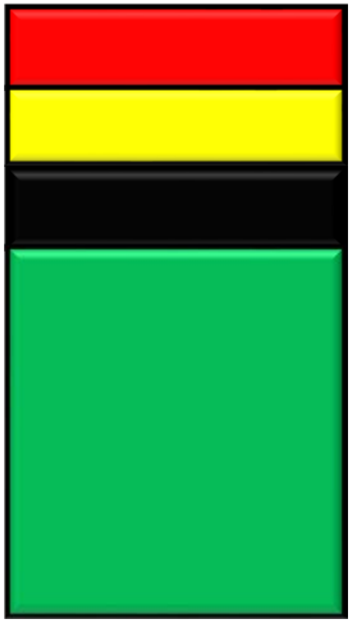

Solution of longitudinal wave equation without and with a source

WITH A THERMAL SOURCE

$$\frac{\partial^2 T}{\partial x^2} - \frac{\rho C}{\kappa}\frac{\partial T}{\partial t} = -\frac{Q}{\kappa}$$

$$Q(x,t) = Q_0 \exp(i\omega t + ikx)$$

$$T(x,\omega) = \frac{Q_0 \cos(kx)}{2\pi\left(\kappa k^2 + i\omega C\right)}$$

$$\frac{\partial^2 u}{\partial x^2} - \frac{1}{c_L^2}\frac{\partial^2 u}{\partial t^2} = \gamma\frac{\partial T}{\partial x}$$

$$u(x,\omega) = \frac{-k\gamma c_L^2 Q_0 \sin(qx)}{2\pi\rho C\left(\alpha k^2 + i\omega\right)\left(\omega^2 - k^2 c_L^2\right)}$$

Kramers rule?

determinant!

$$Q(x,t) = Q_0\delta(t)\cos(kx)$$

$$\Rightarrow Q(x,\omega) = Q_0\cos(kx)$$

c_L: longitudinal speed of sound

C: specific heat capacity

ρ: density

κ: thermal conductivity

γ: thermal expansion coefficient

α = κ/ρC : thermal diffusivity

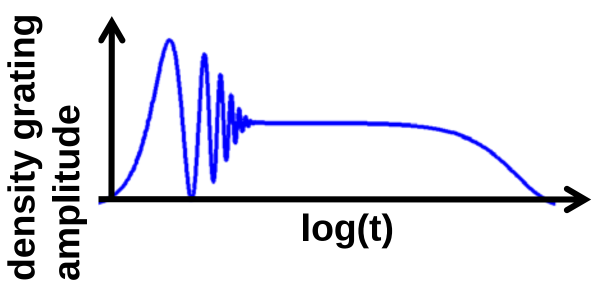

$$T(x,t) = \int_{-\infty}^{+\infty} S(\omega)Q(\omega)\exp(i\omega t)\frac{d\omega}{2\pi}\cos(kx)$$

$$= \int_{-\infty}^{+\infty} \frac{1}{2\pi\left(\kappa k^2 + i\omega C\right)} Q_0 \exp(i\omega t)\frac{d\omega}{2\pi}\cos(kx)$$

Residue theorem?

KU LEUVEN

Solution of longitudinal wave equation without and with a source

WITH A THERMAL SOURCE

$$\frac{\partial^2 T}{\partial x^2} - \frac{\rho C}{\kappa}\frac{\partial T}{\partial t} = -\frac{Q}{\kappa}$$

$$Q(x,t) = Q_0 \exp(i\omega t + ikx)$$

$$T(x,\omega) = \frac{Q_0 \cos(kx)}{2\pi\left(\kappa k^2 + i\omega C\right)}$$

$$\frac{\partial^2 u}{\partial x^2} - \frac{1}{c_L^2}\frac{\partial^2 u}{\partial t^2} = \gamma \frac{\partial T}{\partial x}$$

$$u(x,\omega) = \frac{-k\gamma c_L^2 Q_0 \sin(kx)}{2\pi\rho C\left(\alpha k^2 + i\omega\right)\left(\omega^2 - k^2 c_L^2\right)}$$

determinant!

c_L: longitudinal speed of sound

C: specific heat capacity

ρ: density

κ: thermal conductivity

γ: thermal expansion coefficient

α = κ/ρC : thermal diffusivity

$$Q(x,t) = Q_0 \delta(t)\sin(kx)$$

$$\Rightarrow Q(x,\omega) = Q_0 \sin(kx)$$

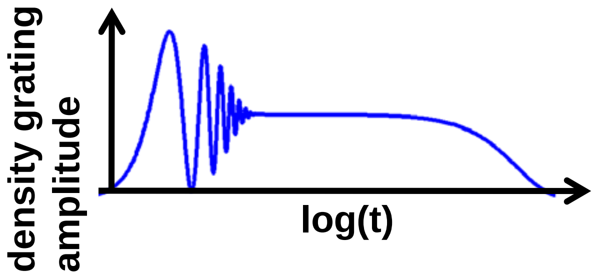

$$u(x,t) = \int_{-\infty}^{+\infty} S(\omega) Q(\omega) \exp(i\omega t)\frac{d\omega}{2\pi}\sin(kx)$$

$$= \int_{-\infty}^{+\infty} \frac{-k\gamma c_L^2}{2\pi\rho C\left(\alpha k^2 + i\omega\right)\left(\omega^2 - k^2 c_L^2\right)} Q_0 \exp(i\omega t)\frac{d\omega}{2\pi}\sin(kx)$$

Residue theorem?

Solution of longitudinal wave equation without and with a source

WITH A THERMAL SOURCE

$$\frac{\partial^2 T}{\partial x^2} - \frac{\rho C}{\kappa}\frac{\partial T}{\partial t} = -\frac{Q}{\kappa}$$

$$Q(x,t) = Q_0 \exp(i\omega t + ikx)$$

$$T(x,\omega) = \frac{Q_0 \cos(kx)}{2\pi\left(\kappa k^2 + i\omega C\right)}$$

$$\frac{\partial^2 u}{\partial x^2} - \frac{1}{c_L^2}\frac{\partial^2 u}{\partial t^2} = \gamma\frac{\partial T}{\partial x}$$

$$u(x,\omega) = \frac{-k\gamma c_L^2 Q_0 \sin(kx)}{2\pi\rho C\left(\alpha k^2 + i\omega\right)\left(\omega^2 - k^2 c_L^2\right)}$$

determinant!

$$Q(x,t) = Q_0 \delta(t)\sin(kx)$$

$$\Rightarrow Q(x,\omega) = Q_0 \sin(kx)$$

c_L: longitudinal speed of sound
C: specific heat capacity
ρ: density
κ: thermal conductivity
γ: thermal expansion coefficient
α = κ/ρC : thermal diffusivity

$$T(x,t) = \frac{Q_0 \sin(kx)}{\rho C}\exp\left(-k^2\alpha t\right)\theta(t)$$

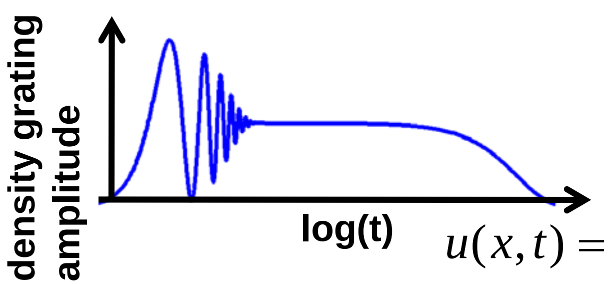

$$u(x,t) = \frac{\gamma Q_0 \sin(kx)}{\rho C k\left(1 + \frac{k^2\alpha^2}{c_L^2}\right)}\left(\exp\left(-k^2\alpha t\right) - \cos(kc_L t) + \frac{\alpha k}{c_L}\sin(kc_L t)\right)\theta(t)$$

KU LEUVEN

Transient grating in reflection mode: displacement response

Thermoelastic excitation

$$T(x,t) = \frac{I_0}{\kappa\sigma} e^{-\sigma z} e^{i(\omega t + kx)} \quad \text{with} \quad \sigma^2 = k^2 + \frac{i\omega}{\alpha}$$

- k,ω domain
- thermal driving source

Displacements at the surface

$$\overline{u}(x,z,t) = \nabla\phi + \nabla \times \psi \quad \text{with} \quad \nabla \cdot \psi = 0$$

Potentials wave equation

$$\frac{\partial^2 \phi_0}{\partial z^2} - p_L^2 \phi_0 = \frac{\beta}{\rho c_L^2} T = \frac{\beta I_0}{\rho c_L^2 \kappa\sigma} e^{-\sigma z} \quad \text{with} \quad p_L = \sqrt{k^2 - \frac{\omega^2}{c_L^2}}$$

$$\frac{\partial^2 \psi_0}{\partial z^2} - p_T^2 \psi_0 = 0 \quad \text{with} \quad p_T = \sqrt{k^2 - \frac{\omega^2}{c_T^2}}$$

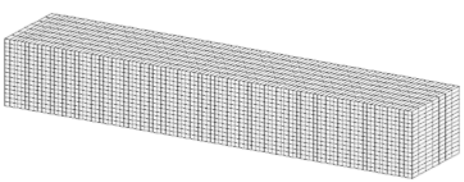

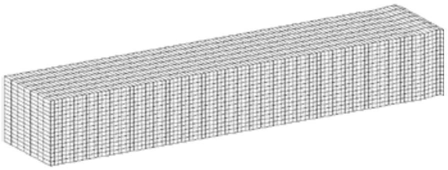

Proposal solutions

$$\phi_0(z) = Ae^{p_L z} + Be^{-p_L z} + Ee^{-\sigma z}$$

$$\psi_0(z) = Ce^{p_T z} + De^{-p_T z}$$

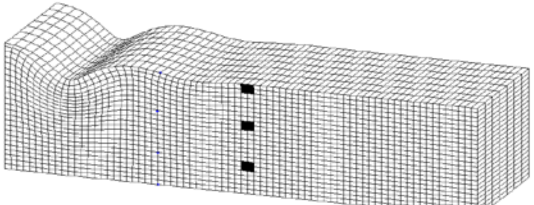

Transient grating in reflection mode: displacement response

Unknowns A,C,E

$$A = 0$$
$$C = 0$$
$$E = \frac{\beta I_0}{\rho c_L^2 \kappa \sigma (\sigma^2 - p_L^2)}$$ ~ source

- effect of surface tension
- effect of gravitation
- thermal driving source

2 remaining unknowns *B* and *D* are determined via 2 boundary conditions

$$\begin{cases} \sigma_{xz}(z=0) = 0 \\ \sigma_{zz}(z=0) = -\gamma \frac{\partial^2 u_z}{\partial x^2} - \rho g u_z \end{cases}$$

Stresses are determined by Duhamel-Neumann relation

$$\sigma_{xz} = \rho c_T^2 \left(\frac{\partial u_x}{\partial z} + \frac{\partial u_z}{\partial x} \right)$$
$$\sigma_{zz} = \rho \left((c_L^2 - 2c_T^2) \frac{\partial u_x}{\partial x} + c_L^2 \frac{\partial u_z}{\partial z} \right) - \beta T$$

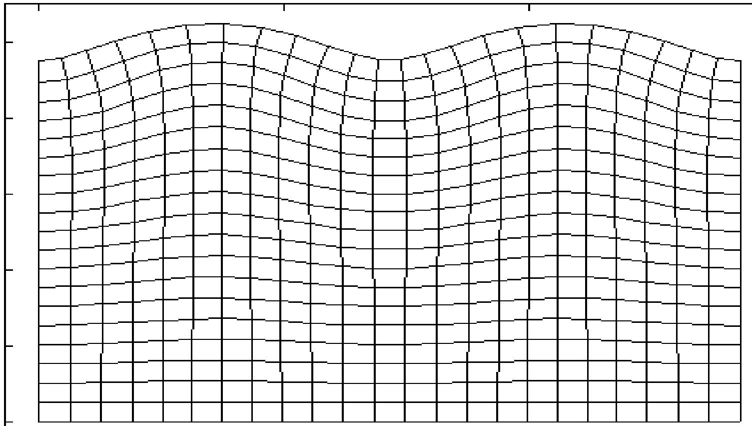

Transient grating in reflection mode: displacement response

2x2 set of equations in unknown coefficients B and D

$$\left\{ \begin{pmatrix} \rho c_T^2(k^2+p_T^2) - \gamma k^2 p_L & 2ik\rho c_T^2 p_T - i\gamma k^3 \\ -2ikp_L\rho c_T^2 & -\rho c_T^2(k^2+p_T^2) \end{pmatrix} \begin{pmatrix} B \\ D \end{pmatrix} = \begin{pmatrix} -\rho c_T^2(k^2+p_T^2) - \gamma k^2\sigma \\ 2ik\sigma\rho c_T^2 \end{pmatrix} E \right.$$

- effect of surface tension
- quasi-Rayleigh determinant

Solution:

$$B = -E\,\frac{\rho^2(2k^2c_T^2-\omega^2)^2 - 4\rho^2c_T^4k^2\sigma p_T - \gamma\rho k^2\omega^2\sigma}{\boxed{(2\rho c_T^2k^2-\rho\omega^2)^2 - 4k^2\rho^2c_T^4p_Lp_T - \gamma\rho k^2\omega^2p_L}}$$

$$D = E\,\frac{2i\rho^2c_T^2k(p_L-\sigma)(2k^2c_T^2-\omega^2)}{\boxed{(2\rho c_T^2k^2-\rho\omega^2)^2 - 4k^2\rho^2c_T^4p_Lp_T - \gamma\rho k^2\omega^2p_L}}$$

$$\phi_0(z) = Ae^{p_L z} + Be^{-p_L z} + Ee^{-\sigma z}$$
$$\psi_0(z) = Ce^{p_T z} + De^{-p_T z}$$

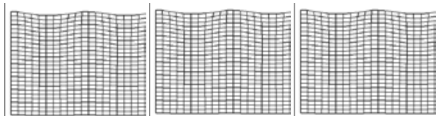

KU LEUVEN

Transient grating in reflection mode: displacement response: arbitrary source

Solution for arbitrary source = 2D (k→x,ω→t) Fourier transform of solution for harmonic excitation, with source spectrum I(ω,k) as weighting function

$$I(x,z,t)=\int_{-\infty}^{+\infty}d\omega\int_{-\infty}^{+\infty}dk\, I(\omega,k)\exp\left(ikx+i\omega t\right)\delta(z)$$

$$\phi_0(x,z,t)=\int_{-\infty}^{+\infty}d\omega\int_{-\infty}^{+\infty}dk\,\frac{I(\omega,k)}{I_0}\left(A(\omega,k)\exp(p_L(\omega,k)z)+B(\omega,k)\exp(-p_L(\omega,k)z)+E(\omega,k)\exp(-\sigma(\omega,k)z)\right)\exp\left(ikx+i\omega t\right)$$

$$\psi_0(x,z,t)=\int_{-\infty}^{+\infty}d\omega\int_{-\infty}^{+\infty}dk\,\frac{I(\omega,k)}{I_0}\left(C(\omega,k)\exp(p_T(\omega,k)z)+D(\omega,k)\exp(-p_T(\omega,k)z)\right)\exp\left(ikx+i\omega t\right)$$

$$\begin{aligned}
u_z(\omega,k,z=0) &= \left(\nabla\phi_0\right)_z\Big|_{z=0}+\left(\nabla\times\psi_0\right)_z\Big|_{z=0}\\
&=\left(\frac{\partial\phi_0}{\partial z}+\frac{\partial\psi_0}{\partial x}\right)\Bigg|_{z=0}\\
&=\left(\left(-p_L B\exp(-p_L z)-\sigma E\exp(-\sigma z)+ikD\exp(-p_T z)\right)\frac{I(\omega,k)}{I_0}\exp\left(ikx+i\omega t\right)\right)\Bigg|_{z=0}\\
&=\left(-p_L B-\sigma E+ikD\right)\frac{I(\omega,k)}{I_0}\exp\left(ikx+i\omega t\right)
\end{aligned}$$

$$I(x,z,t)=\delta(x)\delta(z)\delta(t)\Rightarrow I(\omega,k)=1$$

$$B=-E\frac{\rho^2(2k^2c_T^2-\omega^2)^2-4\rho^2c_T^4k^2\sigma p_T-\gamma\rho k^2\omega^2\sigma}{(2\rho c_T^2k^2-\rho\omega^2)^2-4k^2\rho^2c_T^4p_Lp_T-\gamma\rho k^2\omega^2p_L}$$

$$D=E\frac{2i\rho^2c_T^2k(p_L-\sigma)(2k^2c_T^2-\omega^2)}{(2\rho c_T^2k^2-\rho\omega^2)^2-4k^2\rho^2c_T^4p_Lp_T-\gamma\rho k^2\omega^2p_L}$$

Poles!
→
Residue theorem

$$\Downarrow$$

$$u_z(x,t,z=0)=\int_{-\infty}^{+\infty}d\omega\int_{-\infty}^{+\infty}dk\left(-p_L(\omega,k)B(\omega,k)-\sigma(\omega,k)E(\omega,k)+ikD(\omega,k)\right)\exp\left(ikx+i\omega t\right)$$

Laser ultrasonics for defect detection and application for non-destructive testing

Laser ultrasonic laser Doppler xy scanning imaging: example of material characterization and non-destructive testing

Lamb waves on a thin Cu membrane …
Typical result from full field Doppler xy scanning

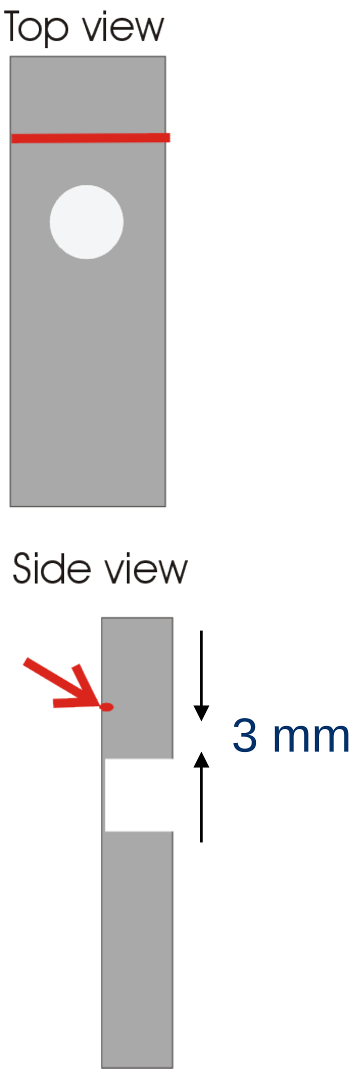

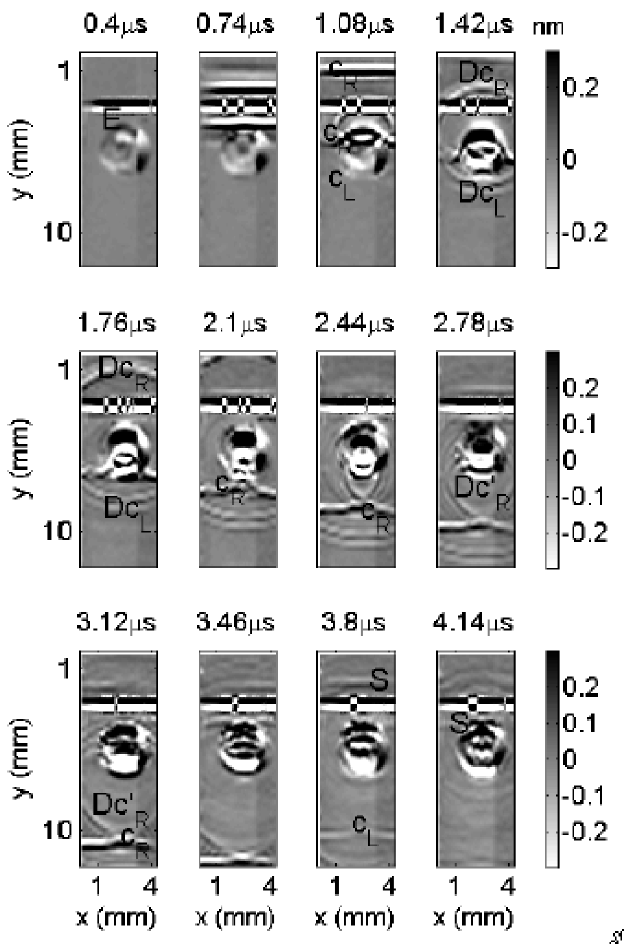

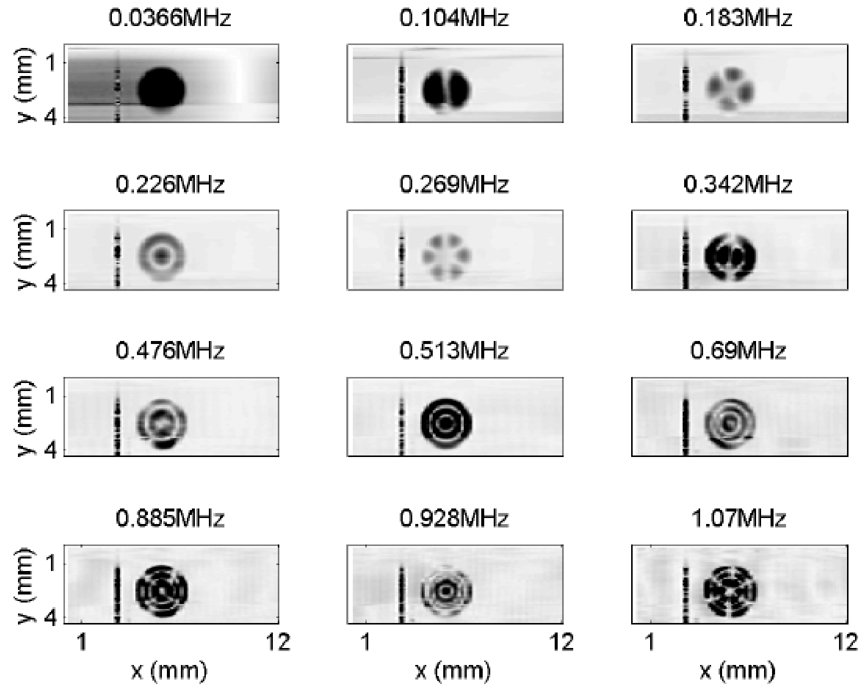

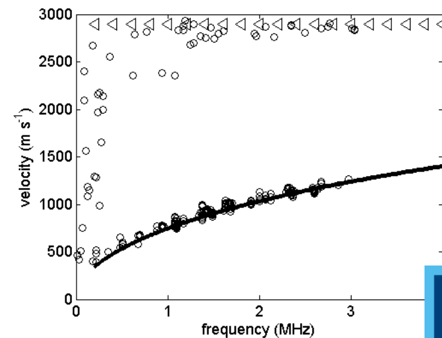

Related references

- Liu, L., Zhong, K., Munro, T., Alvarado, S., Cote, R., Creten, S., Fron, E., Ban, H., Van der Auweraer, M., Roozen, B., Matsuda, O., Glorieux, C. (2015). Wideband fluorescence-based thermometry by neural network recognition: Photothermal application with 10 ns time resolution. *Journal of Applied Physics*, *118* (18), art.nr. 134.58.253.56.
- Kouyate, M., Flores-Cuautle, J., Slenders, E., Sermeus, J., Verstraeten, B., Garay Ramirez, B., San Martin Martinez, E., Kubicar, L., Vretenar, V., Hudec, J., Glorieux, C. (2015). Study of Thermophysical Properties of Silver Nanofluids by ISS-HD, Hot Ball and IPPE Techniques. *International Journal of Thermophysics*, *36* (10-11), 3211-3221.
- Xiong, J., Xu, X., Glorieux, C., Matsuda, O., Cheng, L. (2015). Imaging of transient surface acoustic waves by full-field photorefractive interferometry. *Review of Scientific Instruments*, *86* (5), art.nr. 053107.
- Sermeus, J., Verstraeten, B., Salenbien, R., Pobedinskas, P., Haenen, K., Glorieux, C. (2015). Determination of elastic and thermal properties of a thin nanocrystalline diamond coating using all-optical methods. *Thin Solid Films*, *590*, 284-292.
- Liu, C., Xu, X., Liu, X., Glorieux, C. (2014). Tunable acoustic couplers for two fluids with large impedance mismatch. *Applied Physics Express*, *7* (6), art.nr. 067302.
- Yin, A., Yang, Q., He, F., Wang, X., Glorieux, C. (2014). Textural Through-Thickness Inhomogeneity of Interstitial-Free Steel and its Influence on Plastic Anisotropy Prediction. *Materials Transactions*, *55* (12), 1847-1851.
- Liu, L., Creten, S., Firdaus, Y., Flores Cuautle, J., Kouyaté, M., Van der Auweraer, M., Glorieux, C. (2014). Fluorescence spectra shape based dynamic thermometry. *Applied Physics Letters*, *104* (3), 1-5.
- Sermeus, J., Rochan, S., Vanstreels, K., Vereecken, P., Glorieux, C. (2014). Determination of elastic properties of a MnO2 coating by surface acoustic wave velocity dispersion analysis. *Journal of Applied Physics*, *116*, art.nr. 023503.
- Verstraeten, B., Van Humbeeck, J., Wevers, M., Glorieux, C. (2013). Thermoelastic characterization of changing phase distribution in hardened steel by laser ultrasonics. *International Journal of Thermophysics*, *34* (8-9), art.nr. 10.1007/s10765-013-1405-3, 1754-1761.
- Xiong, J., Glorieux, C. (2013). Spectrally resolved detection of mixed acoustic vibrations by photorefractive interferometry. *Journal of Applied Physics*, *113* (5), art.nr. 054502.
- Shkerdin, G., Glorieux, C. (2013). Interaction of Lamb modes with an inclusion. *Ultrasonics*, *53* (1), 130-140.
- Sermeus, J., Matsuda, O., Salenbien, R., Verstraeten, B., Fivez, J., Glorieux, C. (2012). Thermoelastic Model for Impulsive Stimulated Scattering Monitoring the Evolution from Capillary to Rayleigh TypeWave Propagation on the Surface of Viscoelastic Materials Throughout the Glass Transition. *International Journal of Thermophysics*, *33* (10-11), 2145-2158.
- van Dalen, K., Drijkoningen, G., Smeulders, D., Heller, H., Glorieux, C., Sarens, B., Verstraeten, B. (2011). Medium characterization from interface-wave impedance and ellipticity using simultaneous displacement and pressure measurements. *Journal of the Acoustical Society of America*, *130* (3), 1299-1312.
- Salenbien, R., Cote, R., Goossens, J., Limaye, P., Labie, R., Glorieux, C. (2011). Laser-based surface acoustic wave dispersion spectroscopy for extraction of thicknesses, depth, and elastic parameters of a subsurface layer: Feasibility study on intermetallic layer structure in integrated circuit solder joint. *Journal of Applied Physics*, *109* (9), art.nr. 093104, --.
- Shkerdin, G., Glorieux, C. (2010). Nonlinear clapping modulation of Lamb modes by normally closed delamination. *IEEE Transactions on Ultrasonics, Ferroelectrics and Frequency Control*, *57* (6), 1426-1433.
- Sarens, B., Verstraeten, B., Glorieux, C., Kalogiannakis, G., Van Hemelrijck, D. (2010). Investigation of contact acoustic nonlinearity in delaminations by shearographic imaging, laser doppler vibrometric scanning and finite difference modeling. *IEEE Transactions on Ultrasonics, Ferroelectrics and Frequency Control*, *57* (6), 1383-95.
- Fivez, J., Glorieux, C. (2010). Case-hardening inspection of steel using photothermal phase maxima. *Journal of Applied Physics*, *108*, art.nr. 103506.
- Cote, R., Van der Donck, T., Celis, J., Glorieux, C. (2009). Surface acoustic wave characterization of a thin, rough polymer film. *Thin Solid Films*, *517* (8), 2697-2701.
- Kalogiannakis, G., Sarens, B., Van Hemelrijck, D., Glorieux, C. (2008). On the feasibility of shearographic imaging of acoustic cross-modulation. *Strain*, *44*, 398-408.
- Shkerdin, G., Glorieux, C. (2008). Nonlinear modulation of Lamb modes by clapping delamination. *Journal of the acoustical society of america*, *124* (6), 3397-3409.
- Xu, X., Goossens, J., Shkerdin, G., Glorieux, C. (2008). Effect of loading a plate with different liquids on the propagation of Lamb-like waves studied by laser ultrasonics. *IEEE Transactions on Ultrasonics, Ferroelectrics and Frequency Control*, *55* (3), 675-685.
- Goossens, J., Leclaire, P., Xu, X., Glorieux, C., Martinez, L., Sola, A., Siligardi, C., Cannillo, V., Van der Donck, T., Celis, J. (2007). Surface acoustic wave depth profiling of a functionally graded material. *Journal of Applied Physics*, *102* (5), art.nr. 053508.
- Shkerdin, G., Glorieux, C. (2007). Interaction of lamb modes with delaminations in plates coated by highly absorbing materials. *IEEE Transactions on Ultrasonics, Ferroelectrics and Frequency Control*, *54* (2), 368-77.
- Sarens, B., Kalogiannakis, G., Glorieux, C., Van Hemelrijck, D. (2007). Full-field imaging of non classical acoustic nonlinearity. *Applied Physics Letters*, *91*, art.nr. 264102.
- Matsuda, O., Glorieux, C. (2007). A Green's function method for surface acoustic waves in functionally graded materials. *Journal of the Acoustical Society of America*, *121* (6), 3437-45.
- Leclaire, P., Goossens, J., Martinez, L., Wilkie-Chancellier, N., Serfaty, S., Glorieux, C. (2006). Study of the bending modes in circular quartz resonators. *IEEE transactions on ultrasonics, ferroelectrics and frequency control*, *53* (10), 1934-1943.
- Glorieux, C., Van de Rostyne, K., Goossens, J., Shkerdin, G., Lauriks, W., Nelson, K. (2006). Shear properties of glycerol by interface wave laser ultrasonics. *Journal of Applied Physics*, *99* (1), art.nr. 013511.
- Goossens, J., Martinez, L., Glorieux, C., Wilkie-Chancellier, N., Ehssein, C., Serfaty, S. (2006). Laser ultrasonic analysis of normal modes generated by a voltage pulse on an AT quartz sensor. *Ultrasonics*, *44* (1), e1179-e1182.
- Martinez, L., Goossens, J., Glorieux, C., Wilkie-Chancellier, N., Ehssein, C., Serfaty, S. (2006). 3D Gabor analysis of transient waves propagating along an AT cut quartz disk. *Ultrasonics*, *Ultrasonics*, *44*, *44* (1), E1173-E1177, e1173-e1177.
- Shkerdin, G., Glorieux, C. (2005). Lamb mode conversion in an absorptive bi-layer with a delamination. *Journal of the acoustical society of america*, *118* (4), 2253-2264.
- Boeckx, L., Leclaire, P., Khurana, P., Glorieux, C., Lauriks, W., Allard, J. (2005). Investigation of the phase velocities of guided acoustic waves in soft porous layers. *Journal of the Acoustical Society of America*, *117* (2), 545-554.
- Leys, J., Sinha, G., Glorieux, C., Thoen, J. (2005). Influence of nanosized confinements on 4-n-decyl-4(')-cyanobiphenyl (10CB): A broadband dielectric study. *Physical Review E*, *71* (5), 051709.
- Kalogiannakis, G., Moura, A., Ravi, J., Longuemart, S., Antoniow, J., Van Hemelrijck, D., Glorieux, C. (2005). Experimental modeling of nonlinear photothermal effects in composite materials. *Journal de Physique IV France*, *125*, 487-489.
- Glorieux, C., Beers, J., Bentefour, E., Van de Rostyne, K., Nelson, K. (2004). Phase mask based interferometer: Operation principle, performance, and application to thermoelastic phenomena. *Review of scientific instruments*, *75* (9), 2906-2920.
- Allard, J., Henry, M., Glorieux, C., Lauriks, W., Petillon, S. (2004). Laser induced surface modes at water-elastic and poroelastic solid interfaces. *Journal of Applied Physics*, *95* (2), 528-535.
- Shkerdin, G., Glorieux, C. (2004). Lamb mode conversion in a plate with a delamination. *Journal of the acoustical society of america*, *116* (4), 2089-2100.
- Allard, J., Henry, M., Glorieux, C., Petillon, S., Lauriks, W. (2003). Laser induced surface modes at an air-porous medium interface. *Journal of Applied Physics*, *93* (2), 1298-1304.
- Gao, W., Glorieux, C., Thoen, J. (2003). Laser ultrasonic study of Lamb waves: determination of the thickness and velocities of a thin plate. *International journal of engineering science*, *41* (2), 219-228.
- Glorieux, C., Van de Rostyne, K., Beers, J., Gao, W., Petillon, S., Van Riet, N., Nelson, K., Allard, J., Gusev, V., Lauriks, W., Thoen, J. (2003). Acoustic waves at interfaces studied by laser ultrasonics. *Review of scientific instruments*, *74* (1), 465-469.
- Glorieux, C., Nelson, K., Hinze, G., Fayer, M. (2002). Thermal, structural, and orientational relaxation of supercooled salol studied by polarization-dependent impulsive stimulated scattering. *Journal of Chemical Physics*, *116* (8), 3384-3395.
- Gao, W., Glorieux, C., Thoen, J. (2002). Study of circumferential waves and their interaction with defects on cylindrical shells using line-source laser ultrasonics. *Journal of Applied Physics*, *91* (9), 6114-6119.
- Glorieux, C., Van de Rostyne, K., Gusev, V., Gao, W., Lauriks, W., Thoen, J. (2002). Nonlinearity of acoustic waves at solid-liquid interfaces. *Journal of the acoustical society of america*, *111* (1), 95-103.
- Gao, W., Glorieux, C., Lauriks, W., Thoen, J. (2002). Investigation of titanium nitride coating by broadband laser ultrasonic spectroscopy. *Chinese physics*, *11* (2), 132-138.
- Van de Rostyne, K., Glorieux, C., Gao, W., Lauriks, W., Thoen, J. (2002). Experimental investigation of leaky Lamb modes by an optically induced grating. *IEEE Transactions on ultrasonics ferroelectrics and frequency control*, *49* (9), 1245-1253.
- Paoloni, S., Mayr, P., Glorieux, C., Li Voti, R., Bentefour, E., Thoen, J. (2001). Photothermal depth profiling in the presence of lateral heat flow effects. *Analytical Sciences*, *17 Special Iss. SI*, S406-S409.
- Glorieux, C., Van De Rostyne, K., Nelson, K., Gao, W., Lauriks, W., Thoen, J. (2001). On the character of acoustic waves at the interface between hard and soft solids and liquids. *Journal of the acoustical society of america*, *110* (3), 1299-1306.
- Glorieux, C., Antoniow, J., Chirtoc, M., Chirtoc, I., Thoen, J. (2001). Neural network photothermal depth profiling of a heat source distribution. application to water migration in starch sheets. *Analytical Sciences*, *17 Special Iss. SI*, S398-S401.
- Van De Rostyne, K., Glorieux, C., Lauriks, W., Thoen, J. (2001). Laser ultrasonics generated interface waves for soft matter investigation. *Progress in natural science*, *11*, S317-S324.
- Gao, W., Glorieux, C., Kruger, S., Van De Rostyne, K., Gusev, V., Lauriks, W., Thoen, J. (2001). Investigation of the microstructure of cast iron by laser ultrasonic surface wave spectroscopy. *Materials science and engineering a-structural materials properties microstructure and processing*, *313* (1-2), 170-179.
- Glorieux, C., Gao, W., Kruger, S., Van De Rostyne, K., Lauriks, W., Thoen, J. (2000). Surface acoustic wave depth profiling of elastically inhomogeneous materials. *Journal of Applied Physics*, *88* (7), 4394-4400.
- Gao, W., Glorieux, C., Kruger, S., de Rostyne, K., Gusev, V., Lauriks, W., Thoen, J. (1999). Study of the microstructure of cast iron by analysis of Rayleigh waves. *Acta Physica Sinica -- Overseas Edition*, *8*, S85-S89.
- de Rostyne, K., Glorieux, C., Gao, W., Lauriks, W., Thoen, J. (1999). Laser ultrasonic measurements of acoustic waves generated at solid-liquid interfaces. *Acta Physica Sinica -- Overseas Edition*, *8*, S219-S224.
- Van De Rostyne, K., Glorieux, C., Gao, W., Gusev, V., Nesladek, M., Lauriks, W., Thoen, J. (1999). Investigation of elastic properties of CVD-diamond films using the lowest order flexural leaky lamb wave. *Physica Status Solidi A, Applied Research*, *172* (1), 105-111.
- Glorieux, C., Voti, R., Thoen, J., Bertolotti, M., Sibilia, C. (1999). Depth profiling of thermally inhomogeneous materials by neural network recognition of photothermal time domain data. *Journal of Applied Physics*, *85* (10), 7059-7063.
- Kruger, S., Gao, W., Glorieux, C., Charlier, J., Rebello, J., Lauriks, W., Thoen, J. (1998). Characterization of cast irons by laser-ultrasonic surface acoustic waves. *Materials science and engineering a-structural materials properties microstructure and processing*, *250* (1-2), 312-314.
- Desmet, C., Gusev, V., Glorieux, C., Lauriks, W., Thoen, J. (1998). All-optical investigation of the lowest-order antisymmetrical acoustic modes in liquid-loaded membranes. *Journal of the acoustical society of america*, *103* (1), 618-621.
- Gao, W., Gusev, V., Glorieux, C., Thoen, J., Borghs, G. (1997). Supersonic radiative transport of electron-hole plasma in semiconductors at room temperature studied by laser ultrasonics. *Optics Communications*, *143* (1-3), 19-24.
- Gusev, V., Glorieux, C., Lauriks, W., Thoen, J. (1997). Nonlinear bulk and surface shear acoustic waves in materials with hysteresis and end-point memory. *Physics letters a*, *232* (1-2), 77-86.
- Desmet, C., Gusev, V., Lauriks, W., Glorieux, C., Thoen, J. (1997). All-optical excitation and detection of leaky Rayleigh waves. *Optics letters*, *22* (2), 69-71.
- Glorieux, C., Thoen, J. (1996). Thermal depth profile reconstruction by neural network recognition of the photothermal frequency spectrum. *Journal of Applied Physics*, *80* (11), 6510-6515.
- Gusev, V., Desmet, C., Lauriks, W., Glorieux, C., Thoen, J. (1996). Theory of Scholte, leaky Rayleigh, and lateral wave excitation via the laser-induced thermoelastic effect. *Journal of the acoustical society of america*, *100* (3), 1514-1528.
- Glorieux, C., Desmet, C., Lauriks, W., Wevers, M., Coufal, H. (1996). Photothermal and elastic characterization of a hardened steel rod. *Progress in natural science*, *6*, S406-S408.
- Glorieux, C., Bozoki, Z., Fivez, J., Thoen, J. (1996). Photoacoustic investigation of the nematic director depth profile near the free surface of an inhomogeneously aligned liquid crystal. *Acustica*, *82*, S118-S118.
- Glorieux, C., Caerels, J., Thoen, J. (1996). Magnetic phase transition of gadolinium studied by acoustically detected magnetocaloric effect. *Journal of Applied Physics*, *80* (6), 3412-3421.
- Desmet, C., Gusev, V., Lauriks, W., Glorieux, C., Thoen, J. (1996). Laser-induced thermoelastic excitation of Scholte waves. *Applied Physics Letters*, *68* (21), 2939-2941.
- Desmet, C., Gusev, V., Lauriks, W., Glorieux, C., Thoen, J. (1996). Laser-induced thermoelastic excitation of interface acoustic waves. *Progress in natural science*, *6*, S390-S393.
- Kawald, U., Desmet, C., Lauriks, W., Glorieux, C., Thoen, J. (1996). Investigation of the dispersion relations of surface acoustic waves propagating on a layered cylinder. *Journal of the acoustical society of america*, *99* (2), 926-930.
- Desmet, C., Kawald, U., Mourad, A., Lauriks, W., Glorieux, C., Thoen, J. (1996). Dispersion of surface acoustic waves on a layered cylinder. *Acustica*, *82*, S117-S117.
- Glorieux, C., Bozoki, Z., Fivez, J., Thoen, J. (1995). Photoacoustic depth profiling of the thermal conductivity of an inhomogeneously aligned liquid crystal at a free surface. *Journal of Applied Physics*, *78* (5), 3096-3101.
- Bozoki, Z., Miklos, A., Glorieux, C., Thoen, J., Bicanic, D. (1994). Modeling of the thermoelastic response of composite media by a transfer matrix approach. *Journal de Physique IV*, *4* (C7), 579-582.
- Glorieux, C., Fivez, J., Thoen, J. (1993). Photoacoustic investigation of the thermal properties of layered materials -- calculation of the forward signal and numerical inversion procedure. *Journal of Applied Physics*, *73* (2), 684-690.
- Lauriks, W., Desmet, C., Glorieux, C., Thoen, J. (1993). Investigation of the thermal anisotropy of unidirectional carbon-fiber-reinforced composite plates using optically generated thermal waves and a noncontact optical-detection technique. *Journal of materials research*, *8* (12), 3106-3110.
- Glorieux, C., Degroote, J., Fivez, J., Lauriks, W., Thoen, J. (1993). Application of photoacoustic and photothermal techniques for heat-conduction measurements in a freestanding chemical-vapor-deposited diamond film. *International journal of thermophysics*, *14* (6), 1201-1214.

KU LEUVEN

Prague

Czech Republic

Michal Landa, Pavla Stoklasova,
Hanus Seiner, Petr Sedlak

JAPAN SOCIETY FOR THE PROMOTION OF SCIENCE
日本学術振興会

FWO VLAANDEREN

CONACYT 45 años

Ken Haenen, Paulius Pobedinskas

Hasselt,
Belgium

KU LEUVEN

Osamu Matsuda

Leuven,
Belgium

Bert Verstraeten, Jan Sermeus,
Liwang Liu, Kris Vanstreels

SCK•CEN
STUDIECENTRUM VOOR KERNENERGIE
CENTRE D'ETUDE DE L'ENERGIE NUCLEAIRE

Kelly Martinez, Luis Silvestre
Vaca Oyola, Jonathan Guarachi

Mexico City,
Mexico

Angel Cifuentes, Salvador
Alvarado, Ernesto Marin

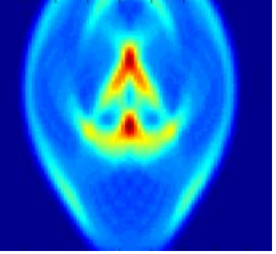

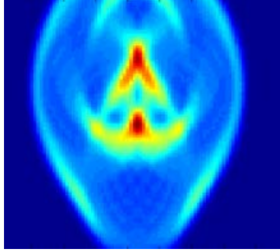

THANK YOU FOR YOUR ATTENTION

Christ.Glorieux@fys.kuleuven.be